University of Szeged
Faculty of Pharmacy
Institute of Pharmaceutical Technology and Regulatory Affairs
Head: Prof. Dr. Ildikó Csóka, Ph.D.

Ph.D. Thesis

Development of buccal mucoadhesive polymer films with sodium alginate and cetirizine dihydrochloride in allergy therapy

Krisztián Pamlényi
Pharmacist

Supervisors:
Dr. Katalin Kristó, Ph.D.
Dr. habil Géza Regdon jr., Ph.D.

Szeged
2023

PUBLICATIONS RELATED TO THE THESIS

1. **Pamlényi, K.**, Kristó, K., Jójárt-Laczkovich, O., Regdon jr., G.:
„Formulation and Optimization of Sodium Alginate Polymer Film as a Buccal Mucoadhesive Drug Delivery System Containing Cetirizine Dihydrochloride”.
Pharmaceutics 13, 619 (2021) doi: 10.3390/pharmaceutics13050619.
Indep. citations: 10 Q1 IF = 6.525 (2021)

2. **Pamlényi, K.,** Kristó, K., Sovány, T., Regdon jr., G.:
„Development and evaluation of bioadhesive buccal films based on sodium alginate for allergy therapy”
Heliyon 8, e10364 (2022) doi: 10.1016/j.heliyon.2022.e10364)
Q1 IF = 3.776 (2021)

3. **Pamlényi, K.,** Regdon jr., G., Nemes, D., Bácskay, I., Fenyvesi, F., Kristó, K.:
„Stability, permeability and cytotoxicity of buccal films in allergy treatment”
Pharmaceutics 14, 1633 (2022) doi: 10.3390/pharmaceutics14081633
Indep. citations: 1 Q1 IF = 6.525 (2021)

PUBLICATIONS NOT RELATED TO THE THESIS

1. Litauszki, K; Kiserdei, É; **Pamlényi, K.**; Szarka, Gy; Kmetty, Á; Kovács, Zs.:
„Controlled Drug Release from Laser Treated Polymeric Carrier”.
J. Pharm. Sci. 111, 3297-3303 (2022) doi: *10.1016/j.xphs.2022.08.018*
Indep. citations: 2 Q2 IF = 3.784 (2021)

2. **Pamlényi, K.**; Kristó, K; Nemes, D., Bácskay, I.; Regdon jr., G:
„Formulation and characterization of pramipexole containing buccal films for using in Parkinson’s disease”
Eur. J. Pharm. Sci. Editor decision: “revision”, we are currently doing it
Q1 IF = 5.112 (2021)

PRESENTATIONS RELATED TO THE THESIS

1. **Pamlényi, K.,** Sovány, T., Kristó, K., Regdon jr., G.: *„Formulation of an innovatve buccal mucoadhesive drug delivery system with sodium alginate polymer film”*, XII. Central European Symposium on Pharmaceutical Technology and Regulatory Affairs conference, Szeged, Sep 2018 –**presenter** (poster presentation)

2. **Pamlényi, K.,** Kristó, K., Regdon jr., G.: „*Szájnyálkahártyán alkalmazható, Na-alginát tartalmú mukoadhezív polimer film előállítása és vizsgálata”,* 2018. évi Tudományos Diákköri Konferencia, *Szeged, Nov 2018* **presenter** (oral presentation)

3. **Pamlényi, K.,** Kristó, K., Regdon jr., G.: *„Szájnyálkahártyán alkalmazható, Na-alginát tartalmú mukoadhezív polimer film előállítása és vizsgálata”,* XXVI. Tudományos Diákköri Konferencia, Marosvásárhely, Apr 2019 – **presenter** (oral presentation)

4. **Pamlényi, K.,** Kristó, K., Regdon jr., G.: „*Szájnyálkahártyán alkalmazható, Na-alginát tartalmú mukoadhezív polimer film előállítása és vizsgálata”,* XXXIV. Országos Tudományos Diákköri Konferencia Debrecen, May 2019 - **presenter** (oral presentation)

5. Regdon jr., G, Módra, Sz., **Pamlényi, K.,** Sovány, T., Kristó, K.: *„Formulation, structural and thermal analysis of an innovative buccal mucoadhesive film drug delivery system from two different polymers”*, 2nd Journal of Thermal Analysis and Calorimetry Conference (2ndJTACC+V4 2019), Budapest, Jun 2019 - **co-author**

6. **Pamlényi, K.,** Kristó, K., Regdon jr., G.: *„Bukkális szájnyálkahártyán alkalmazható innovatív, nátrium-alginát alapú gyógyszerhordozó rendszer kialakítása és termoanalitikai vizsgálata”* Gyógyszertechnológiai és Ipari Gyógyszerészeti Konferencia, Siófok, Sep 2019 – **presenter** (poster presentation)

7. **Pamlényi, K., Kristó, K., Regdon jr., G.:** II. Symposium of Young Researchers on Pharmaceutical Technology, Biotechnology and Regulatory Science, *„Development and characterization of sodium alginate polymer film as a buccal mucoadhesive drug delivery system”,* Szeged, Jan 2020 - **presenter** (oral presentation)

8. **Pamlényi, K.,** Kristó, K., Regdon jr., G.: *„Buccal polymer film as an innovative drug delivery system”*, Medical Conference for PhD Students and Experts of Clinical Sciences (MedPECS 2020), Pécs, Oct 2020 - **presenter** (oral presentation)

9. **Pamlényi, K.,** Kristó, K., Regdon jr., G.: *„Nátrium-alginát, mint bukkális mukoadhezív gyógyszerhordozórendszer”*, III. Fiatal Technológusok Fóruma, Budapest, Dec 2020 –**presenter** (oral presentation)

10. **Pamlényi, K.,** Regdon jr., G., Nemes, D., Bácskay, I., Kristó, K.: *„Preparation and investigation of permeability and physical-chemical properties of buccal films with sodium alginate”*, III. Symposium of Young Researchers on Pharmaceutical Technology, Biotechnology and Regulatory Science, Szeged, Jan 2021 - **presenter** (oral presentation)

11. **Pamlényi, K.**, Kristó, K., Regdon jr., G.: *„Nátrium-alginát alapú bukkális mukoadhezív polimer film gyógszerforma formulálása”* Kárpát-medencei Fiatal Magyar Kutatók Konferenciája (EFOP-3.10.1-17-2017-00001), Budapest, Mar 2021 -**presenter** (oral presentation)

12. **Pamlényi, K.,** Regdon jr., G., Nemes, D., Bácskay, I., Kristó, K.: *„Investigation of stability and permeability of buccal films based on sodium alginate”*, XIII. Central European Symposium on Pharmaceutical Technology and Regulatory Affairs conference, Gdansk, Sep 2021 - **presenter** (oral presentation)

13. **Pamlényi, K.,** Regdon jr., G., Nemes, D., Bácskay, I., Kristó, K.: *„Cetirizin tartalmú nátrium-alginát alapú polimer filmek stabilitási és permeabilitási vizsgálata”*, XIV. Clauder Ottó emlékverseny, Budapest Nov 2021 –**presenter** (oral presentation)

14. **Pamlényi, K.,** Regdon jr., G., Nemes, D., Bácskay, I., Kristó, K.: *„Stability and permeability properties of sodium alginate buccal films”,* IV. Symposium of Young Researchers on Pharmaceutical Technology, Biotechnology and Regulatory Science, Szeged, Jan 2022 - **presenter** (**oral** presentation)

15. **Pamlényi, K.,** Regdon jr., G., Nemes, D., Bácskay, I., Kristó, K.: *„Pramipexolt tartalmazó innovatív bukkális polimer film formulálása és vizsgálata”*, V. Fiatal Technológusok Fóruma, Budapest, May 2022 –**presenter** (oral presentation)

16. **Pamlényi, K.,** Regdon jr., G., Nemes, D., Bácskay, I., Kristó, K.: *„Parkinson-kór kezelésében alkalmazható, pramipexolt tartalmazó innovatív bukkális polimer film formulálása és vizsgálata”*, SZTE Gyógyszerésztudományi Kar 2021. évi ÚNKP díjazottjainak tudományos előadóülése, Szeged, Jun 2022 –**presenter** (oral presentation)

17. **Pamlényi, K.,** Regdon jr., G., Nemes, D., Bácskay, I., Kristó, K.:, *„Preparation of buccal films in Parkinson’s Disease”* 9th BBBB Conference on Pharmaceutical Sciences, Ljubljana, Slovenia, Sep 2022 - **presenter** (oral presentation)

18. **Pamlényi, K.,** Regdon jr., G., Nemes, D., Bácskay, I., Kristó, K.:, *„Formulation of Buccal Films in Parkinson’s Disease”,* V. Symposium of Young Researchers on Pharmaceutical Technology, Biotechnology and Regulatory Science, Szeged, Jan 2023 - **presenter** (oral presentation)

19. **Pamlényi, K.,** Regdon jr., G., Nemes, D., Bácskay, I., Kristó, K.: *„Evaluation of Stability and Cell Line Studies of Alginate Films Containing Cetirizine as Anti-Allergic Agent”,* V. International Conference on PharmScience Research & Development Las Vegas, NV, USA, Feb 2023 - **presenter** (oral presentation)

TABLE OF CONTENTS

ABBREVIATIONS

API	active pharmaceutical ingredient
AC	apical compartment
P_{app}	apparent permeability
CTZ	cetirizine dihydrochloride
CA	citric acid
DSC	differential scanning calorimetry
FSC-SSC	forward and side scatter
FT-IR	Fourier-Transform Infrared Spectra
G	α-L guluronic acid (1–6)
GLY	glycerol
HBSS	Hank's balanced salt solution
HPMC	hydroxypropyl methylcellulose
M	β-D mannuronic acid (1–4)
SA	sodium alginate
SD	standard deviation
SFE	surface free energy
TGA	thermal gravimetric analysis

1. INTRODUCTION

Buccal polymer films offer an alternative and innovative way to deliver an active pharmaceutical ingredient (API) to the systemic circulation without swallowing the dosage form [1, 2]. The characteristics of this dosage form can be exploited in many diseases, for example, in allergy, hypertensive crisis, Parkinson's disease, coma, treatment of children. The pharmaceutical industry has already started to focus on buccal films and recognized them as a potential drug delivery system [3], as evidenced by the availability on the market of a buccal film called Breakyl®, containing fentanyl [4].

Nowadays, the buccal drug delivery system is becoming an important alternative route in drug administration. This possibility of drug application has been untapped and poorly investigated. Buccal drug delivery systems have some bioadhesive solid dosage forms, such as bioadhesive tablets, gels, patches, and mucosal bioadhesive films [5,6]. Patients do not have to swallow this dosage form, they should place the bioadhesive system onto the buccal mucosa of the mouth, and the API can be absorbed into the systemic circulation. Many research groups have already tried to formulate buccal polymers films with different APIs, such as omeprazole, miconazole, ondansetron and prednisolone [7–10], but they did not investigate the prepared films widely because it is not an official dosage form in the Pharmacopeia, so official rules and guidelines for polymer films cannot be found.

In my research work, drug-loaded buccal polymer films were formulated and for the preparation of films SA was applied as a polymer film-forming agent as a novel substance in buccal films. SA was combined with HPMC to create the polymer matrix. In the polymer films, CTZ was used as an API. The mechanical properties of the prepared films were evaluated because these can determine the possibility of the application (the film resists finger pressure and binds to the mucin of the buccal mucosa appropriately). The chemical interactions between the components of the films were also analyzed. In addition, the release of the API was tested and accelerated stability test was carried out. Moreover, the cytotoxicity and permeability of the prepared films were also investigated. My main aim was to find the optimal composition of a buccal film to be used on the buccal mucosa as a potential dosage form.

2. LITERATURE BACKGROUND

2.1. Anatomical structure of the buccal mucosa and characterization of mucin

Patients have to put the polymer film on the buccal area of the mouth (**Figure 1.**). The buccal area is the part of the oral cavity located on the outer side of the teeth. The area of the entire oral cavity is around 170 cm^2, but the medicinally useful area is less than 50 cm^2 because the API can be absorbed into the systemic circulation only from the nonkeratinized epithelium [11–13]. The buccal mucosa has three main parts and several smaller parts. The main parts are the epithelium, the basement membrane and the underlying connecting tissues [14].

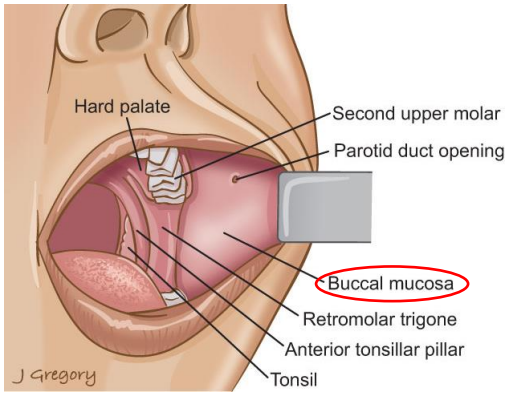

Figure 1. Location of the buccal mucosa in the oral cavity [15]

The cells of the buccal mucosa are covered with a mucus layer, which is made up of 95% water and 5% mucin [13, 16]. Mucin is a glycoprotein-type molecule, which is composed of 80% carbohydrates, 12-25% proteins and 5% sulfate esters [16]. Mucin is a large molecule, its molecular size can reach 50 Mda [17]. It forms a gel layer at buccal pH and can bind to epithelial cells. This bond is made up of several factors. The entanglement of the mucin chains, electrostatic and hydrophobic interactions, and hydrogen bonds result in the gel structure. Mucin can occur on the surface of the mucous membrane in both dissolved and suspended form. The thickness of the mucin layer is different on the individual mucous membranes, in the oral cavity it is 1 μm thick [16,18].

The general structure of mucin is characterized by the fact that it consists of two parts. One part is always from a single-stranded glycoprotein, while the other part can vary. Either large carbohydrate side chains are connected by O-glycosidic bonds, or it is composed of one or two low glycosylated protein parts [19].

There are several types of mucin, two types were distinguished in saliva, type one (MG1) and type two (MG2). Both types are characterized by low solubilization, high elasticity and high viscosity [13,17].

2.2 Definition, theories and mechanism of mucoadhesion

Mucoadhesion is the process when the materials and the mucin of the mucous membrane are held together for a long time by attractive bonding. It is defined as bioadhesion when both connecting materials are biological. Mucin is a hydrophilic macromolecule and possesses a great number of hydrogen atoms and hydroxyl groups and can therefore create primary (covalent, ionic, ester bonding) and secondary (hydrogen bonding, van der Waals forces) bonding with biological structures [20, 21].

Mucoadhesion includes several types of theories, the major categories are [22]:

- **mechanical theory** considers adhesion to be due to the filling of the irregularities on a rough surface by a mucoadhesive liquid. Roughness increases the interfacial area available for interactions, thereby aiding dissipating energy, and it is the most important phenomenon of the process [23].
- **diffusion theory** assumes interdiffusion between the chain of the polymer films and mucin. The phenomenon is determined by concentration gradient at the same time can be limited by the length and mobiliy of molecular chain. The interpenetration depth of polymer and mucin chains can be estimated by the contact time and the diffusion coefficient [23, 24].
- **adsorption theory** supposes that the mucadhesive material adheres to mucin with secondary chemical interactions such as hydrogen bonds, van der Waals, electrostatic and hydrophobic interactions [23, 24].
- **wetting theory** assumes interfacial energy between the solid and the liquid system. The liquid should spread on the solid surface to create bioadhesion. The gas, solid and liquid forms are in equilibrium. It can be characzerized by the wetting degree. We can speak of wetting if $\Theta < 90°$ and the surface is poorly wetted if $\Theta > 90°$. If $\Theta = 0°$, wetting is complete, and if $\Theta = 180°$, the liquid does not wet the solid at all. The wetting degree should be close to 0 degree to achieve the best condition in terms of bioadhesion [23].

- **electronic theory** is based on the premise that mucoadhesive and biological materials have opposing electrical charges. When both materials come into contact, they transfer electrons, leading to the building of a double electronic layer at the interface, where the attractive forces within this electronic double layer determine mucoadhesive strength [24].
- **fracture theory** assumes fraction after adhesion. Generally, the weakest components show this phenomenon. This theory is different from the previous five theories, but it is the most commonly used theory in studies on the mechanical measurement of mucoadhesion [24].

The mechanism of mucoadhesion can be divided into two stages (**Figure 2.**), the contact stage and the consolidation stage. In the contact stage, a direct connection develops between the dehydrated polymer film and the hydrated mucus layer. The polymer film dehydrates the mucus layer, thus the polymer film becomes hydrated. In the stabilization phase, the polymer chains create a permanent chemical bond in the deeper layers of the mucous layer, and a strong mucoadhesion force is formed [24].

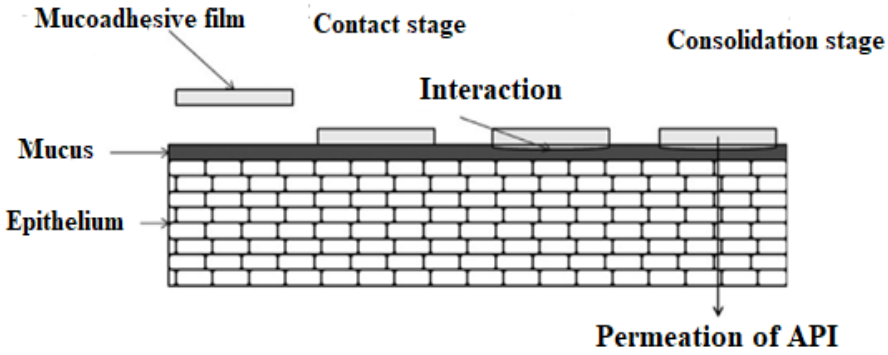

Figure 2. Interaction process between the mucoadhesive film and mucin [18]

The termination of mucoadhesion depends on several parameters. It is mostly determined by the hydration of the polymer film because if it becomes overhydrated, it easily slides off the surface, so the degree of hydration must be controlled. The molecular weight of the polymer also determines the length of mucoadhesion. If the polymer has a low molecular weight, it hydrates quickly and detaches from the surface early. In the case of a high molecular weight, the opposite happens. Another influencing factor is the mobility, charge and concentration of the polymer chains, as well as the lifetime of saliva and mucin, or the movement of buccal tissues [24].

2.3. Advantages and disadvantages of buccal drug administration

According to *Macedo and Patel*, this drug delivery system possesses great advantages. A lower dose of API can be applied compared with other delivery systems. Since the first-pass effect of the liver is avoided, the API can enter the systemic circulation after absorption from the buccal mucosa. Secondly, it can be used in the case of swallowing problems, such as Parkinson's disease, stroke, multiple sclerosis, esophagitis, and allergies [25 ,26]. In geriatrics and pediatrics, it can play a huge role due to its easy and unnoticed application, so in general patients prefer this dosage form to per os tablets [27, 28]. It is a useful form of drug administration from the chemical perspective because the API and gastric acid do not contact each other, so the stomach can be protected from the API and vice versa [29, 30].

Furthermore, local and fast systemic effects can be achieved with these systems, therefore they can be used in emergencies such as hypertensive crisis or anaphylactic shock, and also in chronic illnesses like asthma, allergy, hypertension or other chronic diseases [31–34].

Transcellular and paracellular drug delivery across the lipid membrane of the buccal mucosa is equally good, which can result in good transport for hydrophilic and lipophilic APIs [35]. Buccal polymer films might be preferred to buccal tablets. They are more flexible and comfortable as they can be washed from the buccal mucosa by the saliva and thus be removed easily [25].

However, this dosage form also has difficulties. In the polymer film, a dose of less than 50 mg of API can be used successfully due to the fact that the surface of the buccal mucosa is small, so a small dose of API can be absorbed from the small absorption surface [36]. Buccal films as a dosage form are not official in the Pharmacopoeias [37].

2.4. Polymers in terms of mucoadhesion

Mucoadhesion force and the time of mucoadhesion are also important for the application because if one of these two parameters is not sufficient, the absorption of the active pharmaceutical ingredient (API) cannot occur. The first step in the development is the selection of the polymer material with mucoadhesive properties. Many polymers are available with different parameters [38]. Polymers can be from natural sources, semi-synthetic, and synthetic. The most commonly used polymers are cellulose derivatives such

as hydroxypropyl cellulose (HPC), hydroxypropyl-methylcellulose (HPMC), but chitosan, sodium alginate (SA), polyacrylic acid (PAA) and polyethylene glycol (PEG) are also common [9, 39–41]. Plasticizers are also important additives in the formulation. They can increase the elasticity of the films and make the application easier, such are, for example, glycerol and mannitol [42]. In addition, many additives can be applied in polymer films, such as solvents, taste-masking agents, permeation enhancers, saliva-stimulating agents, etc. [43–45]. In the literature, there are some studies that investigated the effect of the polymer material and the plasticizer or any other ingredient in films, but in these studies the authors did not apply an API despite the fact that the API can remarkably change the properties of films and in terms of use, it would be important to investigate them together [40, 46–48]. The selected API has to meet some criteria. The applied amount of the API should not exceed 40–50 mg per one dose, it should be soluble in water or in other solvent, and without these criteria formulation is not possible [37, 48].

Oral and buccal controlled drug delivery systems are used widely with hydrophilic polymers [34, 49]. Oral buccal polymer films must have at least medium mucoadhesive strength; therefore, one or more polymer film-forming excipients, such as sodium alginate (SA) and hydroxypropyl methylcellulose (HPMC), can be chosen [30].

2.5. Characterization of sodium alginate and other components

SA is a natural water-soluble, nontoxic, biodegradable, anionic, biocompatible polymer with appropriate mucoadhesive properties [50–52]. It can be extracted from brownseeds (Phaeophyceae), Macrocystis Pyriferal and Ascophyllum Nodosum [53, 54]. It is a member of the polysaccharides (linear) chemical family. It is built by two types of monomers, β-D mannuronic acid (1–4) (M) and α-L guluronic acid (1–6) (G) as it can be seen in **Figure 3**. G and M can be arranged as homopolymer G blocks and M blocks, or as heteropolymer mixed blocks (MG) [54]. The sequence of the G and M blocks can be different (GG, MM, GM, MG). The different sequence can affect the molecular weight and physical properties of SA [55]. The molecular weight of SA can vary within a wide range, from 10 to 1000 kDa [55]. Sodium, potassium, and ammonium salts with a molecular weight of 60-70 kDa can be found on the market [56]. SA can also form a salt with divalent ions, especially with calcium [57, 58]. A strong interaction can occur between the carboxylic group of SA and calcium ions, and it can be determined as an egg-box structure [59]. The GG blocks are responsible for the crosslinking between SA and calcium, MM and MG

blocks for gel flexibility. It can be said that the SA gel structure depends on the percentage of G and M blocks [56, 60].

SA has a hydroxyl group too, which can bind to the mucin of the buccal mucosa (carboxyl group as well) [7]. SA is used in the pharmaceutical and the food and beverage industries. In the pharmaceutical industry, it is often used as a coating component, gel and emulsion stabilizer, and a polymer film-forming excipient for drug delivery in hydrogels, micro-, nanoparticles. The listed properties make SA suitable to be applied in buccal mucoadhesive films [7, 54, 61, 62].

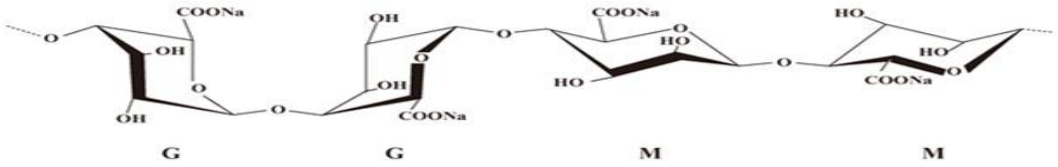

Figure 3. Chemical structure of sodium alginate (SA) [63]

In our previous work, the film-forming properties of HPMC were studied [40]. HPMC is a popular, water-soluble, semisynthetic polymer. It is a white, solid, nontoxic polysaccharide (cellulose ether) molecule. In the literature, many researchers have reported that HPMC has good mucoadhesive properties [64–67]. Due to its large number of methoxy, carboxyl, and hydroxyl groups, it can create stable hydrogen bonds with the mucin of the buccal mucosa. *Kumria et al*. concluded that the larger HPMC content can raise the mucoadhesion time and mucoadhesion force of films [68]. According to *Peh and Wong*, HPMC films swelled to a greater extent in simulated saliva solution [69]. This fact proves the great mucoadhesivity of HPMC. HPMC is a polymer with high hydrophilicity for an oral-controlled drug delivery system [65, 66, 70]. It is used as a film-forming agent, thickener agent, coating agent, and alternative to gelatin, and it is a polymer matrix system in tablets, capsules, gels, and eye drops. In addition, it is applied in agriculture, food, and cosmetics [71].

2.6. Allergy and cetirizine

Allergy is a condition caused by the hypersensitivity of the immune system, an increased sensitivity that results from a harmful substance triggering an immunological response [72]; it is also known as allergic disease. Allergies affect more and more people all around the world [73]. Allergic reactions can be classified into four different groups, Types I, II, III, IV [74]. Types I, II, III are immediate reactions, appearing within 24 hours of

exposure to the allergen [74]. Type IV is a delayed allergic reaction that usually occurs after 24 hours of exposure [74]. In my work, I focused on Type I allergy. The symptoms of Type I allergic diseases may include red skin, red eyes, a runny nose, sneezing, shortness of breath or swallowing problems. Medications can be used to improve the symptoms of allergy [72, 75, 76]. The most commonly applied medications in the treatment of allergies are antihistamines, which can block the H1 receptor [76].

Cetirizine dihydrochloride (CTZ) is a second-generation, non-sedative antihistamine [77, 78]; it is the active metabolite of the first-generation H1 receptor blocker, hydroxyzine (**Figure 4.**) [79]. It is a member of BCS I classification. CTZ has three ionizable groups, a strong basic amino group, a strong carboxylic acid group, and a weak basic amino group, and it is a zwitterion structure between pH 3.0 and 8.0 [80]. CTZ has two remarkable forms (conformers), a folded and an extended one. The folded conformer has notable lipophobicity, low polarity, and a very low energy form due to the resulting intramolecular ionic bond between the positive and the negative charges. However, the extended form is characterized by high polarity, good lipophilicity, and it can form intramolecular hydrogen bondings, Van der Waals forces, and ionic bonds [81].

Due to its antihistamine properties, it can be used effectively in the treatment of seasonal or chronic allergic rhinitis, urticaria and bronchial asthma [79, 83]. Some studies reported that it can reduce bronchoconstriction and swallowing problems. CTZ is available on the market in tablets and solution dosage forms [84].

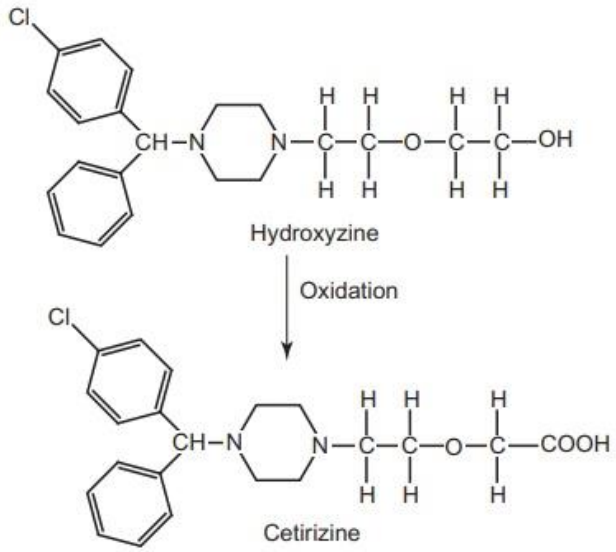

Figure 4. Chemical structure and metabolization of cetirizine [82]

In addition, it is used intravenously in emergencies (anaphylaxis) by paramedics after the administration of adrenaline and intravenous steroids. In normal application the patients have to swallow the dosage form with CTZ, but in the case of an anaphylactic reaction, it is impossible because there is a swallowing problem due to laryngeal oedema. In this case, the patient has to apply an injection or wait for medical help.

In our case, CTZ can act immediately after permeation, so it can quickly reduce serious symptoms without medical help.

Bioadhesive drug delivery systems are becoming increasingly frequent on the market. One such system is buccal tablets, films and gels. This administration route is easy to use, so patient compliance is better than in the case of the intravenous or per os route, etc. [30]. Children, elderly people and people who suffer from swallowing problems can also use it [85]. A further advantage of this alternative route is that the active pharmaceutical ingredient can enter the systemic circulation without transformation because it avoids the first-pass effect of the liver [86].

Summarizing all facts, buccal films containing CTZ are able to reduce and moderate allergic symptoms in a short time, and depending on the formulation, they are also capable of protecting allergic patients from a life-threatening condition.

3. AIM OF THE EXPERIMENTAL WORK

In my research work, I prepared buccal mucoadhesive polymer films with SA and CTZ as a potential buccal drug delivery system.

In the first part of my work, my main goal was to prepare and investigate polymer films of different compositions without API. The aim of my work was to:

- evaluate the film-forming ability of SA
- optimize the prepared films with preformulation
- study the mechanical properties of films
  (thickness, breaking hardness, in vitro mucoadhesivity)
- investigate the effect of different amounts of GLY on the polymer system
- evaluate the chemical interactions between the components of films
  (FT-IR spectroscopy, TGA, DSC)
- develop a drug delivery polymer matrix based on SA for buccal application

- evaluate the data of the films with statistical analysis (factorial design) by mixed two-level and three-level factorial designs. With this analysis, we are able to predict the properties of certain compositions without measurement, so efficiency can increase.

In the second part of my research work, my main aim was to choose the API to be incorporated in the polymer film system. I chose CTZ as the drug for the films. The API can influence the bonds and interactions between the components of the films, as a result of which the properties of the films can be changed. Therefore, my further goals were as follows:

- investigate the mechanical properties of films
  (thickness, breaking hardness, in vitro mucoadhesivity, contact angle (CA) measurement and surface free energy (SFE) calculation)
- study the effect of the GLY and CTZ on the polymer system
- evaluate the interactions between the API and the components of films
  (FT-IR and RAMAN spectroscopy, TGA, DSC)
- study the release of the API from the different compositions of films (dissolution test)
- evaluate the data of the films with statistical analysis (factorial design) by mixed two-level and three-level factorial designs

In the last part of my scientific work, my main goal was to investigate the stability of the prepared films, as well as the relation of the promising compositions based on my earlier research work with the living cells. The knowledge of these properties is very important from the point of view of storage and application. The aims were the following:

- study the stability of the prepared film
  - mechanical stability (thickness, breaking hardness, in vitro mucoadhesivity)
  - physicochemical stability (FT-IR spectroscopy)
  - API content
- based on data from the literature, citric acid (CA) enhances permeation, therefore, it was incorporated into the films to improve permeation [43, 82].
- investigate the cytotoxicity of the polymer films
- examine the permeation of CTZ from buccal films across an artificial membrane
- evaluate the permeation of CTZ from the films on the TR 146 buccal cell line

My final aim was to select the best composition with suitable mechanical and chemical properties, good stability, appropriate cytotoxicity and high permeability.

4. MATERIALS AND METHODS

4.1. Materials

Sodium alginate (SA) (Biochemica GmbH, Darmstadt, Germany) (10,000–600,000 g/mol) and hydroxy methylcellulose (HPMC) (Pharmacoat® 603, Shin Etsu Chemical Co., Ltd., Tokyo, Japan) were used as film-forming agents in the polymer film. Glycerol (GLY) 85% (w/w %) was added to the film as a plasticizer (Ph. Eur. 8.). Citric acid (CA) (Ph. Eur. 8.) was incorporated in the polymer film system as a permeation enhancer. Cetirizine dihydrochloride (CTZ) (Ph. Eur. 8.) was the API, which was a gift from ExtractumPharma Pharmaceutical Manufacturing, Marketing and Consulting Inc., Kunfehértó, Hungary. Mucin (Carl Roth GmbH + Co. KG, Karlsruhe, Germany) (10 w/w %) dispersion was used in the in vitro mucoadhesion test.

4.2. Preparation of buccal films

The films were prepared at room temperature with the solvent casting method. As the first step of preparation, SA (1, 1.33, 1.5, 2, 3, 4 w/w %) was dissolved in distilled water and mixed (900 rpm) at room temperature. The solution was heated to 70 °C and mixed (900 rpm), and CTZ was then incorporated in the warm solution (70 °C, 0.5523 g/100 g solution), and the mixing was continued for 5 h. In certain cases, as the third step, HPMC (0, 0.66, 1, 1.5 w/w %) and CA were added to the solution with mixing without heating. In the fourth step, GLY (0, 1, 3, 5 w/w %) was added to the solution the following day. Mixing was decreased to 100 rpm for 3 h to help the air bubbles disappear from the solution.

The solution was cast on a glass surface in Petri dishes, with 10 g of solution/dish; then, it was dried at room temperature (24.4 ± 0.5 °C). The dried polymer films were removed from the surface and were placed in closed containers (24.4 ± 1 °C, 60 ± 2 % RH), and the other part of the prepared films was also placed in closed containers, but at 40 °C ± 2 °C, 75 % RH ± 5 % RH. The prepared films contained 10 mg of CTZ on an area of 4 cm^2, which is the therapeutic dose of this API. **Table 1.** shows the different compositions of the prepared polymer films.

I studied how the parameters changed in the case of purely SA-based films without HPMC (Samples 1–18). I also investigated the parameters of films with different combinations of SA and HPMC (Samples 19-42). Finally, I incorporated CA into the promising compositions (Samples 43-48).

Table 1. Composition of different SA- and HPMC-based films

Samples	SA (w/w %)	HPMC (w/w %)	GLY (w/w %)	CA (w/w %)	CTZ (10 mg/4 cm^2)
1	2	0	0	-	-
2	3	0	0	-	-
3	4	0	0	-	-
4	2	0	1	-	-
5	2	0	3	-	-
6	2	0	5	-	-
7	3	0	1	-	-
8	3	0	3	-	-
9	3	0	5	-	-
10	2	0	1	-	+
11	2	0	3	-	+
12	2	0	5	-	+
13	3	0	1	-	+
14	3	0	3	-	+
15	3	0	5	-	+
16	4	0	1	-	-
17	4	0	3	-	-
18	4	0	5	-	-
19	1	1	1	-	-
20	1	1	1	-	+
21	1	1	3	-	-
22	1	1	3	-	+
23	1	1	5	-	-
24	1	1	5	-	+
25	1.33	0.66	1	-	-
26	1.33	0.66	1	-	+
27	1.33	0.66	3	-	-
28	1.33	0.66	3	-	+
29	1.33	0.66	5	-	-
30	1.33	0.66	5	-	+
31	1.5	1.5	1	-	-
32	1.5	1.5	1	-	+
33	1.5	1.5	3	-	-
34	1.5	1.5	3	-	+
35	1.5	1.5	5	-	-
36	1.5	1.5	5	-	+
37	2	1	1	-	-
38	2	1	1	-	+
39	2	1	3	-	-
40	2	1	3	-	+

Samples	SA (w/w %)	HPMC (w/w %)	GLY (w/w %)	CA (w/w %)	CTZ (10 mg/4 cm^2)
41	2	1	5	-	-
42	2	1	5	-	+
43	3	0	1	+	+
44	3	0	3	+	+
45	1.5	1.5	1	+	+
46	1.5	1.5	3	+	+
47	2	1	1	+	+
48	2	1	3	+	+

4.3. Methods

4.3.1. Thickness

The thickness of the polymer films was measured with a screw micrometre (Mitutoyo Co. Ltd, Japan), sensitivity was 0.001 mm. Six points were selected randomly from all films (n = 6). The means and standard deviations (SD) were evaluated from these data.

4.3.2. Breaking hardness

Breaking hardness was tested with a self-developed device and software. The device and the software were developed at our institute [47, 88]. The device has two different types of sample holder as probes (needle-like probe, rod-like probe). The equipment has a fix disc and a vertically moving jowl. Force, force-displacement and time can be registered. A different sample holder can be applied depending on the test. The breaking hardness of the films can be examined with the needle-like probe (its area was 201 mm^2). At the beginning of the test, the sample was fixed on the bottom part of the equipment and the probe was lowered at constant speed (20 mm/min). The probe moved towards the film and finally it broke the film. The equipment detected the time, force and deformation during the test. The test was finished when the film was broken. The measuring range was 0–200 N, the sampling rate was 50 Hz, the output was 0–5 V and the sensitivity was 0.1 N [40]. The test was repeated six times (n = 6) for each film. Tablets, pellets, films can also be investigated with this equipment. The means and standard deviations were calculated.

4.3.3. In vitro mucoadhesivity measurement

Mucoadhesion was investigated with the same texture analyser with different settings and parameter modifications [47, 51, 89, 90]. In this study, a rod-like sample holder with a diameter of 5 mm was used. A double-faced adhesive tape was fixed on the surface of the sample holder, and the polymer film was fixed to the other face of the adhesive tape. On the bottom part of the tester, a fixed disc with a diameter of 35 mm was applied, and 40 µL of freshly prepared mucin dispersion (10 w/w %) was spread on it. The rod-like sample holder went to the fixed, bottom disc and pressed the polymer film to the mucin-covered bottom disc with 30 ± 0.1 N for 30 s. This steady-state part can be found in the force–time curve. Thereafter, the sample holder went back to the original place, and the force was decreased until the sample started to separate from the mucin, which can be seen as a well-defined, sharp peak in the force–time curve, indicating the in vitro mucoadhesion force of the films. The test was done six times (n = 6), and the means and standard deviations were calculated.

4.3.4. Contact angle measurement and surface free energy (SFE) calculation

Polymer films were placed on the microscope glass slides. One drop of distilled water and diiodomethane was used to measure the contact angle (Θ) of polymer films for 15 s, with the circle fitting method, by using a contact angle apparatus (OCA20-DataPhysics Instrument GmbH, Filderstadt, Germany). One drop of different liquids was applied, the volume of which was 10 µL and 2 µL in the case of distilled water and diiodomethane, respectively.

The means and standard deviations (SD) were calculated from 6 identical samples of each combination of films (n = 6). The means and standard deviations were used to calculate the SFE of films. SFE was calculated with Wu's method. This method defines the amounts of the polar (γ^p) and the dispersive (γ^d) components of solids. The SFE of solids can be calculated by using the following connection if the two parameters and the contact angle of the solid are known (Equation 1):

$$(1+\cos\Theta)\cdot\gamma = \frac{4\left(\gamma_s^{\,d}\cdot\gamma_l^{\,d}\right)}{\gamma_s^{\,d}+\gamma_l^{\,d}} + \frac{\left(\gamma_s^{\,p}\cdot\gamma_l^{\,p}\right)}{\gamma_s^{\,p}+\gamma_l^{\,p}} \qquad (1)$$

where Θ is the contact angle of the solid–liquid surface, γ_l is the liquid surface tension, γ_s is the solid surface energy, which is the sum of their polar and dispersive components.

According to Wu, the SFE of distilled water is 72.8 mN/m (polar part (γ^p) = 50.2 mN/m; dispersive part (γ^d) = 22.6 mN/m), while the SFE of diiodomethane is 50.8 mN/m (polar part (γ^p) = 1.8 mN/m; dispersive part (γ^d) = 49.0 mN/m) [47]. Knowing the polar and the dispersive parts of polymer films, the polarity of films can be established by using the following formula [where γ^{tot} (mN/m) = γ^p (mN/m) + γ^d (mN/m)] (Equation 2):

$$\text{Polarity (\%)} = (\gamma^p \text{ (mN/m)}/\gamma^{tot} \text{ (mN/m)}) \times 100 \quad (2)$$

4.3.5. FT-IR spectroscopy

An Avatar 330 FT-IR apparatus (Thermo-Scientific, Waltham, MA, USA) was used to analyse the Fourier-Transform Infrared Spectra of the raw materials and the prepared polymer films. The apparatus was equipped with a coupled Zn/Se horizontal attenuated total reflectance (HATR) unit. The films were put on a clean crystal of the apparatus. The range of wavelength was 600 to 4000 cm^{-1} during the investigation. The spectra were collected from 128 scans at the spectral resolution of 4 cm^{-1} with CO_2 and H_2O for correction.

4.3.6. Raman spectroscopy

Transmission Raman Spectroscopy is used for the noninvasive and fast qualitative investigation of pharmaceutical dosage forms and intermediate products. In our method, the distribution of CTZ was analyzed by Raman surface mapping in CTZ-containing free buccal films.

To investigate the distribution of API, Raman spectra were acquired with a Thermo Fisher DXR Dispersive Raman (Thermo Fisher Sco. Inc., Waltham, MA., USA) equipped with a CCD camera and a diode laser operating at a wavelength of 780 nm. Raman measurements were carried out with a laser power of 24 mW at a 25-µm slit aperture size on a 2-µm spot size. The discrete spectra of the individual substances such as CTZ, HPMC, and SA, and different compositions of polymer films were collected using an exposure time of 6 s, the number of exposures was 20, and the number of background exposures was 512. Smart background was used during the whole investigation. The applied spectral range was 3200–200 cm^{-1} with cosmic ray and fluorescence corrections.

4.3.7. Thermoanalytical measurement (thermogravimetric analyses (TGA), differential scanning calorimetry (DSC))

The thermoanalytical measurement of the prepared films was carried out with a Mettler-Toledo TGA/DSC1 instrument (Mettler Toledo, Switzerland). Small pieces of films (approximately 10 mg) were placed in aluminium pans (40 μL), and were inserted into the instrument. During the measurement, the start temperature was 25 °C and the end temperature was 500 °C. The heating rate was 10 °C/min. The samples were investigated in flowing nitrogen atmosphere, the flow rate was 50 ml/min. The curves were evaluated from the average of two parallel measurements with STARe software [91, 92].

4.3.8. Dissolution test

Polymer films of a size of 2 cm × 2 cm (containing 10 mg of CTZ) were investigated in the dissolution test. The dissolution test was made by an Erweka DT700 dissolution basket tester at a mixing speed of 100 rpm. 900 milliliters of phosphate buffer (pH = 6.8) was used as the dissolution medium, and its temperature was 37 °C [8, 93, 94]. Aliquots of 5 mL were analyzed in 5, 10, 15, 20, 30, 40, 50, 60, 90, and 120 min with Genesys 10S UV-VIS (Thermo Fisher Scientific, USA) UV-spectrophotometry at λ = 207 nm.

4.3.9. Stability test

During product development, it is essential and unavoidable to assess the stability of the drug and the drug delivery system. In my research work, stability studies were done according to ICH guidelines. The prepared films were placed in closed containers and stored at 40 °C ± 2 °C, 75 % RH ± 5 % RH for a period of 6 months [95].

Different methods were applied to obtain information about the changes in the properties of the films. During the stability test, breaking hardness, in vitro mucoadhesivity and active agent content were analysed to determine changes in the physical properties of the films.

Furthermore, the interactions I also examined with FT-IR spectroscopy, and the drug content was also detected during the 6-month period. The methods of thickness, breaking hardness, in vitro mucoadhesivity, FT-IR spectroscopy and drug content were the same as described above. I investigated the promising film composition in its freshly prepared state, 3 months later and 6 months later.

4.3.10. Cell viability test

In order to study the cell viability of CTZ films, a Guava® easyCyte™ 5HT (Luminex, Austin, TX, USA) flow cytometer was used for our experiments. TR-146 cells were collected from cell culture flasks with a trypsin–EDTA solution and redistributed into separate tubes, and 1 million cells were treated with 1 mL of CTZ solution (CTZ films dissolved in HBSS in equal concentration as in the case of the permeation tests). After 30 min of incubation, the cells were centrifuged, the test solutions were removed, and the cells were gently washed with cold HBSS and centrifuged again.

The supernatant was removed, and a 1 million cells/mL cell suspension was prepared with HBSS and then stained with 1 µL of 100 µg/mL propidium iodide solution. After 15 min, the suspensions were distributed on 96-well microplates in a volume of 200 µL (3 wells/group) and analysed. Propidium iodide was excited with a 488-nm laser and detected at the 525/30 nm channel (green parameter).

On the Forward and Side Scatter Patterns (FSC-SSC) scatterplot, the non-cellular events were excluded. The remaining events (8,000–10,000) were analysed on a scatterplot, and gates were created to determine stained (necrotic) and non-stained (living) cells [96]. The experiment was carried out in triplicate. As negative control, HBSS was used, and cells treated with HBSS instead of the dissolved films were considered 100%, to which all treated groups were compared. As positive control, cells were treated with 1% Triton-X 100.

4.3.11. Permeation test

The permeation property of CTZ was investigated with two different permeation methods. As the first step, in the Enhancer Cell, the permeation of the API was examined from the polymer films across an artificial cellulose acetate membrane. In the next step, the permeation of the API was measured on the TR146 buccal cell line under in vitro conditions [97–99].

4.3.11.1. Permeation test across artificial membrane

The permeation of CTZ was studied in the Enhancer Cell across an artificial cellulose acetate membrane (Whatman®, SN:WHA10404106, pore size 0.2 µm, surface 2.54 cm^2) [100]. The size of the measured films was 1 × 1 cm. The films were put on the surface of the membrane and placed into the donor phase, which was 2 mL phosphate buffer (pH = 6.8), modelling saliva. The acceptor phase was also phosphate buffer (pH = 7.4, 300 mL), which

simulated the pH of blood. The test was run in an Erweka DT700 dissolution basket tester at a mixing speed of 100 rpm. Aliquots of 5 mL were analysed at 15, 30, 60, 90, 120, 180 and 240 min with Genesys 10S UV–VIS (Thermo Fisher Scientific, Waltham, MA, USA) UV-spectrophotometry at $\lambda = 207$ nm wavelength.

4.3.11.2. Cell culturing

TR-146 cells (European Collection of Authenticated Cell Cultures Catalogue No: 10032305) were cultured in Dulbecco's modified Eagle's medium with L-glutamine and D-glucose supplemented with 10 v/v % FBS, 3.7 g/L sodium hydrogen carbonate, 1 v/v % non-essential amino acid solution and 100 IU/mL penicillin K, with 100 µg/mL streptomycin sulfate at 37 °C in an atmosphere of 5% CO_2 in plastic cell culture flasks. The cells were routinely maintained by regular passaging. Cells used for our experiments were between passage numbers 20 and 28.

4.3.11.3. In vitro permeation test

For the permeation test, 1×10^5 cells were seeded on ThinCert® PET cell culture inserts with a pore size of 0.4 µm, a pore density of $2 \times 10^6/cm^2$ and a culturing surface of 33.6 mm^2 (Greiner BioOne, Mosonmagyaróvár, Hungary). The culture medium was changed twice per week on the inserts, and the cells were grown for 2 weeks in 24-well plates. A Millicell ERS 1 device was used to measure transepithelial electrical resistance (Merck, Budapest, Hungary). After 2 weeks, only inserts with a resistance value over 130 $\Omega \cdot cm^2$ were used, which correlates well with previous reports [101]. The films were cut to equal weight with an overall CTZ content of 0.35 mg.

Each film was dissolved in Hank's balanced salt solution (HBSS) with pH = 7.2 before the experiment. The cell culture medium was removed from the inserts, and 400 µL of the dissolved films was added to the apical compartment (AC) and 1000 µL to the basolateral compartment (BC). After 30, 60 and 90 min, 2×100 µL of solution was removed from the wells after gentle mixing. The removed volume was replaced with HBSS. The samples were placed into UV-Star 96-well plates (Greiner BioOne, Mosonmagyaróvár, Hungary), and their absorbance was measured at 248 nm with a Multiskan Go microplate reader (Thermo-Fisher, Waltham, MA, USA). Apparent permeability (P_{app}) was calculated as: $(\Delta Q/\Delta t) \times (1/(0.336\ cm^2 \times C_0))$, where C_0 is the concentration of the tested compound

(mg/mL); $\Delta Q/\Delta t$ is the rate of permeability of the tested compound ((mg/mL)·s $^{-1}$) between 60 and 90 min.

4.3.12. Statistical analysis

The collected data were analyzed with the factorial ANOVA method by Tibco Statistica v13.4.0.14 (Statsoft, Tulsa, OK, USA) software. The results were evaluated by mixed two-level and three-level factorial designs. The equations describe the relationship between the two factors (x_1–concentration of SA and x_2–concentration of GLY) and the five optimalization parameters (y_1–thickness; y_2–breaking hardness, y_3–mucoadhesion force, y_4–surface free energy, and y_5–dissolution). The low, zero and high levels of the factors are shown in **Table 2**.

Table 2. The values of factors for mixed two-level and three-level factorial designs

Total Polymer Concentration (%)	Factors	Low Level	Zero Level	High Level
2%	Concentration of SA (x_1)	1	-	1.33
	Concentration of GLY (x_2)	1	3	5
3%	Concentration of SA (x_1)	1.5	-	2
	Concentration of GLY (x_2)	1	3	5

The significance test of breaking hardness and in vitro mucoadhesivity was evaluated with Microsoft Excel (version 15, Redmond, Washington, USA) as software. A Two-Sample T-Test was applied. In all cases, the samples were compared to the composition without CTZ. In each case, we used a significance level $p < 0.05$. Significance is labelled as ns = ns = $p \geq 0.05$; * = $p < 0.05$.

In the stability study (breaking hardness, in vitro mucoadhesivity) the samples were compared to the freshly prepared sample (0 month). The apparent permeability values of the films were analysed with the Kruskal–Wallis test with Dunn's test as post hoc test. In each case, we used a significance level of $p < 0.05$. Significance is labelled as ns = $p \geq 0.05$; * = $p < 0.05$; ** = $p < 0.01$.

5. RESULTS AND DISCUSSION

5.1. Thickness and breaking hardness measurement

Figure 5. shows that the thickness (y_1) of different compositions of films rises depending on the polymer and GLY concentration. The 3% polymer films are thicker than the 2% ones; therefore, the polymer concentration can increase the thickness of the films due to the higher amount of polymer (Equations 3–6). The type of polymer does not influence thickness notably; films with a higher amount of SA (without HPMC) are thicker than the 2:1 SA and HPMC films. The 2:1 SA and HPMC films are thicker than the 1:1 SA and HPMC films, but there is no significant difference between the SA films without HPMC (Samples 4-6, 10-12 and 7-9, 13-15), 1:1 SA and HPMC (Samples 19–24 and 31–36) and 2:1 SA and HPMC films (Samples 25–30 and 37–42). It can be seen that the C_{SA} (x_1) coefficients were very low in all cases, and they were not significant. C_{GLY} (x_2) can also influence thickness, and this was statistically significant ($p < 0.05$) in all cases. According to *Gao and et al.*, GLY possesses a water retention effect, so GLY can enhance the distance of bonding; therefore, the thickness of the films can be increased [102]. CTZ can also enhance thickness, which can be explained by the fact that CTZ increases the dry matter content of the films. In the **Table 3.** it can be found the thickness and breaking hardness of films.

Thickness of the films:

$$y_1 = 138.9 + 40.53\,x_2 + 3.94 \cdot x_2^2 + 5.69 \cdot x_1\,x_2 \quad \text{(2\% polymer films containing CTZ)} \quad (3)$$

$$R^2 = 0.9218$$

$$y_1 = 168.02 + 4.59 \cdot x_1 + 54.89 \cdot x_2 + 17.43 \cdot x_1\,x_2^2 \quad \text{(3\% polymer films containing CTZ)} \quad (4)$$

$$R^2 = 0.9784$$

$$y_1 = 116.12 + 1.66 \cdot x_1 + 46.98 \cdot x_2 - 4.47 \cdot x_1 \cdot x_2 \quad \text{(2\% polymer films without CTZ)} \quad (5)$$

$$R^2 = 0.9461$$

$$y_1 = 145.45 + 2.85 \cdot x_1 + 54.95 \cdot x_2 + 7.7 \cdot x_1 \cdot x_2 \quad \text{(3\% polymer films without CTZ)} \quad (6)$$

$$R^2 = 0.9972$$

According to *Paolicelli et al.*, GLY can make the film elastic, soft, and flexible. In my work, GLY was found to decrease the breaking hardness (y_2) of films [103]. This observation is due to the fact that GLY can interact with other components of films (CTZ, SA, and HPMC), typically in the form of hydrogen bonds, and retains water. In addition, GLY can enhance the bonding distance, so films with a high GLY concentration can break more easily.

Table 3. Mechanical properties of the polymer films

Samples	Thickness (µm)	Breaking hardness (N)	Samples	Thickness (µm)	Breaking hardness (N)
1	67.45 ± 8.53	116.95 ± 2.11	25	81.50 ± 6.66	18.15 ± 1.45
2	99.34 ± 10.38	161.33 ± 2.34	26	86.74 ± 6.34	27.37 ± 0.28
3	212.43 ± 4.92	180.18 ± 1.51	27	105.31 ± 8.18	12.85 ± 2.37
4	98.29 ± 6.38	142.34 ± 3.32	28	146.00 ± 6.06	14.56 ± 2.18
5	135.66 ± 9.86	110.52 ± 1.31	29	166.52 ± 3.87	9.10 ± 1.91
6	199.33 ± 7.53	66.78 ± 1.16	30	179.19 ± 4.99	16.92 ± 1.46
7	106.63 ± 8.42	178.00 ± 3.78	31	93.53 ± 6.35	8.53 ± 0.57
8	123.12 ± 3.36	126.43 ± 2.56	32	125.29 ± 5.56	28.06 ± 3.76
9	177.38 ± 6.92	107.61 ± 2.24	33	146.22 ± 5.91	11.39 ± 0.91
10	105.23 ± 5.18	158.54 ± 1.91	34	164.79 ± 5.88	26.47 ± 1.42
11	148.03 ± 13.88	144.56 ± 2.06	35	188.03 ± 2.71	4.58 ± 0.37
12	212.32 ± 3.43	113.45 ± 1.44	36	200.22 ± 8.14	16.28 ± 2.92
13	158.05 ± 4.34	195.45 ± 2.72	37	87.23 ± 1.26	17.96 ± 1.52
14	194.14 ± 2.97	153.62 ± 2.56	38	102.00 ± 2.71	32.68 ± 3.03
15	253.17 ± 11.30	142.34 ± 2.79	39	145.12 ± 3.46	23.47 ± 2.49
16	not measured	164.74 ± 2.15	40	169.20 ± 2.49	27.68 ± 3.65
17	not measured	166.33 ± 2.01	41	212.55 ± 9.98	16.96 ± 1.95
18	not measured	168.28 ± 2.26	42	246.65 ± 5.51	20.75 ± 0.22
19	56.25 ± 8.54	5.61 ± 0.01	43	not measured	33.19 ± 3.49
20	104.75 ± 7.27	13.89 ± 0.92	44	not measured	41.80 ± 5.05
21	128.00 + 7.7	6.07 ± 1.07	45	not measured	31.39 ± 1.16
22	142.32 ± 8.52	9.90 ± 1.19	46	not measured	13.17 ± 0.18
23	159.14 ± 6.32	5.50 ± 1.95	47	not measured	38.17 ± 1.70
24	174.43 ± 6.02	6.33 ± 0.75	48	not measured	24.61 ± 2.86

The average values of breaking hardness of films (14.82 N and 9.55 N) were found to be lower in the case of 2% polymer concentration than in the case of 3% (25.32 N and 13.81 N). The total polymer increases breaking hardness because it can form a cohesive, strong, stable structure in the films due to the bonding of polymer chains. Moreover, the results show that a higher amount of SA (x_1) (Samples 25–30 and Samples 37–42) can result in a stronger structure compared to an equal amount of the polymer. This is shown by the value of the coefficients x_1 shown in (Equations 7–10), which is positive in all cases and statistically significant in two cases (Equations 9 and 10). It is possible that SA can create stronger and a larger number of bonds with CTZ than HPMC can with CTZ and itself. Another finding is that 3% polymer films have larger strengths than 2% polymer films.

Finally, it can be said that 2% polymer films with lower c_{SA} (Samples 19–24) have low breaking hardness (less than 10 N), and these films break easily. This property is not acceptable from the aspect of application. The other film compositions have high breaking

hardness and can be used properly for buccal application because they do not break from the force of the finger.

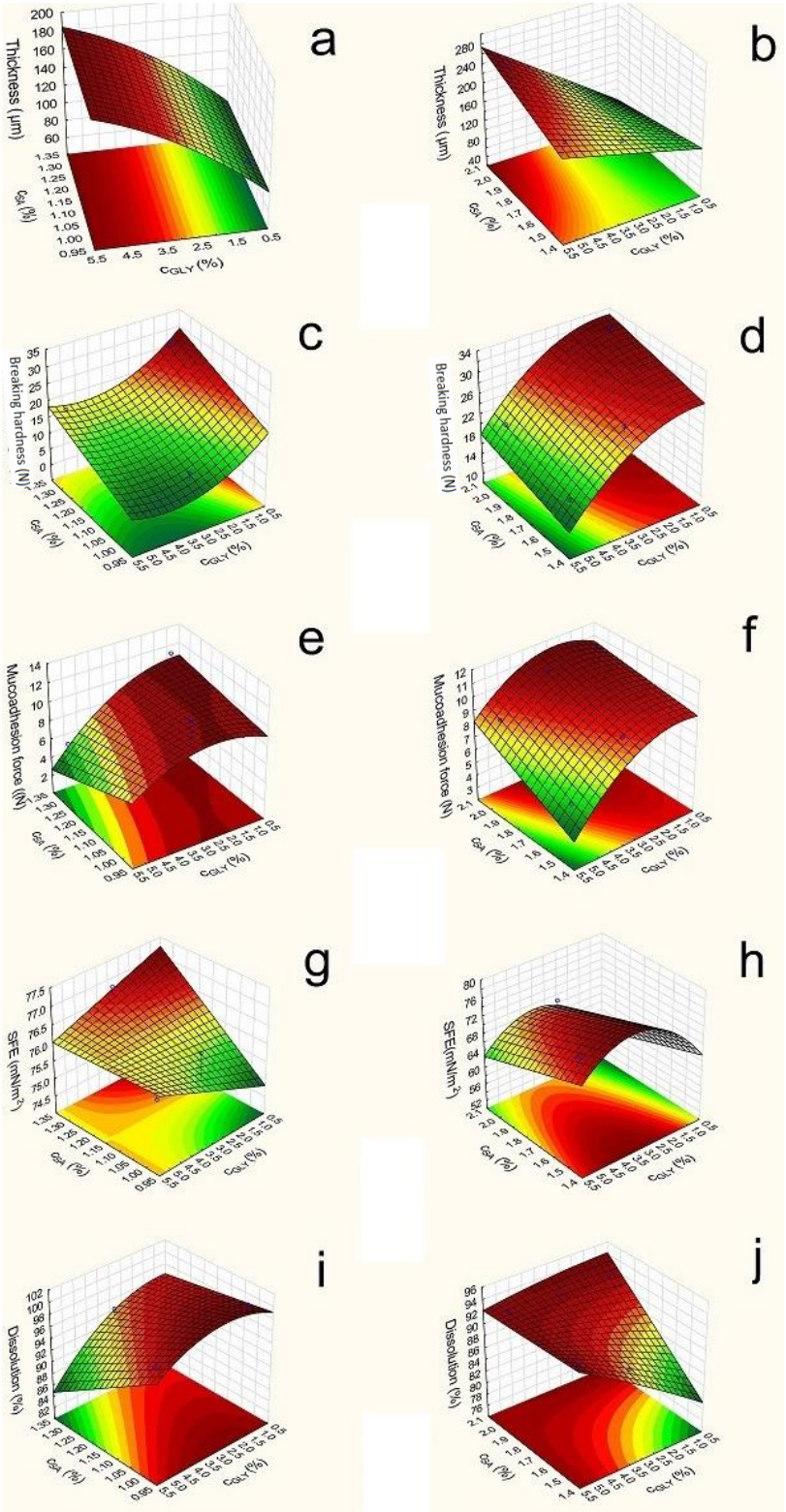

Figure 5. Response surfaces of polymer films containing CTZ (**left** - 2%; **right** - 3% polymer)
(**a**, **b**): Film thickness; (**c**, **d**): Breaking hardness; (**e**, **f**): Mucoadhesion force; (**g**, **h**): Surface free energy; (**i**, **j**): Dissolution

The data and **Figure 5.** show that, in the 2% polymer films, SA and GLY have a significant effect. The SA concentration can increase breaking hardness, but GLY has a reverse effect on breaking hardness; it can decrease the breaking hardness of the films. A similar effect can be observed in the 3% polymer films, but the effect of GLY is not significant. Equations 7–10 are given below for the different compositions. The significant parameters are marked with red letters.

Breaking hardness:

$y_2 = 14.82 + 4.79 \cdot x_1 - 4.50 \cdot x_2 - 1.95 \cdot x_2^2$ (2% polymer films containing CTZ) (7)

$R^2 = 0.9218$

$y_2 = 25.32 + 1.72 \cdot x_1 - 5.93 \cdot x_2 + 1.32 \cdot x_2^2$ (3% polymer films containing CTZ) (8)

$R^2 = 0.9784$

$y_2 = 9.55 + 3.81 \cdot x_1 - 2.29 \cdot x_2 - 2.24 \cdot x_1 \cdot x_2$ (2% polymer films without CTZ) (9)

$R^2 = 0.9955$

$y_2 = 13.81 + 5.66 \cdot x_1 - 1.24 \cdot x_2 + 2.70 \cdot x_2^2 + 0.73 \cdot x_1 \cdot x_2$ (3% polymer films without CTZ) (10)

$R^2 = 0.9979$

5.2. In vitro mucoadhesivity measurement

The mucoadhesion of the prepared films is presented in **Figure 6**. The CTZ-free films had high mucoadhesion force values, most of them more than 10 N and some samples above 15 N (Samples 3, 4, 7, 19, 21, 31, 33, 37, 39). The CTZ-containing samples had significantly lower mucoadhesion force, so CTZ decreases the mucoadhesion of polymer films, possibly due to the interaction between the carboxylic groups of SA, HPMC and CTZ molecules, thus fewer groups are able to bind to the mucin. These samples have moderate mucoadhesion, but they can be used for a buccal drug delivery system because this lower force is enough for buccal mucoadhesion. The increasing amount of polymers increased mucoadhesion due to the higher number of free binding groups in the system, which can bind to the mucin of the buccal mucous.

GLY can influence mucoadhesion force. The increasing amount of GLY decreased mucoadhesion force, probably because of the hydrogen bond which can be formed between GLY and the film-forming polymers, and also due to the fact that no binding is formed with the chains of mucin because of the lower number of free chains in the polymer.

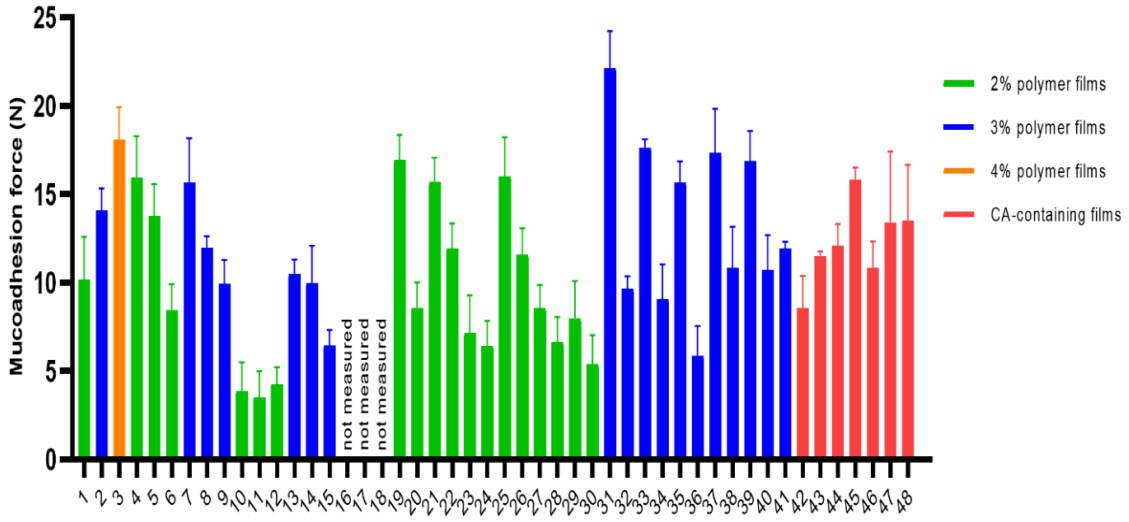

Figure 6. Mucoadhesion force of the prepared films

During statistical analysis, the mucoadhesion force of films of all compositions (CTZ-free and CTZ-containing) was found to be decreased significantly by GLY. Similarly, SA also decreased it in the CTZ-free films because SA has moderate mucoadhesion force, while HPMC has higher one, so a greater HPMC concentration can cause higher mucoadhesion in the films. The reason for this effect can probably be the interaction between the functional groups of SA and CTZ, thus SA will have fewer groups left capable of binding to the mucin (**Figure 5.**) as it can be stated in the FT-IR and in the Raman measurements as well. Equations 11-14 can be found below.

Mucoadhesion force:

$y_3=8.41-2.09\cdot x_2-1.01\cdot x_1\cdot x_2$ (2% polymer films containing CTZ) (11)

$R^2=0.6133$

$y_3=9.10+0.92\cdot x_1-1.53\cdot x_2+0.58\ x_2^2+0.39\cdot x_1\cdot x_2$ (3% polymer films containing CTZ) (12)

$R^2=0.9981$

$y_3=18.96-1.21\cdot x_1-4.47\cdot x_2+0.44\cdot x_1\cdot x_2$ (2% polymer films without CTZ) (13)

$R^2=0.8408$

$y_3=23.82-1.53\cdot x_1-2.96\cdot x_2$ (3% polymer films without CTZ) (14)

$R^2=0.9120$

5.3. Contact angle measurement and surface free energy (SFE) calculation

The SFEs (y_4) of the polymer films are presented in **Table 4**. This measurement is very important and critical from the aspect of applying this pharmaceutical dosage form

because the saliva has to spread on the surface of the films extensively in order for mucoadhesion to develop.

The CTZ-free films exhibited medium SFE 51.99 mN/m and 57.81 mN/m average values (Equations (15) and (16)), while the CTZ-containing films have significantly higher SFE, the average value was 69 and 76.11 (Equations 15 and 16), so CTZ raises the SFE of films, particularly the polar part of SFE. CTZ-containing films also show significantly higher polarity, which may be caused by the carboxylic group of the CTZ molecule. From these results, it can be concluded that an extended conformer of CTZ can be found in the prepared films [80]. Contact angle showed lower values in the CTZ-containing films. The SFE of CTZ-free films changed particularly as a function of increasing GLY concentration (x_2) and only slightly as a function of the SA concentration (x_1). This observation was not true for the CTZ films because in those films, the SFEs had roughly constant values independently of the concentration of GLY and polymer concentration (**Figure 5.**).

Table 4. SFE (γ^{tot}) values of polymer films

Samples	γ^{tot} (mN/m)	γ^{d} (mN/m)	γ^{p} (mN/m)	Polarity (%)
19	49.59	32.54	17.05	34.38
20	74.88	38.85	36.03	48.12
21	51.65	36.34	15.31	29.64
22	76.33	37.44	38.89	50.95
23	62.60	36.35	26.25	41.93
24	75.72	35.60	40.12	52.98
25	53.56	32.28	21.29	39.75
26	76.86	39.17	37.69	49.04
27	66.21	31.85	34.36	51.90
28	76.89	40.57	36.32	47.24
29	63.23	28.15	35.08	55.48
30	75.98	38.26	37.73	49.66
31	54.32	33.12	21.20	39.03
32	68.61	38.80	29.87	43.54
33	57.36	36.21	21.15	36.87
34	73.78	35.14	38.65	52.39
35	50.84	33.59	17.25	33.93
36	73.72	36.07	37.65	51.07
37	47.99	33.56	14.43	30.07
38	61.05	35.11	25.93	42.47
39	48.72	31.61	17.11	35.12
40	71.73	37.12	34.61	48.25
41	52.68	36.01	16.67	31.64
42	65.12	38.40	26.72	41.03

During the next step of the statistical analysis, SFE was determined in the different compositions of films. In 2% polymer films with and without CTZ, SFE is increased by SA and GLY, while in films with 3% polymer API and without API, SFE is reduced by SA. See Equations 15-18 below.

Surface free energy:

$y_5 = 76.11 + 0.46 \cdot x_1 + 0.375 \cdot x_2^2 - 0.43 \cdot x_1 \cdot x_2$ (2% polymer films containing CTZ) (15)

$R^2 = 0.9638$

$y_5 = 69.00 - 3.04 \cdot x_1 + 2.30 \cdot x_2 + 2.82 \cdot x_2^2$ (3% polymer films containing CTZ) (16)

$R^2 = 0.9054$

$y_5 = 57.81 + 3.19 \cdot x_1 + 5.67 \cdot x_2 + 0.84 \cdot x_2^2$ (2% polymer films without CTZ) (17)

$R^2 = 0.7854$

$y_5 = 51.99 - 2.19 \cdot x_1 + 2.04 \cdot x_1 \cdot x_2$ (3% polymer films without CTZ) (18)

$R^2 = 0.7237$

5.4. FT-IR spectroscopy

The polymer films were examined with FT-IR spectroscopy to identify the interactions between the components of the films. According to *Paczkowsa et al.*, the carboxyl group of CTZ can be explored at 1739 cm^{-1} in FT-IR spectra (**Figure 6.**) [104]. In the spectra of the API, this peak can be separated sharply. However, in the spectra of the films, this peak is shifted and disappears, depending on the concentration of the polymer. In the 2% polymer films, the CTZ peak is shifted towards the larger wavenumber, but the intensity of the peak is smaller than in the case of the raw material. In case of the 3% polymer films, the peak disappears completely, which means that interactions can develop between CTZ and the SA and HPMC in the films. The carboxyl group of CTZ can be found at 1739 cm^{-1}, so it can be asserted that hydrogen bondings are created between SA, HPMC, and the carboxylic group of CTZ. Due to the low polymer concentration, the films have fewer OH groups of SA and HPMC, which can create hydrogen bonds, so, in this case, the peak is only slightly shifted. However, the 3% polymer films have more OH groups, thus more hydrogen bonds can be created, which can cause a more remarkable structure change, so the peak can disappear completely.

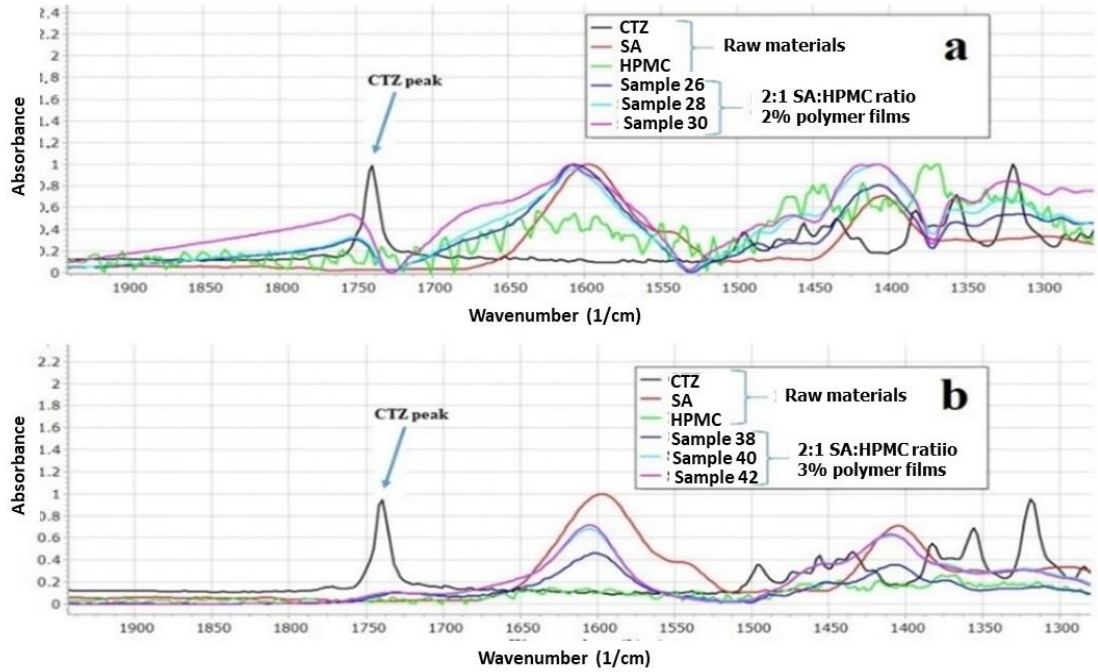

Figure 6. Individual FT-IR spectra of SA, HPMC, CTZ, and prepared films (**a**): 2% polymer films and (**b**): 3% polymer films

Moreover, a spectral peak can be found at 2384 cm^{-1}; this is the stretching vibration of the N-H group of CTZ [105]. In both 2% and 3% concentration polymer films, this peak disappears regardless of the GLY concentration. This observation can suggest that in the films interaction may develop between the N-H-group of CTZ and the other excipients of films. A peak of SA appears at 2937 cm^{-1} [106]. This peak belongs to the C-H stretching vibration. In the polymer films, this peak is shifted to a larger wavenumber and merges with the GLY peak. With these findings, the FT-IR results sufficiently demonstrated the interactions that can occur in the films. The results of Raman spectroscopy also confirm these interactions.

5.5. RAMAN spectroscopy

The Raman spectra of raw materials can be seen in **Figure 7**. Based on the comparison of the spectra of the components, a CTZ peak was chosen at 1598.15 cm^{-1}. It is assigned to the C-C stretchings in the phenyl and chlorophenyl groups in the chemical structure of CTZ [103]. This sharp peak was chosen for the chemical mapping profile because it characterizes the API individually.

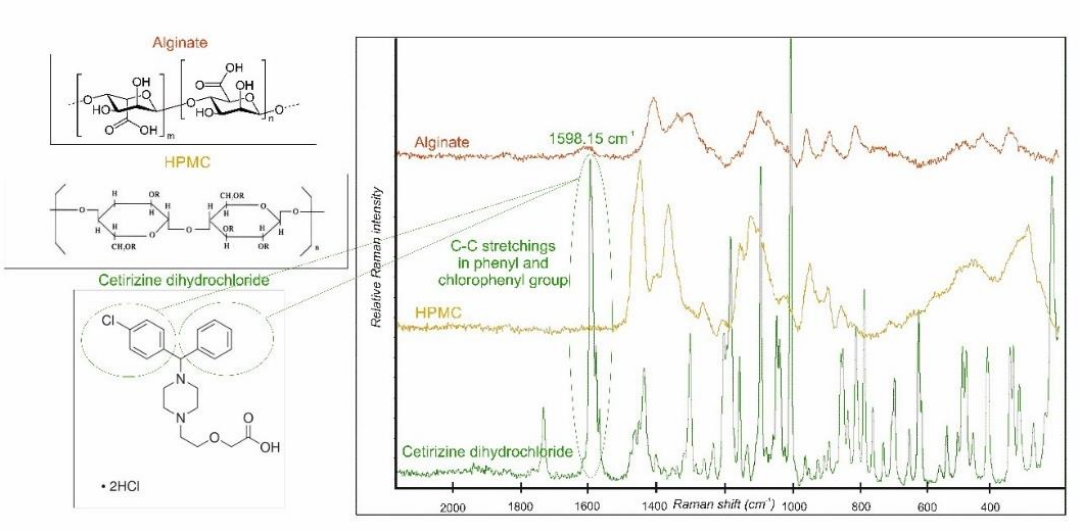

Figure 7. Individual Raman spectra of SA, HPMC and CTZ

Chemical maps are shown in **Figure 8**. The distribution of CTZ was homogeneous in the polymer films with different GLY contents. The warm (red and orange) colors indicate a greater API content in the samples. In the film with 1% GLY content, the API can be in crystalline agglomerates (yellow, orange spots) in the samples. In the other two cases, especially in the case of the sample containing 3% GLY, the color distribution of the maps is very smooth. It means a possible molecular disperse distribution of the API in the film. As a conclusion, the water-soluble API is in a dissolved form in the films because a higher GLY concentration also means higher water content due to the moisturizing property of GLY. This property of the films can be disadvantageous because it can cause the physical instability of the samples. Besides, higher GLY concentrations can be harmful during the mucoadhesion of buccal films because GLY reduces the amount of mucoadhesive polymer chains which are able to bind.

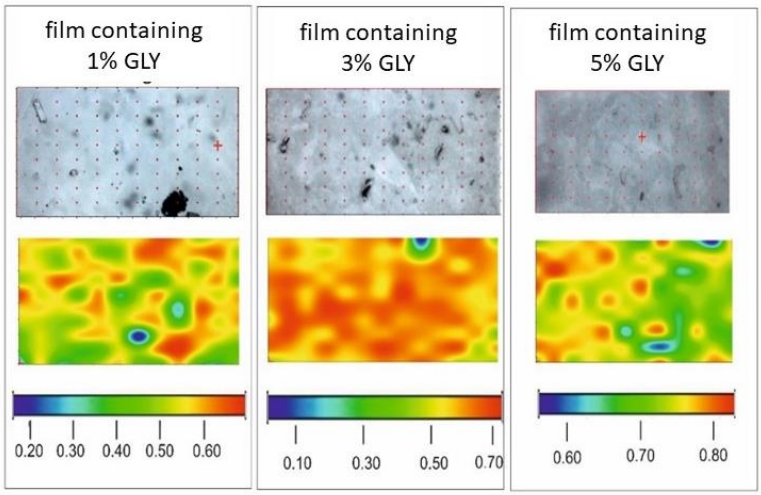

Figure 8. Chemical mapping of films with different GLY contents

5.6. Thermoanalytical measurement (thermogravimetric analyses (TGA), differential scanning calorimetry (DSC))

In **Figure 9.** the TGA and DSC curves of the raw materials can be seen. The TGA curves in **Figure 9.** show that the mass loss of the film-forming agent is 11.84% until 180 °C, and 47.56% until 500 °C. The decomposition process starts from 75 °C. For GLY, the mass loss is almost similar until 180 °C, but it is more than 86% until 500 °C. The mass loss curve of CTZ reveals that decomposition starts above 200 °C, so CTZ can be said to be a thermostable API.

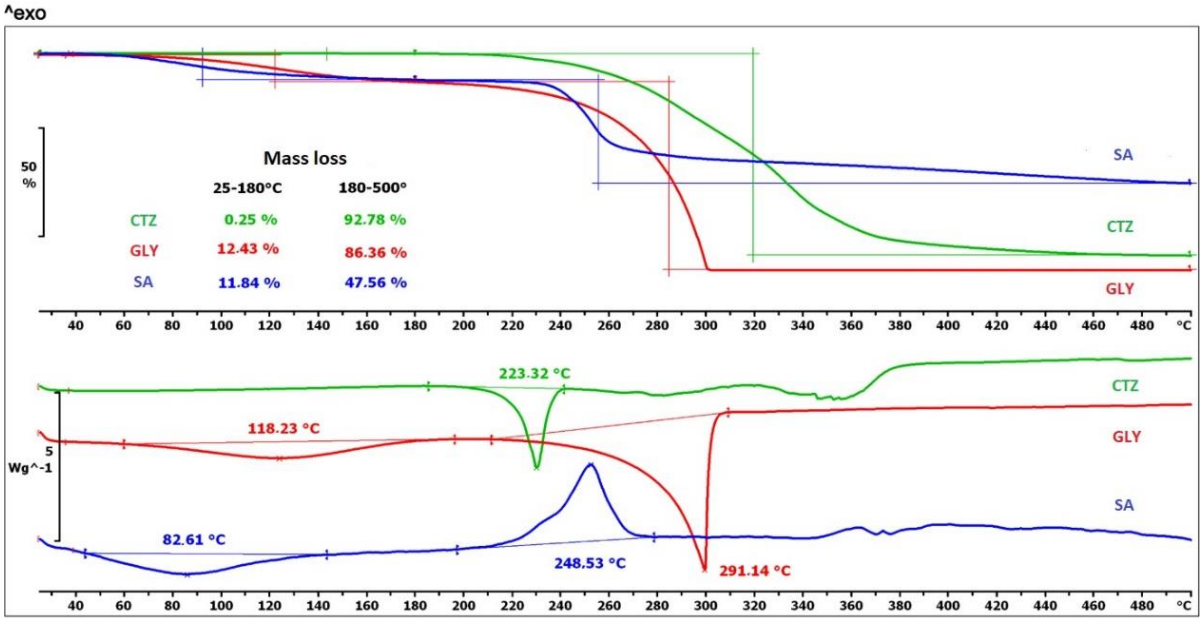

Figure 9. Thermal properties of raw materials as shown by TGA and DSC curves

The DSC curve of SA shows an endothermic peak from 40 °C to 150 °C and an exothermic peak is visible from 200 °C to 280 °C. For GLY, 2 peaks can also be detected. The first peak appears at 118.23 °C, it is an endothermic peak. The second peak starts from 215 °C and ends at 320 °C. This peak indicates the decomposition of GLY. The decomposition of CTZ starts after the melting point, which can be seen at 223.32 °C, followed by the general decomposition of CTZ.

After the examination of the excipients, we wished to investigate the behaviour of the prepared films and explore the interaction between the excipients. The results of the thermal behaviour of films can be found in **Figure 10.,** which shows the thermoanalytical curves of 3% polymer films. The decomposition of buccal films can take place in two steps. In the first step (until 180 °C), it is visible that films with the lowest GLY concentration (Sample 10) (it is not visible in **Figure 10.**) have the lowest mass loss, which can be

explained by the lower water content of films with low GLY concentration. In the case of larger GLY and SA concentrations, which result in a higher water content, there is no significant difference in the mass loss of Samples 11-15. **In Figure 10.**, the same observations can be made in the case of the second step of the decomposition process, but the mass loss values of the films with different compositions were higher, ranging from 62% to 70%.

Two characteristic peaks of SA can be seen in the DSC curves of films with different compositions (**Figure 10.**). The first peak shifted towards the higher temperature with increasing GLY concentration. This observation revealed a moderate interaction between the components of the films, which could indicate the presence of hydrogen bonds, which was also confirmed by the results of the FT-IR spectroscopy measurements. The exothermic peak of the DSC curves also showed a shift with increasing GLY concentration, the peak moved towards the lower temperature. This relationship was also observed in the case of films with 2 and 3% SA concentration.

In summary, it can be said that the decomposition processes usually started at 70 °C, so the polymer films can be considered thermally stable up to this temperature.

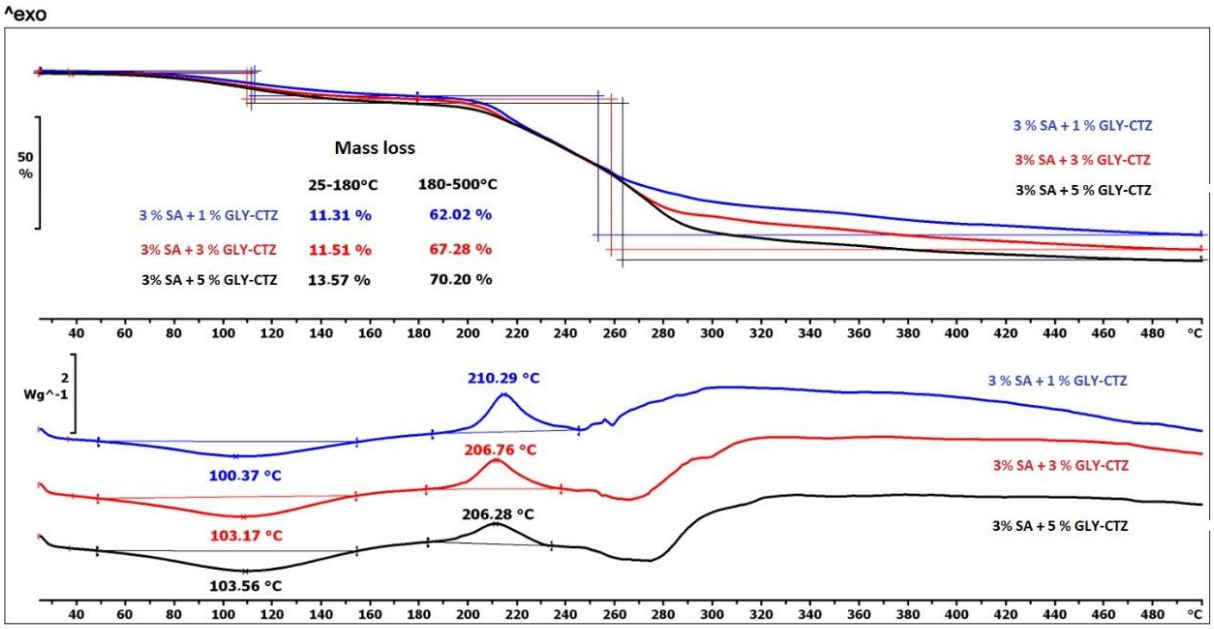

Figure 10. Thermal properties of the 3% polymer films as shown by TGA and DSC curves

5.7. Dissolution test

The dissolution study is one of the most important dosage form tests. The results of the dissolution study of the films with 2% and 3% polymer concentrations are shown in **Figure 10**. During the whole test (120 min), the total amount of CTZ dissolved from the different compositions of the films.

In the first 20 min, almost 100% of the API can dissolve from the films with 2% polymer concentration (**Figure 10/a**). CTZ can dissolve from the thinner polymer layer faster than from thicker films, and on the other hand, in the case of thinner films, HPMC is able to dissolve more easily. Films with a lower SA concentration have faster API dissolution, which can be slowed down by GLY. When the SA and GLY concentrations were increased, dissolution became slower in the case of 3% polymer concentration in the first 20 min (Equation 20), the API cannot be released fully; 65% to 96% of the API dissolved from the different film compositions. It is noteworthy in the figure that, at the beginning of the test (first 5 min), the API dissolved faster from the films with equal polymer concentration. The reason for this is that in the case of 3% polymer concentration a stable, cohesive structure is formed between the chains of the polymers, GLY and API, as visible from the thickness and hardness tests and also supported by FT-IR spectroscopy measurement, therefore, GLY cannot affect dissolution significantly. Compared to 2% films, the effect of GLY is less than expected in 3% films.

When the dissolved drug was investigated after 20 min with a statistical analysis, it can be seen that in the 2% polymer films cSA (x1) can decrease it, while in the 3% films cSA can enhance it. GLY concentration (x2) can increase the dissolution rate when a high SA concentration is applied (Equation 20) (**Figure 10**.). Equations (19) and (20) can be observed below.

Dissolution:

$y_5 = 95.66 - 3.1 \cdot x_1 - 2.89 \cdot x_2 + 0.97 \cdot x_2^2 - 1.55 \cdot x_1 \cdot x_2$ (2% polymer films containing CTZ) (19)

$R^2 = 0.9671$

$y_5 = 89.85 + 2.54 \cdot x_1 + 2.40 \cdot x_2 + 0.12 \cdot x_2^2 - 2.29 \cdot x_1 \cdot x_2$ (3% polymer films containing CTZ) (20)

$R^2 = 0.9996$

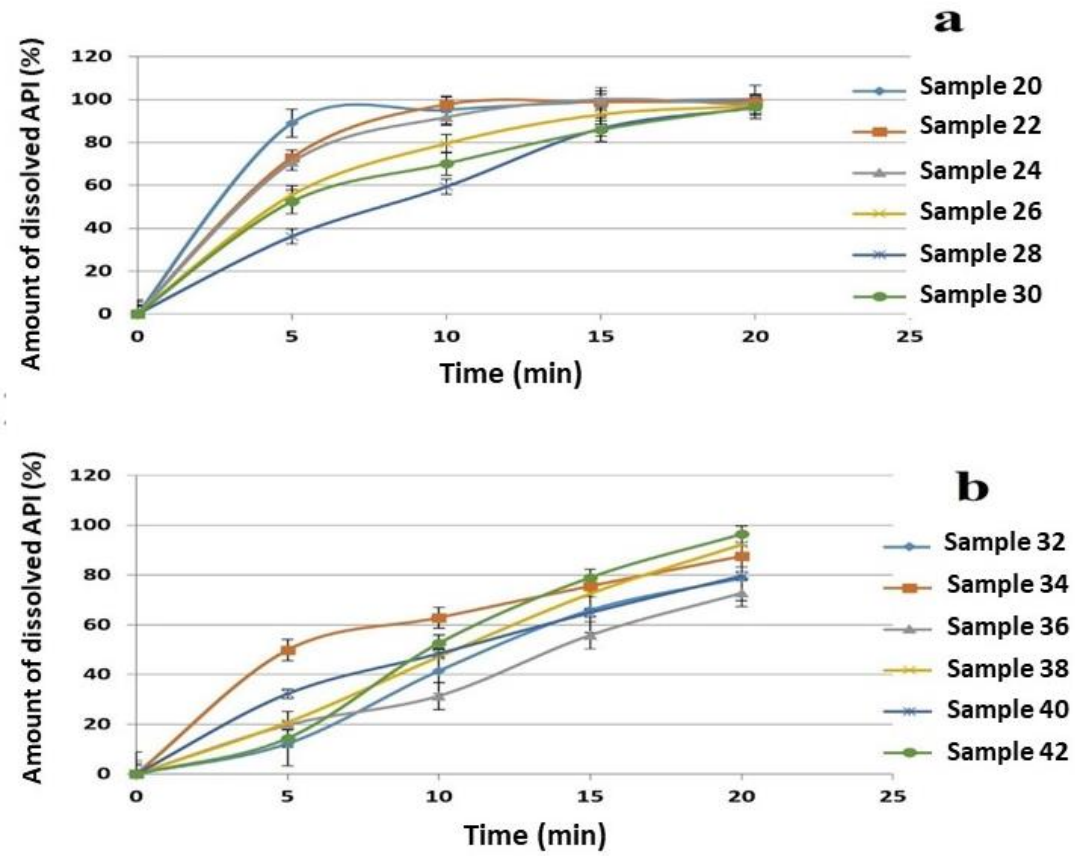

Figure 10. Dissolution curves of the prepared films in the first 20 minutes
(**a**: 2% polymer films, **b**: 3% polymer films)

5.8. Stability test

5.8.1. Breaking hardness measurement

The results of the breaking hardness measurements are presented in **Figure 11**. The changes in the extent of the breaking hardness of the films during the 6-month period are marked in different colours. Breaking hardness decreased for every composition during the period. At the beginning of the investigation, the breaking hardness of the films containing CA was higher than that of the films without CA. At the same time, in the case of CA-containing films (Samples 43, 44, 45, 46, 47, 48,) the decrease in breaking hardness was higher than without CA (Samples 13, 14, 32, 34, 38, 40). As the GLY concentration increased, the breaking hardness of the films decreased. During storage, GLY can decompose, which can cause the decrease in the breaking hardness of the films, and due to this fact, the water content of the films also decreases. This assumption is also supported by the results of the FT-IR measurements. Because of these facts, it can be said that the films that do not contain CA and contain a low GLY amount have adequate stability in terms of breaking hardness (Samples 13, 32, 38).

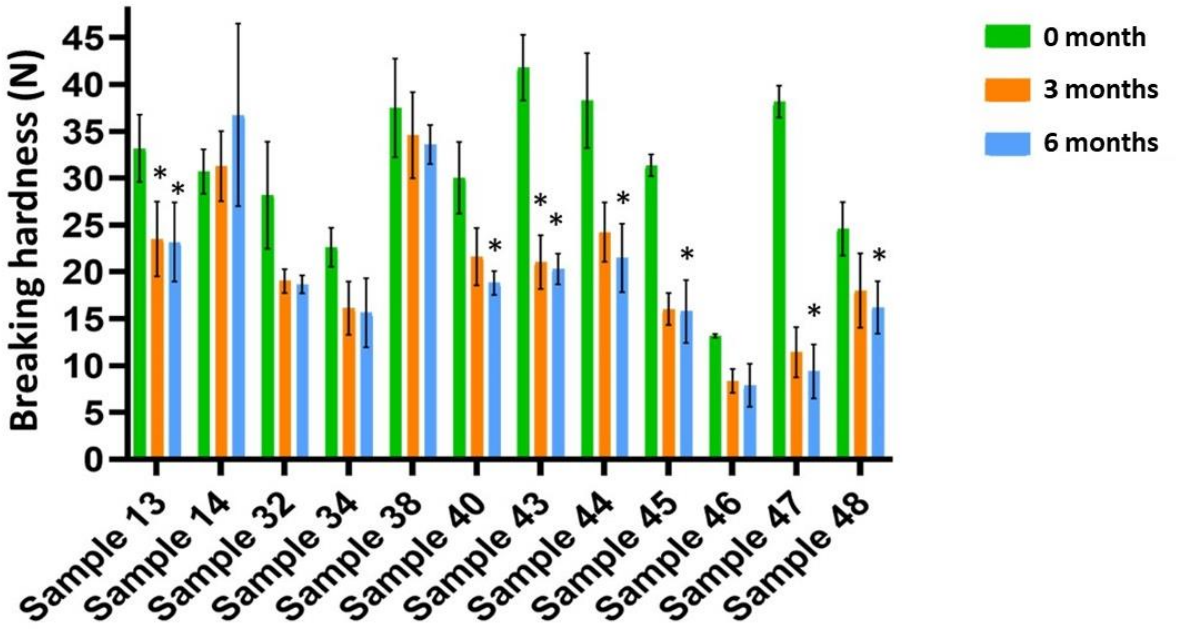

Figure 11. Breaking hardness of the prepared films (Samples 43, 44, 45, 46, 47, 48 contain CA) (* $p < 0.05$; $n = 6$). The samples were compared to the freshly prepared sample (0 month).

5.8.2. In vitro mucoadhesivity measurement

Figure 12. shows the mucoadhesivity of the films with different colours at different times. As can be seen, mucoadhesion force increased for almost every sample during the 6-month period. This is a positive fact because it means that the films can connect to the buccal mucosa in a stronger way after storage time. This phenomenon can probably be explained by the fact that more free chains are formed during storage, so carboxyl and hydroxyl groups can connect to the oligosaccharide chain of mucin on the buccal mucosa.

Films without HPMC showed a higher rise in mucoadhesion force compared with the films without HPMC (Samples 13, 14, 43, 44), so it can be said that HPMC can enhance the stability of the films. Moreover, these results suggest that the films containing CA have higher in vitro mucoadhesion force, especially in the case of the six-month samples, than the films without CA. The GLY concentration can also influence the mucoadhesivity of films. Films with a higher GLY concentration may cause lower growth and growth rate in mucoadhesivity. This observation may be due to the fact that high amounts of GLY can build in the polymer film structure better, therefore during storage fewer chains are free which are able to bind to the mucin of the buccal mucosa.

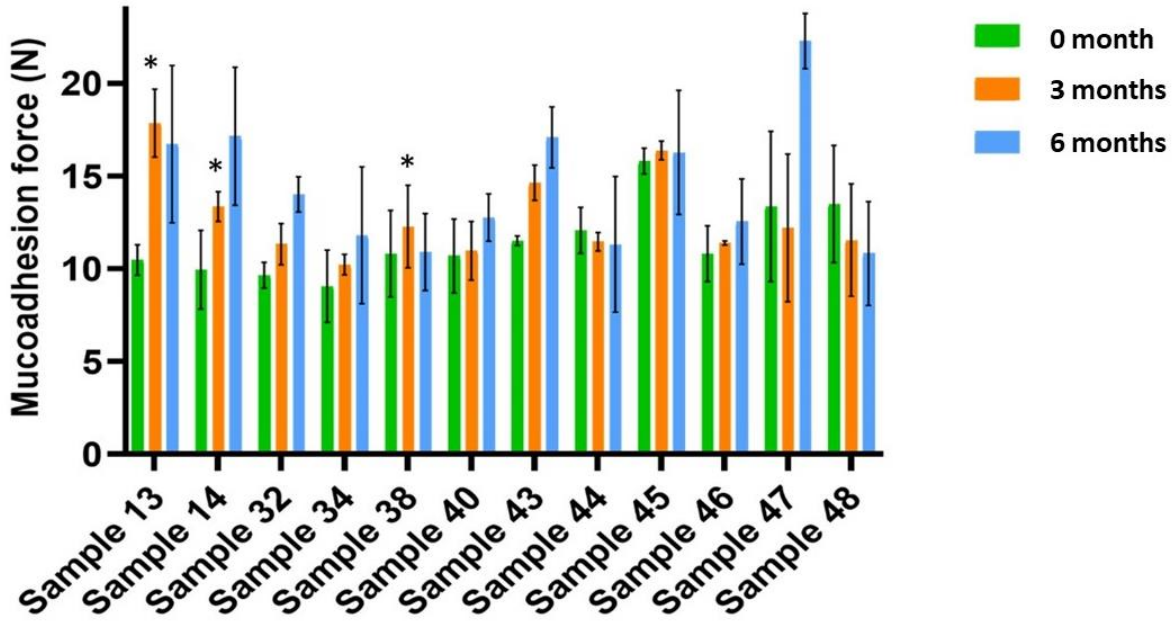

Figure 12. Mucoadhesivity of the prepared films (Samples 43, 44, 45, 46, 47, 48 contain CA)

(* $p < 0.05$; $n = 6$). The samples were compared to the freshly prepared sample (0 months).

5.8.3. Active agent content

Figure 13. shows the results of the change in content during 6 months of storage. As expected, a decrease can be observed for each sample under the forced condition during storage. The reductions in the amount of the API were higher at the beginning of the investigation (between 0 month and 3 months), while later (between 3 months and 6 months), the changes were smaller. The changes were larger for films containing CA, so it can be concluded that CA can decrease the stability of films. GLY can also enhance the decomposition of the API. It was found that films with a larger amount of GLY had a lower amount of API after 6 months than films with a low amount of GLY, so higher GLY concentrations in the films can also reduce film stability. The reason for this is that films with a high GLY concentration have a higher water content because of the water retention effect of GLY, and a higher water content can increase decomposition. As can be seen, Sample 13 and Sample 32 can preserve the required amount of the API (higher than 85%) after 6 months, while Sample 38, 45, 47 can preserve it after 3 months.

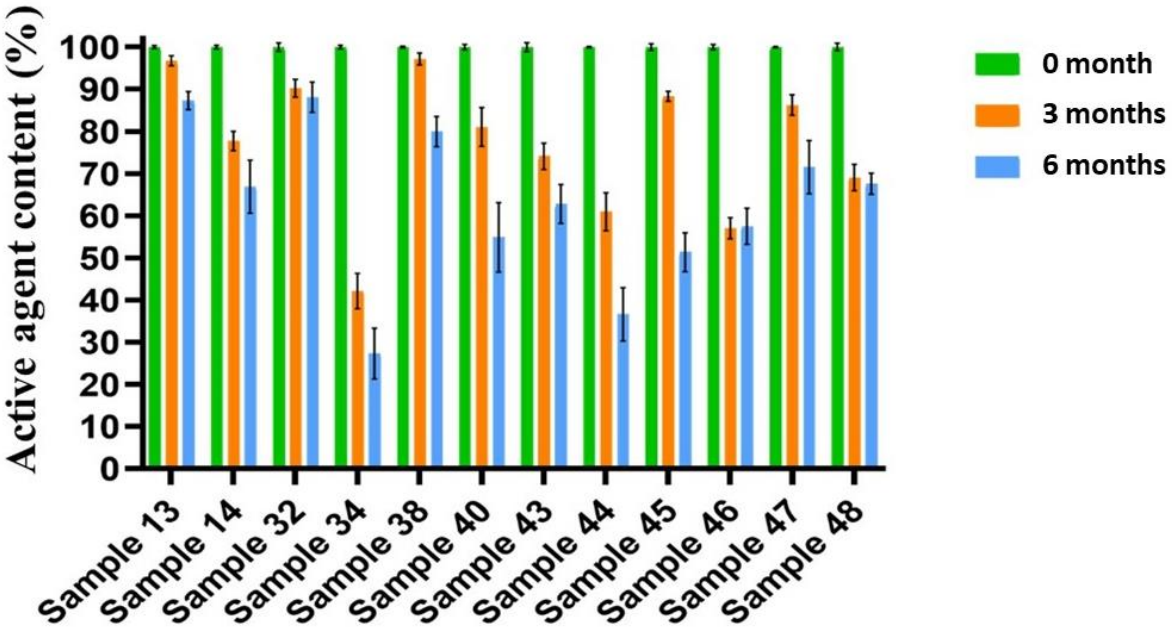

Figure 13. API content for different films during accelerated stability study (Samples 43, 44, 45, 46, 47, 48 contain CA) (n = 6).

5.8.4. FT-IR spectroscopy

In **Figure 14.**, the FT-IR spectra of the films can be seen. Part „A" of **Figure 14**. shows the film composition with the largest amount of API (Sample 13) after six months, while in the bottom figure the film composition with the least amount of API is presented (Sample 46). As can be seen, the carboxyl group of CTZ can be detected at 1739 cm^{-1} in the FT-IR spectrum. In the spectrum of CTZ as a raw material, this peak can be sharply distinguished. However, in the films, this peak is shifted to the higher wavenumbers. In case of Sample 13 (Part „A" of **Figure 14.**), the CTZ peak is shifted towards a higher wavenumber, but the intensity of the peak is smaller than in the case of the raw material. In Part „B" of **Figure 14.**, for Sample 46, the peak disappears completely after sixth months, which shows that the amount of the API decreased because of the forced condition during storage, and hydrogen bonds are formed between SA, HPMC and the carboxylic group of CTZ, which can cause more remarkable structural changes.

A spectral peak can be found at 2384 cm^{-1}, it shows the stretching vibration of the N-H group of CTZ. This peak disappears in every sample, regardless of the GLY concentration. This observation may suggest that interactions develop in the films between the N-H-group of CTZ and the other components of the films. Overall, it can be stated that the decomposition of the API is greater in CA-containing films than in the ones without CA. Moreover, interactions can occur between the components of the films.

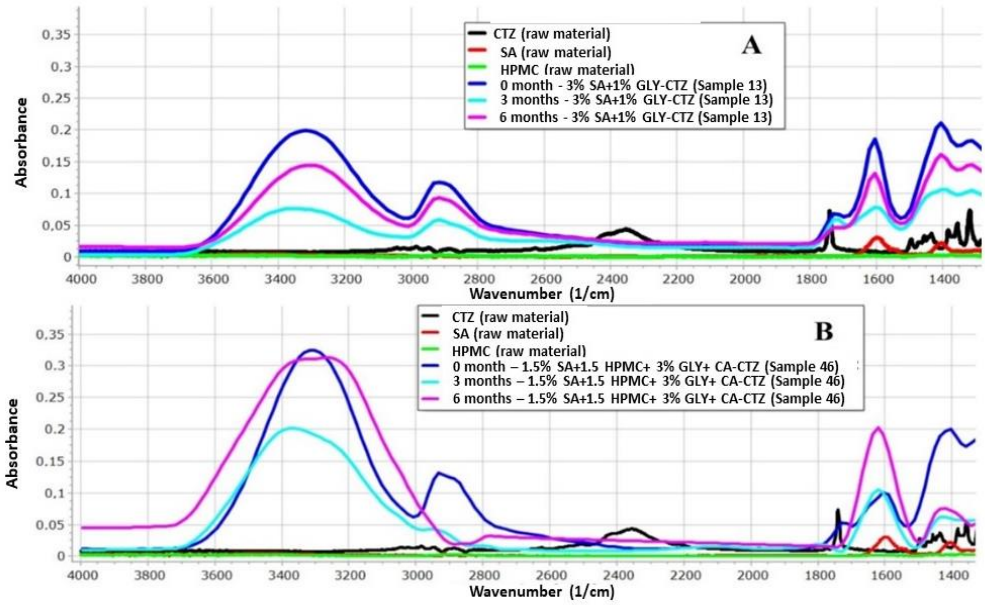

Figure 14. Results of the FT-IR spectra of the prepared films (Part „A" Sample 13, Part „B" Sample 46)

5.9. Cell viability test

The TR-146 cells were treated with the dissolved films, in the concentration of 0.35 mg/mL CTZ in HBSS as a solvent. **Table 5.** shows the results of the cell viability test according to flow cytometry stained with propidium iodide. It can be seen that some formulations had a high impact on cell viability. Samples 34 and 47 were below 40%. However, Samples 14, 32 and 48 had almost no cytotoxic effect. The other samples had a cell viability value between 55 and 87%.

Table 5. Cell viability of the prepared films according to flow cytometry. The experiment was carried out in triplicate. (Samples 43, 44, 45, 46, 47, 48 contain CA)

Samples	Cell viability compared to control (%)
13	67.1 ± 2.7
14	92.8 ± 0.4
32	99.3 ± 0.8
34	33.6 ± 0.7
38	87.2 ± 0.5
40	56.4 ± 4.6
43	78.7 ± 0.6
44	56.3 ± 1.0
45	55.9 ± 0.2
46	87.7 ± 0.1
47	17.4 ± 0.3
48	91.3 ± 1.5
Triton X	0.2 ± 0.1

Cellular transport experiments were performed only with Samples 13, 14, 32, 38, 43, 46 and 48, which had cell viability values over 60%. The direct cytotoxicity of CTZ is not well-published. *Majumder et al.* have identified that, in a concentration of 400 µM, mouse macrophage RAW 264.7 and mouse myoblast C2C12 cell lines showed only ~50% and ~60% cell viability, respectively [107]. For human lymphocytes, it was described that a concentration of 200 µg/mL reduced cell viability to 50% [108]. In our cytotoxicity and cell viability experiments, the concentration of CTZ was higher, 744 µM actually.

5.10. Permeation test

5.10.1. Permeation test across artificial membrane

Figure 15. shows the results of the permeation test across an artificial cellulose membrane. From most compositions, more than 40% of the API can permeate to the acceptor compartment. The SA concentration can influence the amount of the permeated API. A higher amount of the API can permeate to the acceptor compartment from the films with a higher SA concentration than from the ones with a lower SA concentration. This correlation is shown in **Figure 15.**, where Sample 13 (black curve) has a higher permeation rate than the comparable samples (Sample 32—green curve, Sample 38—brown curve). The same correlation can be observed for Sample 14 (red curve) and Sample 40 (blue curve). Furthermore, it can also be stated that the GLY concentration did not influence the permeation rate and speed of the API. These results can be considered good because the entire amount of the permeated API can have an effect compared to per os tablets because of the first-pass effect of the liver.

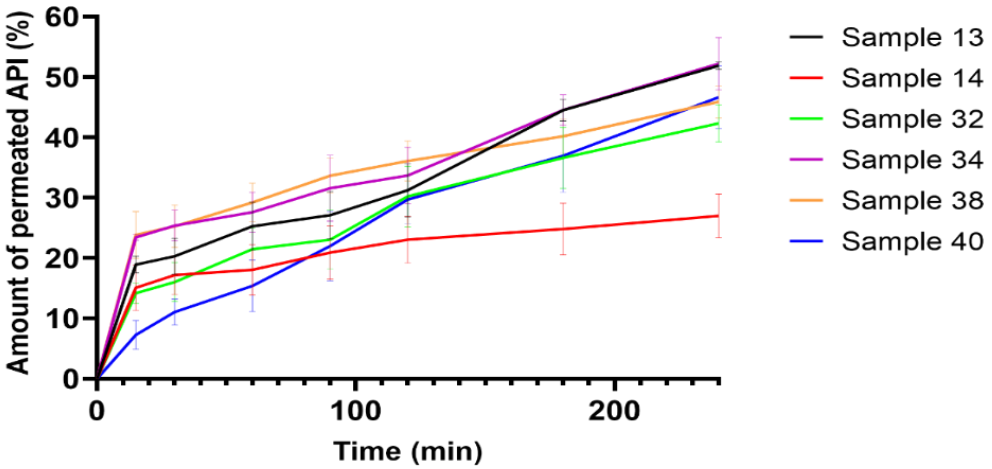

Figure 15. Permeation curves of polymer films on artificial membrane (n = 6)

5.10.2. In vitro permeation test

TR-146 cells are an accepted model for the in vitro testing of buccal absorption. The prepared films were dissolved in HBSS, and their cellular transports were observed for 90 minutes. As shown in **Figure 16.**, Sample 43 had exceptionally high permeation, while Sample 48 had the lowest value. The presence of CA had no direct effect on cellular transport. Moreover, films with HPMC content had smaller permeability. A significant difference was found only between Sample 43 and Sample 48. (*= $p < 0.05$)

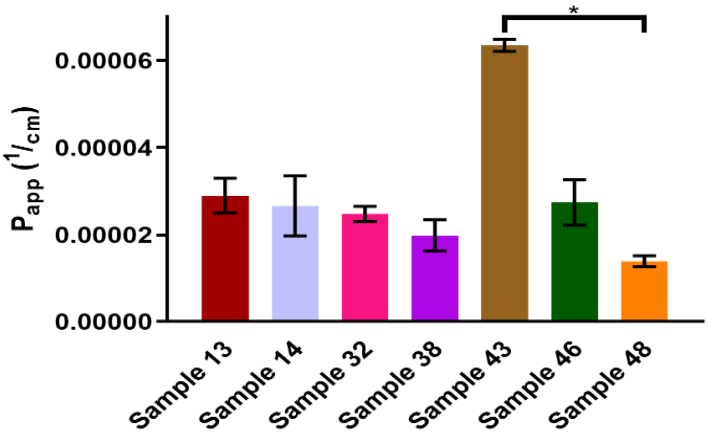

Figure 16. Apparent permeability values of prepared films calculated from the permeability rate of CTZ between 60 and 90 min. Each film was investigated in three separate parallel cell culture inserts (n=3).

As can be seen in **Figure 17.**, most films had a linear transport rate through the cells between 30 and 90 minutes. With the exception of Sample 43, all films had a faster transport rate in the first 30 minutes, after which the transport slowed. The dissolution and the transport of CTZ from all films were stable, with no observed dose dumping.

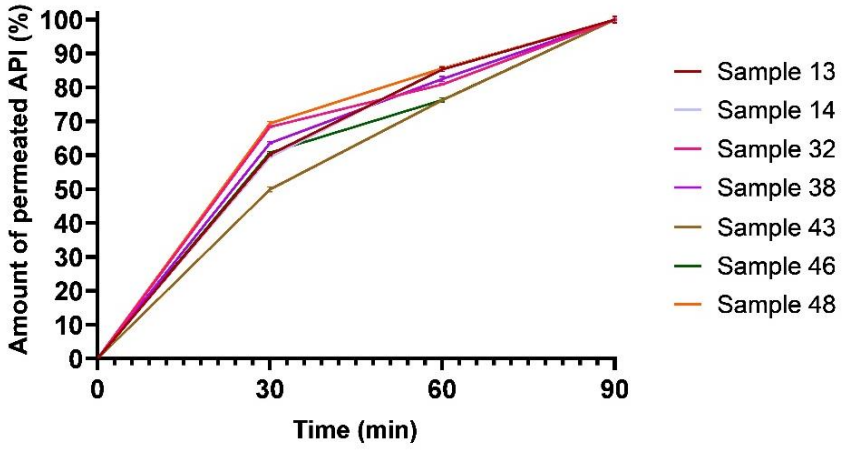

Figure 17. Transported CTZ-time curves of buccal films on the TR-146 cell line. Each film was investigated in three separate, parallel cell culture inserts. (n=3)

6. SUMMARY

In my research work, I focused on the development of buccal film as a potential drug delivery system in allergy. I used SA as a novel film-forming agent to prepare buccal films. First, I studied the film-forming ability of SA without API. To learn about the properties of SA-based films, I incorporated CTZ as an API in the polymer film matrix with other excipients. I characterized the prepared films with several methods to get to know the films in depth. I investigated the physical properties of the films, such as thickness, breaking hardness, in vitro mucoadhesivity, contact angle and surface free energy. I also studied the chemical behavior of the films with FT-IR, RAMAN spectroscopy and thermoanalytical measurements (TGA, DSC). I tested the release of API from the films and the permeation of API both across artificial membrane and on buccal cell line (TR146). I also obtained information about the cell viability of the films with a cytotoxicity test. Finally, I learned information about the stability of my films, which is important from the point of view of transport, storage and application. Based on the results, it can be said that I formulated buccal polymer films with CTZ successfully. The mechanical properties of the films can be changed within a wide range. SA, GLY and CTZ can increase the breaking hardness of films. SA enhances the mucoadhesivity of films, while GLY and CTZ decrease it. A chemical interaction can be found between SA, HPMC, GLY and CTZ, which can be manifested mainly in the form of hydrogen bonds. The API is distributed in the films completely homogeneously and, depending on the GLY concentration, it can be found in the form of crystalline and molecular disperse distribution. The films are stable up to 70 °C, therefore heating is possible during preparation and drying, so the process can be faster. In the first 20 minutes, more than 80% of the API can dissolve from most compositions. More than 40% of the API can permeate from the donor compartment examined through the artificial membrane. The speed of CTZ transport was nearly constant from all compositions, and none of the components influenced it significantly on the buccal cell line. Samples 14, 32, 8, 38, 46 and 48 have appropriate and acceptable cytocompatibility. The stability test revealed that CA, GLY can enhance the reduction of the API significantly. I found some formulations which can preserve the API content according to pharmacopeia expectations (Samples 13, 32, 38, 45, 47) after 3 or 6 months.

Finally, I developed a fast-dissolving polymer film from SA and found a promising (optimal) composition, Sample 32, which is suitable and possible to apply as a buccal drug delivery system.

7. CONCLUSION, NOVELTY AND PRACTICAL USEFULNESS

Buccal mucoadhesive polymer films can allow systemic and local drug application. In addition, they can also be used advantageously in case of swallowing difficulties (allergic reaction or fear of swallowing tablets). They have not played a significant role among our medicines yet, but they will surely do so later. They are not official in the Pharmacopeia, so it is important to study them widely.

Based on the preformulation study, I focused on the film-forming ability of SA and on formulating buccal films with SA, and it can be concluded that:

- SA can create a strong, cohesive structure, and due to these properties, all compositions had very large breaking hardness. The amount of SA can increase the breaking hardness of the films, but GLY reduces it.
- SA has good mucoadhesive properties, while GLY reduces the mucoadhesion force of films.
- By the FT-IR measurement, weak and strong interactions between the different excipients can also be detected. These interactions can typically be identified as hydrogen bondings.
- Thermal analysis can also detect interactions between the different materials in the films. This interaction determines that hydrogen bondings can be created in the films.
- The observation of interaction between the excipients was proved with two different measurements.
- The films are thermally stable up to 70 °C, so it is possible to increase the temperature of preparation to speed up the production.

In the next step of the development, I formulated mucoadhesive polymer films, which contained CTZ as an API. Moreover, I used HPMC to influence the mucoadhesivity of my polymer system. I used several methods to characterize the properties of the films widely.

The main findings from studying the API-containing films are as follows:

- GLY was a statistically significant factor for film thickness and breaking hardness for the 3% total polymer film, but the coefficient also had a high value in the case

of 2% total polymer. CTZ and GLY can increase the thickness and the breaking hardness of the films.

- In the mucoadhesion test, GLY concentration was found to be a significant factor with an inverse relationship. It can decrease mucoadhesion force; therefore, only 1% GLY concentration is recommended. CTZ and GLY can decrease mucoadhesion force, but most of the polymer film samples have sufficient mucoadhesion force.
- CZT-containing films had lower contact angle values, the fluid could spread on the surface of the film. It proves that CTZ-containing films have a hydrophilic surface. CTZ can also increase SFEs because it has hydrophilic molecule groups and can increase the hydrophilicity of the polymer film system. In these cases, no statistically significant factor was found.
- Interactions can be found between the polymer components and the CTZ molecules, which depend on the polymer concentration. In the 3% polymer films, the development of hydrogen bonds is remarkable.
- The distribution of CTZ is homogeneous in the films.
- GLY can influence the form of CTZ in the films. In the films with 1% GLY concentration, CTZ is crystalline, while in the films with 3% and 5% GLY concentration the API is in molecular disperse distribution.
- In 20 min, a higher amount of API can dissolve from the thicker and lower polymer concentration polymer film samples because they are not able to form a stable, strong structure.
- In the film samples with a higher polymer concentration, the polymer molecules and GLY and CTZ can create strong bonds, so CTZ can dissolve more slowly. GLY can decrease the dissolution rate of CTZ.
- Samples with 1% and 3% of GLY proved to be appropriate for application on the buccal mucosa. Samples 13, 14, 32, 34, 38, 40 were found to be promising compositions.

In the last stage of my work, I further investigated the promising compositions and formulated new compositions with CA. Based on the stability test, cytotoxicity and permeation test, the following main findings can be established:

- The breaking hardness of all films decreased during storage. The decrease was higher for CA-containing films.
- During storage, the mucoadhesivity of the films can increase to a great extent, which is a positive fact.
- CA was able to enhance the mucoadhesion force of the films, and the low GLY concentration may also result in beneficial mucoadhesion properties in the films.
- The CA-containing films have smaller drug content, CA enhanced the reduction in the API, and the high GLY concentration can also reduce the amount of the API during storage.
- There are compositions that can preserve the API content according to pharmacopeia expectations (Samples 13, 32, 38, 45, 47) after 3 or 6 months.
- Through the FT-IR investigation, chemical interactions were found in the buccal films between the N-H-group of CTZ and the other components of films, mainly in the form of hydrogen bonds.
- The decomposition of CTZ is greater in CA-containing films than in the ones without CA.
- Interactions can occur between the components of the films, mostly in the form of hydrogen bonds, which can greatly affect the breaking hardness and mucoadhesivity of the films.
- No direct correlation was found between cell viability and the presence of citric acid. Samples 14, 32, 8, 38, 46 and 48 have appropriate and acceptable cytocompatibility.
- More than 40% of CTZ was able to permeate to the acceptor compartment from almost all compositions. The SA concentration can influence the amount of the permeated API. A higher amount of the API was able to permeate to the acceptor compartment from the films with a higher SA concentration than from the ones with a lower SA concentration.
- The speed of transport of CTZ was nearly constant from all compositions; no excipient caused significantly faster or slower permeation. Apparent permeability

was the highest for Sample 43, which was transported across the buccal cell line in a large quantity.

- CA did not enhance the permeation rate of CTZ in the films, but high alginate content resulted in relatively high permeability.
- HPMC seemed to decrease apparent permeability.
- Sample 32 (1.5% SA + 1.5% HPMC + 1% GLY) demonstrated the best stability, cell viability and permeability properties, so this composition is recommended for application on the buccal mucosa.

The novelties of my research work are the following:

- Films were investigated extensively, which, in addition to the examination of the usual physical parameters, also focused on chemical analyses, as well as the dissolution and passage of the API through cells, biocompatibility examination and stability study.
- Chemical interactions can be found between the components of films, which are mostly hydrogen bonds, and it was demonstrated that these interactions can determine and influence the physical properties of the films as well as the release of the API, so the use of analytical methods during development is unavoidable and indispensable.
- The amount of GLY does not only affect the physical properties and stability of the films (among many parameters), but can also influence the chemical form of the API in the films.
- Although CA can increase the permeation of the API, its application in films is not recommended as it greatly reduces the stability of the films.
- The investigation of polymer films was successfully performed on the TR146 buccal cell line in order to model, under in vitro conditions, the amount of the API that passed through the cells, which is able to exert an effect immediately after entering the systemic circulation. The transport of the API from the buccal films through the cells was linear and a sufficient amount passed through, more than 60% in 30 minutes.

8. REFERENCES

[1] A.M. Avachat, K.N. Gujar, K.V. Wagh, Development and evaluation of tamarind seed xyloglucan-based mucoadhesive buccal films of rizatriptan benzoate, Carbohydr Polym. 91 (2013) 537–542. https://doi.org/10.1016/j.carbpol.2012.08.062.

[2] A. Göbel, J.B. da Silva, M. Cook, J. Breitkreutz, Development of buccal film formulations and their mucoadhesive performance in biomimetic models, Int. J. Pharm. 610 (2021) 121233. https://doi.org/10.1016/j.ijpharm.2021.121233.

[3] V. Hearnden, V. Sankar, K. Hull, D.V. Juras, M. Greenberg, A.R. Kerr, P.B. Lockhart, L.L. Patton, S. Porter, M.H. Thornhill, New developments and opportunities in oral mucosal drug delivery for local and systemic disease, Adv. Drug Deliv. Rev. 64 (2012) 16–28. https://doi.org/10.1016/j.addr.2011.02.008.

[4] V. Gibaja, L. Javot, J. Tournebize, P. Gillet, Données récentes de pharmacosurveillance du fentanyl d'action rapide : alerte sur le mésusage, Therapies. 76 (2021) 165. https://doi.org/10.1016/j.therap.2021.01.017.

[5] H. Koradia, K. Chaudhari, Formulation of unidirectional buccal tablet of Mirtazapine: An in vitro and ex vivo evaluation, J. Drug Deliv. Sci. Technol. 43 (2018) 233–242. https://doi.org/10.1016/j.jddst.2017.10.012.

[6] G.K. Eleftheriadis, P.K. Monou, N. Bouropoulos, J. Boetker, J. Rantanen, J. Jacobsen, I.S. Vizirianakis, D.G. Fatouros, Fabrication of Mucoadhesive Buccal Films for Local Administration of Ketoprofen and Lidocaine Hydrochloride by Combining Fused Deposition Modeling and Inkjet Printing, J. Pharm. Sci. 109 (2020) 2757–2766. https://doi.org/10.1016/j.xphs.2020.05.022.

[7] S. Khan, J.S. Boateng, J. Mitchell, V. Trivedi, Formulation, Characterisation and Stabilisation of Buccal Films for Paediatric Drug Delivery of Omeprazole, AAPS PharmSciTech. 16 (2015) 800–810. https://doi.org/10.1208/s12249-014-0268-7.

[8] G. Tejada, M.C. Lamas, L. Svetaz, C.J. Salomón, V.A. Alvarez, D. Leonardi, Effect of drug incorporation technique and polymer combination on the performance of biopolymeric antifungal buccal films, Int. J. Pharm.. 548 (2018) 431–442. https://doi.org/10.1016/j.ijpharm.2018.07.023.

[9] R. Trastullo, A. Abruzzo, B. Saladini, M.C. Gallucci, T. Cerchiara, B. Luppi, F. Bigucci, Design and evaluation of buccal films as paediatric dosage form for transmucosal delivery of ondansetron, Eur. J. Pharm. Biopharm. 105 (2016) 115–121. https://doi.org/10.1016/j.ejpb.2016.05.026.

[10] R. Kumria, A.B. Nair, G. Goomber, S. Gupta, Buccal films of prednisolone with enhanced bioavailability, Drug Deliv. 23 (2016) 471–478. https://doi.org/10.3109/10717544.2014.920058.

[11] J.W. Lee, J.H. Park, J.R. Robinson, Bioadhesive-Based Dosage Forms: The Next Generation, J. Pharm. Sci. 89 (2000) 850–866. https://doi.org/10.1002/1520-6017(200007)89:7<850::AID-JPS2>3.0.CO;2-G.

[12] L.M.C. Collins, C. Dawes, The Surface Area of the Adult Human Mouth and Thickness of the Salivary Film Covering the Teeth and Oral Mucosa, J Dent Res. 66 (1987) 1300–1302. https://doi.org/10.1177/00220345870660080201.

[13] M. Gottnek, K. Hódi, G. Regdon jr., Szájnyálkahártyán alkalmazható mukoadhezív filmek I. rész: A szájnyálkahártya és a nyál anatómiai, élettani áttekintése, Gyógyszerészet. 57 (2013). 24-31.

[14] J.D. Smart, Lectin-mediated drug delivery in the oral cavity, Adv. Drug Deliv. Rev. 56 (2004) 481–489. https://doi.org/10.1016/j.addr.2003.10.016.

[15] https://thancguide.org/cancer-types/oral/buccal/anatomy/, (n.d.).

[16] J.M. Gu, J.R. Robinson, S.H. Leung, Binding of acrylic polymers to mucin/epithelial surfaces: structure-property relationships, Crit Rev Ther Drug Carrier Syst. 5 (1988) 21–67.

[17] L.A. Tabak, Structure And Function of Human Salivary Mucins, Critical Reviews in Oral Biology & Medicine. 1 (1990) 229–234. https://doi.org/10.1177/10454411900010040201.

[18] M. Gottnek, K. Hódi, G. jr., Szájnyálkahártyán alkalmazható mukoadhezív filmek II. rész: Bukkális mukoadhezív filmekben alkalmazott hatóanyagok. Mukoadhezív filmek előállítása és vizsgálata, Gyógyszerészet. 57 (2013). 69-75.

[19] I. Fiebrig, S.E. Harding, A.J. Rowe, S.C. Hyman, S.S. Davis, Transmission electron microscopy studies on pig gastric mucin and its interactions with chitosan, Carbohydr. Polym. 28 (1995) 239–244. https://doi.org/10.1016/0144-8617(95)00105-0.

[20] G. Sandri, M. Ruggeri, S. Rossi, M.C. Bonferoni, B. Vigani, F. Ferrari, (Trans)buccal drug delivery, in: Nanotechnology for Oral Drug Delivery, Elsevier, 2020: pp. 225–250. https://doi.org/10.1016/B978-0-12-818038-9.00013-2.

[21] P. Laurén, H. Paukkonen, T. Lipiäinen, Y. Dong, T. Oksanen, H. Räikkönen, H. Ehlers, P. Laaksonen, M. Yliperttula, T. Laaksonen, Pectin and Mucin Enhance the Bioadhesion of Drug Loaded Nanofibrillated Cellulose Films, Pharm Res. 35 (2018) 145. https://doi.org/10.1007/s11095-018-2428-z.

[22] M.L. Bruschi, S.B. de Souza Ferreira, J. Bassi da Silva, Mucoadhesive and mucus-penetrating polymers for drug delivery, in: Nanotechnology for Oral Drug Delivery, Elsevier, 2020: pp. 77–141. https://doi.org/10.1016/B978-0-12-818038-9.00011-9.

[23] M. Gottnek, Ph.D. Thesis Design and characterization of mucoadhesive hydroxypropyl cellulose oral films, (2017).

[24] J. Smart, The basics and underlying mechanisms of mucoadhesion, Adv. Drug Deliv. Rev. 57 (2005) 1556–1568. https://doi.org/10.1016/j.addr.2005.07.001.

[25] C. Itin, R. Komargodski, A.J. Domb, A. Hoffman, Controlled Delivery of Apomorphine Through Buccal Mucosa, Towards a Noninvasive Administration Method in Parkinson's Disease: A Preclinical Mechanistic Study, J. Pharm. Sci. 109 (2020) 2729–2734. https://doi.org/10.1016/j.xphs.2020.05.017.

[26] B.E. Al-Dhubiab, A.B. Nair, R. Kumria, M. Attimarad, S. Harsha, Development and evaluation of buccal films impregnated with selegiline-loaded nanospheres, Drug Deliv. 23 (2016) 2154–2162. https://doi.org/10.3109/10717544.2014.948644.

[27] M. Orlu, S.R. Ranmal, Y. Sheng, C. Tuleu, P. Seddon, Acceptability of orodispersible films for delivery of medicines to infants and preschool children, Drug Deliv. 24 (2017) 1243–1248. https://doi.org/10.1080/10717544.2017.1370512.

[28] K. Chachlioutaki, E.K. Tzimtzimis, D. Tzetzis, M.-W. Chang, Z. Ahmad, C. Karavasili, D.G. Fatouros, Electrospun Orodispersible Films of Isoniazid for Pediatric Tuberculosis Treatment, Pharmaceutics. 12 (2020) 470. https://doi.org/10.3390/pharmaceutics12050470.

[29] V.F. Patel, F. Liu, M.B. Brown, Advances in oral transmucosal drug delivery, J. Control. Release. 153 (2011) 106–116. https://doi.org/10.1016/j.jconrel.2011.01.027.

[30] A.S. Macedo, P.M. Castro, L. Roque, N.G. Thomé, C.P. Reis, M.E. Pintado, P. Fonte, Novel and revisited approaches in nanoparticle systems for buccal drug delivery, J. Control. Release. 320 (2020) 125–141. https://doi.org/10.1016/j.jconrel.2020.01.006.

[31] A.I. Raafat, G.A. Mahmoud, A.E.-H. Ali, N.A. Badawy, M.F. Elshahawy, In vitro evaluation of mucoadhesive and self-disinfection efficiency of (acrylic acid/polyethylene glycol)-silver nanocomposites for buccal drug delivery, J. Bioact. Compat. Polym. 33 (2018) 95–115. https://doi.org/10.1177/0883911517710665.

[32] M.A. Rogawski, A.H. Heller, Diazepam buccal film for the treatment of acute seizures, Epilepsy & Behavior. 101 (2019) 106537. https://doi.org/10.1016/j.yebeh.2019.106537.

[33] A. Flo, A.C. Calpena, L. Halbaut, E.I. Araya, F. Fernández, B. Clares, Melatonin Delivery: Transdermal and Transbuccal Evaluation in Different Vehicles, Pharm Res. 33 (2016) 1615–1627. https://doi.org/10.1007/s11095-016-1901-9.

[34] R. Kumria, A.B. Nair, G. Goomber, S. Gupta, Buccal films of prednisolone with enhanced bioavailability, Drug Deliv.. 23 (2016) 471–478. https://doi.org/10.3109/10717544.2014.920058.

[35] U.D. Kulkarni, R. Mahalingam, X. Li, I. Pather, B. Jasti, Effect of Experimental Temperature on the Permeation of Model Diffusants Across Porcine Buccal Mucosa, AAPS PharmSciTech. 12 (2011) 579–586. https://doi.org/10.1208/s12249-011-9624-z.

[36] D.R. Serrano, R. Fernandez-Garcia, M. Mele, A.M. Healy, A. Lalatsa, Designing Fast-Dissolving Orodispersible Films of Amphotericin B for Oropharyngeal Candidiasis, Pharmaceutics. 11 (2019) 369. https://doi.org/10.3390/pharmaceutics11080369.

[37] A.B. Nair, R. Kumria, S. Harsha, M. Attimarad, B.E. Al-Dhubiab, I.A. Alhaider, In vitro techniques to evaluate buccal films, J. Control. Release. 166 (2013) 10–21. https://doi.org/10.1016/j.jconrel.2012.11.019.

[38] F. Laffleur, Mucoadhesive polymers for buccal drug delivery, Drug Develop. Ind. Pharm. 40 (2014) 591–598. https://doi.org/10.3109/03639045.2014.892959.

[39] O.C. Okeke, J.S. Boateng, Composite HPMC and sodium alginate based buccal formulations for nicotine replacement therapy, International Journal of Biological Macromolecules. 91 (2016) 31–44. https://doi.org/10.1016/j.ijbiomac.2016.05.079.

[40] A. Kelemen, B. Katona, S. Módra, Z. Aigner, I. Sebe, K. Pintye-Hódi, R. Zelkó, G. Regdon, K. Kristó, Effects of Sucrose Palmitate on the Physico-Chemical and Mucoadhesive Properties of Buccal Films, Molecules. 25 (2020) 5248. https://doi.org/10.3390/molecules25225248.

[41] K.-G.H. Desai, S.R. Mallery, A.S. Holpuch, S.P. Schwendeman, Development and In Vitro-In Vivo Evaluation of Fenretinide-Loaded Oral Mucoadhesive Patches for Site-Specific Chemoprevention of Oral Cancer, Pharm Res. 28 (2011) 2599–2609. https://doi.org/10.1007/s11095-011-0489-3.

[42] M. Montenegro-Nicolini, J.O. Morales, Overview and Future Potential of Buccal Mucoadhesive Films as Drug Delivery Systems for Biologics, AAPS PharmSciTech. 18 (2017) 3–14. https://doi.org/10.1208/s12249-016-0525-z.

[43] J.O. Morales, J.T. McConville, Manufacture and characterization of mucoadhesive buccal films, European J. Pharm. Biopharm. 77 (2011) 187–199. https://doi.org/10.1016/j.ejpb.2010.11.023.

[44] Y.H.-E.Y. Ibrahim, G. Regdon, K. Kristó, A. Kelemen, M.E. Adam, E.I. Hamedelniel, T. Sovány, Design and characterization of chitosan/citrate films as carrier for oral macromolecule delivery, Eur. J. Pharm. Sci. 146 (2020) 105270. https://doi.org/10.1016/j.ejps.2020.105270.

[45] S. Farias, J.S. Boateng, In vitro, ex vivo and in vivo evaluation of taste masked low dose acetylsalicylic acid loaded composite wafers as platforms for buccal administration in geriatric patients with dysphagia, Int. J. Pharm. 589 (2020) 119807. https://doi.org/10.1016/j.ijpharm.2020.119807.

[46] A.M. Ili Balqis, M.A.R. Nor Khaizura, A.R. Russly, Z.A. Nur Hanani, Effects of plasticizers on the physicochemical properties of kappa-carrageenan films extracted from Eucheuma cottonii, International J. Biol. Macromol. 103 (2017) 721–732. https://doi.org/10.1016/j.ijbiomac.2017.05.105.

[47] M. Gottnek, K. Süvegh, K. Pintye-Hódi, G. Regdon, Effects of excipients on the tensile strength, surface properties and free volume of Klucel® free films of pharmaceutical importance, Radiat. Phys. Chem. 89 (2013) 57–63. https://doi.org/10.1016/j.radphyschem.2013.04.017.

[48] A. Miro, I. d'Angelo, A. Nappi, P. La Manna, M. Biondi, L. Mayol, P. Musto, R. Russo, M.I.L. Rotonda, F. Ungaro, F. Quaglia, Engineering poly(ethylene oxide) buccal films with cyclodextrin: A novel role for an old excipient?, Int. J. Pharm. 452 (2013) 283–291. https://doi.org/10.1016/j.ijpharm.2013.05.030.

[49] A. Karagianni, L. Peltonen, Production of Itraconazole Nanocrystal-Based Polymeric Film Formulations for Immediate Drug Release, Pharmaceutics. 12 (2020) 960. https://doi.org/10.3390/pharmaceutics12100960.

[50] L. Wang, Y. Wu, J. Li, H. Qiao, L. Di, Rheological and mucoadhesive properties of polysaccharide from Bletilla striata with potential use in pharmaceutics as bio-adhesive excipient, Int. J. Biol. Macromol. 120 (2018) 529–536. https://doi.org/10.1016/j.ijbiomac.2018.08.127.

[51] K. Pamlényi, K. Kristó, O. Jójárt-Laczkovich, G. Regdon, Formulation and Optimization of Sodium Alginate Polymer Film as a Buccal Mucoadhesive Drug Delivery System Containing Cetirizine Dihydrochloride, Pharmaceutics. 13 (2021) 619. https://doi.org/10.3390/pharmaceutics13050619.

[52] M. Gottnek, K. Hódi, G. Regdon jr., Szájnyálkahártyán alkalmazható mukoadhezív filmek III. rész: Bukkális mukoadhezív filmek esetén alkalmazott polimerek és segédanyagok, Gyógyszerészet, 57 (2013) 274–282.

[53] C. Xiao, H. Liu, Y. Lu, L. Zhang, BLEND FILMS FROM SODIUM ALGINATE AND GELATIN SOLUTIONS, J. Macromol. Sci., Part A. 38 (2001) 317–328. https://doi.org/10.1081/MA-100103352.

[54] S. Galus, A. Lenart, Development and characterization of composite edible films based on sodium alginate and pectin, J. Food Eng. 115 (2013) 459–465. https://doi.org/10.1016/j.jfoodeng.2012.03.006.

[55] J. Kurczewska, Recent Reports on Polysaccharide-Based Materials for Drug Delivery, Polymers. 14 (2022) 4189. https://doi.org/10.3390/polym14194189.

[56] A. Zamboulis, G. Michailidou, I. Koumentakou, D.N. Bikiaris, Polysaccharide 3D Printing for Drug Delivery Applications, Pharmaceutics. 14 (2022) 145. https://doi.org/10.3390/pharmaceutics14010145.

[57] Q. Zhou, H. Kang, M. Bielec, X. Wu, Q. Cheng, W. Wei, H. Dai, Influence of different divalent ions cross-linking sodium alginate-polyacrylamide hydrogels on antibacterial properties and wound healing, Carbohydr. Polym. 197 (2018) 292–304. https://doi.org/10.1016/j.carbpol.2018.05.078.

[58] Z. Li, J. Guo, F. Guan, J. Yin, Q. Yang, S. Zhang, J. Tian, Y. Zhang, M. Ding, W. Wang, Oxidized sodium alginate cross-linked calcium alginate/antarctic krill protein composite fiber for improving

strength and water resistance, Colloids and Surfaces A: Physicochemical and Engineering Aspects. 656 (2023) 130317. https://doi.org/10.1016/j.colsurfa.2022.130317.

[59] P. dos Santos Araújo, G.B. Belini, G.P. Mambrini, F.M. Yamaji, W.R. Waldman, Thermal degradation of calcium and sodium alginate: A greener synthesis towards calcium oxide micro/nanoparticles, International J. Biol. Macromol. 140 (2019) 749–760. https://doi.org/10.1016/j.ijbiomac.2019.08.103.

[60] R. Abka-khajouei, L. Tounsi, N. Shahabi, A.K. Patel, S. Abdelkafi, P. Michaud, Structures, Properties and Applications of Alginates, Marine Drugs. 20 (2022) 364. https://doi.org/10.3390/md20060364.

[61] O.C. Okeke, J.S. Boateng, Nicotine stabilization in composite sodium alginate based wafers and films for nicotine replacement therapy, Carbohydr. Polym. 155 (2017) 78–88. https://doi.org/10.1016/j.carbpol.2016.08.053.

[62] C. Juliano, M. Cossu, P. Pigozzi, G. Rassu, P. Giunchedi, Preparation, In Vitro Characterization and Preliminary In Vivo Evaluation of Buccal Polymeric Films Containing Chlorhexidine, AAPS PharmSciTech. 9 (2008) 1153–1158. https://doi.org/10.1208/s12249-008-9153-6.

[63] H. Daemi, M. Barikani, M. Barmar, Compatible compositions based on aqueous polyurethane dispersions and sodium alginate, Carbohydr Polym. 92 (2013) 490–496. https://doi.org/10.1016/j.carbpol.2012.09.046.

[64] T. Tagami, M. Ando, N. Nagata, E. Goto, N. Yoshimura, T. Takeuchi, T. Noda, T. Ozeki, Fabrication of Naftopidil-Loaded Tablets Using a Semisolid Extrusion-Type 3D Printer and the Characteristics of the Printed Hydrogel and Resulting Tablets, J. Pharm. Sci. 108 (2019) 907–913. https://doi.org/10.1016/j.xphs.2018.08.026.

[65] X.C. Fu, G.P. Wang, W.Q. Liang, M.S.S. Chow, Prediction of drug release from HPMC matrices: effect of physicochemical properties of drug and polymer concentration, J. Control. Release. 95 (2004) 209–216. https://doi.org/10.1016/j.jconrel.2003.11.007.

[66] A. Viridén, B. Wittgren, A. Larsson, Investigation of critical polymer properties for polymer release and swelling of HPMC matrix tablets, Eur. J. Pharm. Sci. 36 (2009) 297–309. https://doi.org/10.1016/j.ejps.2008.10.021.

[67] A. Sosnik, J. das Neves, B. Sarmento, Mucoadhesive polymers in the design of nano-drug delivery systems for administration by non-parenteral routes: A review, Prog. Polym. Sci. 39 (2014) 2030–2075. https://doi.org/10.1016/j.progpolymsci.2014.07.010.

[68] R. Kumria, A.B. Nair, B.E. Al-Dhubiab, Loratidine buccal films for allergic rhinitis: development and evaluation, Drug Dev. Ind. Pharm. 40 (2014) 625–631. https://doi.org/10.3109/03639045.2014.884125.

[69] K.K. Peh, C.F. Wong, Polymeric films as vehicle for buccal delivery: swelling, mechanical, and bioadhesive properties, J Pharm Pharm Sci. 2 (1999) 53–61.

[70] H. Castán, M.A. Ruiz, B. Clares, M.E. Morales, Design, development and characterization of buccal bioadhesive films of Doxepin for treatment of odontalgia, Drug Deliv. 22 (2015) 869–876. https://doi.org/10.3109/10717544.2014.896958.

[71] K. Deshmukh, M. Basheer Ahamed, R.R. Deshmukh, S.K. Khadheer Pasha, P.R. Bhagat, K. Chidambaram, Biopolymer Composites With High Dielectric Performance: Interface Engineering, in: Biopolymer Composites in Electronics, Elsevier, 2017: pp. 27–128. https://doi.org/10.1016/B978-0-12-809261-3.00003-6.

[72] T.H. McConnell, The nature of disease: pathology for the health professions, Lippincott Williams & Wilkins, Baltimore, 2007.

[73] R. Dahl, A. Stender, S. Rak, Specific immunotherapy with SQ standardized grass allergen tablets in asthmatics with rhinoconjunctivitis., Allergy. 61 (2006) 185–190. https://doi.org/10.1111/j.1398-9995.2005.00949.x.

[74] M. Averbeck, C. Gebhardt, F. Emmrich, R. Treudler, J.C. Simon, CME. Immunologic Principles of Allergic Disease, JDDG. 5 (2007) 1015–1027. https://doi.org/10.1111/j.1610-0387.2007.06538.x.

[75] L.M. Wheatley, A. Togias, Allergic Rhinitis, N Engl J Med. 372 (2015) 456–463. https://doi.org/10.1056/NEJMcp1412282.

[76] J.N. Larsen, L. Broge, H. Jacobi, Allergy immunotherapy: the future of allergy treatment, Drug Discov. 21 (2016) 26–37. https://doi.org/10.1016/j.drudis.2015.07.010.

[77] S.T. Holgate, R. Polosa, Treatment strategies for allergy and asthma, Nat Rev Immunol. 8 (2008) 218–230. https://doi.org/10.1038/nri2262.

[78] D. Sharma, G. Singh, D. Kumar, M. Singh, Formulation Development and Evaluation of Fast Disintegrating Tablets of Salbutamol Sulphate, Cetirizine Hydrochloride in Combined Pharmaceutical

Dosage Form: A New Era in Novel Drug Delivery for Pediatrics and Geriatrics, J. Drug Deliv. 2015 (2015) 1–10. https://doi.org/10.1155/2015/640529.

[79] P. Bizikova, M.G. Papich, T. Olivry, Hydroxyzine and cetirizine pharmacokinetics and pharmacodynamics after oral and intravenous administration of hydroxyzine to healthy dogs, Vet. Dermatol. 19 (2008) 348–357. https://doi.org/10.1111/j.1365-3164.2008.00697.x.

[80] G. Plemper van Balen, G. Caron, G. Ermondi, A. Pagliara, T. Grandi, G. Bouchard, R. Fruttero, P. Carrupt, B. Testa, [Lipophilicity Behaviour of the Zwitterionic Antihistamine Cetirizine in Phosphatidylcholine Liposomes/Water Systems], Pharm. Res. 18 (2001) 694–701. https://doi.org/10.1023/A:1011049830615.

[81] B. Testa, A. Pagliara, P.A. Carrupt, The molecular behaviour of cetirizine, Clin. Experim. Allergy. 27 (1997) 13–18. https://doi.org/10.1111/j.1365-2222.1997.tb02578.x.

[82] D.M. Campoli-Richards, M.M.-T. Buckley, A. Fitton, Cetirizine: A Review of its Pharmacological Properties and Clinical Potential in Allergic Rhinitis, Pollen-Induced Asthma, and Chronic Urticaria, Drugs. 40 (1990) 762–781. https://doi.org/10.2165/00003495-199040050-00009.

[83] J. Durda, B. Wedi, V. Martin, K. Breuer, Hyperresponsiveness to antihistamines in spontaneous urticaria and heat urticaria, ALS. 1 (2017) 222–226. https://doi.org/10.5414/ALX01554E.

[84] J.R. May, W.K. Dolen, Management of Allergic Rhinitis: A Review for the Community Pharmacist, Clin.Ther. 39 (2017) 2410–2419. https://doi.org/10.1016/j.clinthera.2017.10.006.

[85] B. Fonseca-Santos, M. Chorilli, An overview of polymeric dosage forms in buccal drug delivery: State of art, design of formulations and their in vivo performance evaluation, Mater. Sci. Eng. C. 86 (2018) 129–143. https://doi.org/10.1016/j.msec.2017.12.022.

[86] J. Xu, S. Strandman, J.X.X. Zhu, J. Barralet, M. Cerruti, Genipin-crosslinked catechol-chitosan mucoadhesive hydrogels for buccal drug delivery, Biomaterials. 37 (2015) 395–404. https://doi.org/10.1016/j.biomaterials.2014.10.024.

[87] M.C. Bonferoni, G. Sandri, S. Rossi, F. Ferrari, S. Gibin, C. Caramella, Chitosan citrate as multifunctional polymer for vaginal delivery, Eur. J. Pharm. Sci. 33 (2008) 166–176. https://doi.org/10.1016/j.ejps.2007.11.004.

[88] A. Kelemen, M. Gottnek, G. Regdon, K. Pintye-Hódi, New equipment for measurement of the force of adhesion of mucoadhesive films, J. Adhes. Sci. Technol. 29 (2015) 1360–1367. https://doi.org/10.1080/01694243.2015.1029059.

[89] K. Pamlényi, G. Regdon, D. Nemes, F. Fenyvesi, I. Bácskay, K. Kristó, Stability, Permeability and Cytotoxicity of Buccal Films in Allergy Treatment, Pharmaceutics. 14 (2022) 1633. https://doi.org/10.3390/pharmaceutics14081633.

[90] K. Pamlényi, K. Kristó, T. Sovány, G. Regdon jr., Development and evaluation of bioadhesive buccal films based on sodium alginate for allergy therapy, Heliyon. 8 (2022) e10364. https://doi.org/10.1016/j.heliyon.2022.e10364.

[91] G. Regdon, A. Kósa, I. Erős, K. Pintye-Hódi, Thermoanalytical behaviour of some coating free films, J Therm Anal Calorim. 89 (2007) 793–797. https://doi.org/10.1007/s10973-006-7566-6.

[92] M. Gottnek, K. Pintye-Hódi, G. Regdon, Tracking of the behaviour of lidocaine base containing hydroxypropylcellulose free films with thermoanalytical method, J Therm Anal Calorim. 120 (2015) 201–208. https://doi.org/10.1007/s10973-015-4407-5.

[93] V.F. Patel, F. Liu, M.B. Brown, Modeling the oral cavity: In vitro and in vivo evaluations of buccal drug delivery systems, J. Control. Release. 161 (2012) 746–756. https://doi.org/10.1016/j.jconrel.2012.05.026.

[94] R. Madhavi B, Buccal Film Drug Delivery System-An Innovative and Emerging Technology, J Mol Pharm Org Process Res. 1 (2013). https://doi.org/10.4172/2329-9053.1000107.

[95] O. González-González, I.O. Ramirez, B.I. Ramirez, P. O'Connell, M.P. Ballesteros, J.J. Torrado, D.R. Serrano, Drug Stability: ICH versus Accelerated Predictive Stability Studies, Pharmaceutics. 14 (2022) 2324. https://doi.org/10.3390/pharmaceutics14112324.

[96] H. Pham Le Khanh, D. Nemes, Á. Rusznyák, Z. Ujhelyi, P. Fehér, F. Fenyvesi, J. Váradi, M. Vecsernyés, I. Bácskay, Comparative Investigation of Cellular Effects of Polyethylene Glycol (PEG) Derivatives, Polymers. 14 (2022) 279. https://doi.org/10.3390/polym14020279.

[97] C. Sander, H.M. Nielsen, J. Jacobsen, Buccal delivery of metformin: TR146 cell culture model evaluating the use of bioadhesive chitosan discs for drug permeability enhancement, Int. J. Pharm. 458 (2013) 254–261. https://doi.org/10.1016/j.ijpharm.2013.10.026.

[98] C. Tetyczka, M. Griesbacher, M. Absenger-Novak, E. Fröhlich, E. Roblegg, Development of nanostructured lipid carriers for intraoral delivery of Domperidone, Int. J. Pharm. 526 (2017) 188–198. https://doi.org/10.1016/j.ijpharm.2017.04.076.

[99] H.M. Nielsen, J.C. Verhoef, M. Ponec, M.R. Rassing, TR146 cells grown on filters as a model of human buccal epithelium: permeability of fluorescein isothiocyanate-labelled dextrans in the presence of sodium glycocholate, J. Control. Release. 60 (1999) 223–233. https://doi.org/10.1016/S0168-3659(99)00081-4.

[100] S. Azarmi, W. Roa, R. Löbenberg, Current perspectives in dissolution testing of conventional and novel dosage forms, Int. J. Pharm. 328 (2007) 12–21. https://doi.org/10.1016/j.ijpharm.2006.10.001.

[101] J. Jacobsen, B. van Deurs, M. Pedersen, M.R. Rassing, TR146 cells grown on filters as a model for human buccal epithelium: I. Morphology, growth, barrier properties, and permeability, Int. J. Pharm. 125 (1995) 165–184. https://doi.org/10.1016/0378-5173(95)00109-V.

[102] W. Gao, P. Liu, X. Li, L. Qiu, H. Hou, B. Cui, The co-plasticization effects of glycerol and small molecular sugars on starch-based nanocomposite films prepared by extrusion blowing, Int. J. Biol. Macromol. 133 (2019) 1175–1181. https://doi.org/10.1016/j.ijbiomac.2019.04.193.

[103] P. Paolicelli, S. Petralito, G. Varani, M. Nardoni, S. Pacelli, L. Di Muzio, J. Tirillò, C. Bartuli, S. Cesa, M.A. Casadei, A. Adrover, Effect of glycerol on the physical and mechanical properties of thin gellan gum films for oral drug delivery, Int. J. Pharm. 547 (2018) 226–234. https://doi.org/10.1016/j.ijpharm.2018.05.046.

[104] M. Paczkowska, M. Mizera, K. Lewandowska, M. Kozak, A. Miklaszewski, J. Cielecka-Piontek, Effects of inclusion of cetirizine hydrochloride in β-cyclodextrin, J Incl Phenom Macrocycl Chem. 91 (2018) 149–159. https://doi.org/10.1007/s10847-018-0808-y.

[105] M.S. Arshad, S. Hassan, A. Hussain, N. Abbas, I. Kucuk, K. Nazari, R. Ali, S. Ramzan, A. Alqahtani, E.G. Andriotis, D.G. Fatouros, M.-W. Chang, Z. Ahmad, Improved transdermal delivery of cetirizine hydrochloride using polymeric microneedles, DARU J Pharm Sci. 27 (2019) 673–681. https://doi.org/10.1007/s40199-019-00301-3.

[106] S. Sellimi, I. Younes, H.B. Ayed, H. Maalej, V. Montero, M. Rinaudo, M. Dahia, T. Mechichi, M. Hajji, M. Nasri, Structural, physicochemical and antioxidant properties of sodium alginate isolated from a Tunisian brown seaweed, Int. J. Biol. Macromol. 72 (2015) 1358–1367. https://doi.org/10.1016/j.ijbiomac.2014.10.016.

[107] J. Majumder, J. Deb, A. Husain, S.S. Jana, P. Dastidar, Cetirizine derived supramolecular topical gel in action: rational design, characterization and in vivo self-delivery application in treating skin allergy in mice, J. Mater. Chem. B. 3 (2015) 6634–6644. https://doi.org/10.1039/C5TB00676G.

[108] A. Salimi, M. Razian, J. Pourahmad, Analysis of Toxicity Effects of Buspirone, Cetirizine and Olanzapine on Human Blood Lymphocytes: in Vitro Model, CCP. 13 (2018) 120–127. https://doi.org/10.2174/1574884713666180516112920.

ACKNOWLEDGEMENTS

I wish to thank **Prof. Dr. Judit Hohmann**, Head of the Doctoral School of Pharmaceutical Sciences and I would like to thank **Prof. Dr. Ildikó Csóka**, Head of the Institute of Pharmaceutical Technology and Regulatory Affairs, for ensuring that I could continue the work I had started as a graduate student.

I would like to express my grateful thanks to my supervisors, **Dr. Katalin Kristó** and **Dr. Géza Regdon Jr.** for their guidance, useful advice, patience, support and their selfless help that I received from them during my Ph.D. work.

I wish to thank **Dr. Tamás Sovány** for his help in the measurements of FT-IR spectroscopy.

I would like to express my thank to **Dr. Orsolya Jójártné Laczkovich** for her advice and help, especially in Raman measurements and evaluations.

I express my kindest gratitude to **Prof. Dr. Ildikó Bácskay** and **Dr. Dániel Nemes**, from the Department of Pharmaceutical Technology, University of Debrecen, for their immense help in the cytotoxicity and in vitro permeability tests during my Ph.D. work.

I wish to especially thank **Prof. Dr. Bruno Sarmento** and **all members of the NTDD (Nanomedicnes & Translational Drug Delivery) research group** for their inspiring help in my studies during Erasmus traineeship in i3S - Instituto de Investigação e Inovação em Saúde Universidade do Porto.

I thank the **members of the first research group**, and **all members of the Institute of Pharmaceutical Technology and Regulatory Affairs** for their help.

My sincere thanks also go to the **Richter Gedeon Talentum Foundation**, Budapest, who provided me with the opportunity to participate in the Ph.D. program.

I express my thanks to **my muse**, **the girl** who got me started in the experimental work and this topic.

Finally, I am especially thankful to **my parents**, **my sister** and **my brothers**, as well as **all members of my family** for their support, tremendous help, their patience, and for ensuring a peaceful background during my studies. I would like to thank **my friends** for their love and tireless support, encouragement, and understanding.

ANNEX

I.

pharmaceutics

MDPI

Article

Formulation and Optimization of Sodium Alginate Polymer Film as a Buccal Mucoadhesive Drug Delivery System Containing Cetirizine Dihydrochloride

Krisztián Pamlényi, Katalin Kristó, Orsolya Jójárt-Laczkovich and Géza Regdon, Jr. *

Institute of Pharmaceutical Technology and Regulatory Affairs, University of Szeged, Eötvös u. 6., H-6720 Szeged, Hungary; pamlenyi.krisztian@szte.hu (K.P.); kristo.katalin@szte.hu (K.K.); jojartne.laczkovich.orsolya@szte.hu (O.J.-L.)

* Correspondence: geza.regdon@pharm.u-szeged.hu or geza.regdon@gmail.com; Tel.: +36-62-545574; Fax: +36-62-545571

Abstract: Currently, pharmaceutical companies are working on innovative methods, processes and products. Oral mucoadhesive systems, such as tablets, gels, and polymer films, are among these possible products. Oral mucoadhesive systems possess many advantages, including the possibility to be applied in swallowing problems. The present study focused on formulating buccal mucoadhesive polymer films and investigating the physical and physical–chemical properties of films. Sodium alginate (SA) and hydroxypropyl methylcellulose (HPMC) were used as film-forming agents, glycerol (GLY) was added as a plasticizer, and cetirizine dihydrochloride (CTZ) was used as an active pharmaceutical ingredient (API). The polymer films were prepared at room temperature with the solvent casting method by mixed two-level and three-level factorial designs. The thickness, tensile strength (hardness), mucoadhesivity, surface free energy (SFE), FTIR, and Raman spectra, as well as the dissolution of the prepared films, were investigated. The investigations showed that GLY can reduce the mucoadhesivity of films, and CTZ can increase the tensile strength of films. The distribution of CTZ proved to be homogeneous in the films. The API could dissolve completely from all the films. We can conclude that polymer films with 1% and 3% GLY concentrations are appropriate to be formulated for application on the buccal mucosa as a drug delivery system.

Keywords: buccal; mucoadhesive; drug delivery system; polymer film; alginate; cetirizine; FTIR; RAMAN mapping; statistical analysis

Citation: Pamlényi, K.; Kristó, K.; Jójárt-Laczkovich, O.; Regdon, G., Jr. Formulation and Optimization of Sodium Alginate Polymer Film as a Buccal Mucoadhesive Drug Delivery System Containing Cetirizine Dihydrochloride. *Pharmaceutics* **2021**, *13*, 619. https://doi.org/10.3390/pharmaceutics13050619

Academic Editor: Jelena Parojčić

Received: 23 March 2021
Accepted: 23 April 2021
Published: 26 April 2021

1. Introduction

Nowadays, the buccal drug delivery system is becoming an important alternative route in drug administration. This possibility of drug application has been untapped and poorly investigated. A buccal drug delivery system has some bioadhesive solid dosage forms, such as bioadhesive tablets, gels, patches, and mucosal bioadhesive films [1–3]. The patients have to place the bioadhesive system onto the buccal mucosa of the mouth. According to Macedo and Patel, this drug delivery system possesses great advantages. A lower dose of API can be applied compared with other delivery systems. Since the first-pass effect of the liver is avoided, the API can enter the systemic circulation after absorption from the buccal mucosa. Secondly, it can be used in the case of swallowing problems, such as Parkinson's disease, stroke, multiple sclerosis, esophagitis, and allergies [4,5]. In geriatrics and pediatrics, it can play a huge role due to its easy and unnoticed application, so patients prefer this dosage form to per os tablets [6,7]. It is a useful form of drug administration from the chemical perspective, because the API and gastric acid do not contact each other, so the stomach can be protected from the API and vice versa [8,9]. However, this dosage form also has difficulties. In the polymer film, a dose of less than 20 mg of the API can be used successfully [10] due to the fact that the surface of the buccal mucosa is small, so a small

dose of API can be absorbed from the small absorption surface. Buccal polymer films might be preferred to buccal tablets. They are more flexible and comfortable as they can be washed from the buccal mucosa by the saliva and, thus, be removed easily [5]. Oral and buccal controlled drug delivery systems are used widely with hydrophilic polymers [11,12]. Oral buccal polymer films must have at least medium mucoadhesive strength; therefore, one or more polymer film-forming excipients, such as sodium alginate (SA) and hydroxypropyl methylcellulose (HPMC), can be chosen [8].

SA is a natural water-soluble, nontoxic, biodegradable anionic polymer extracted from brownseeds (Phaeophyceae), *Macrocystis Pyriferal* and *Ascophyllum Nodosum* [13,14]. It is a member of the polysaccharides (linear) chemical family. It is built by two types of monomers, β-D mannuronic acid (1–4) (M) and α-L guluronic acid (1–6) (G). G and M can be arranged as homopolymer G blocks and M blocks or as heteropolymer mixed blocks (MG) [14]. SA has hydroxyl and carboxyl groups, which can bind to the mucin of the buccal mucosa [15]. The G blocks of SA can form a gel with divalent ions. SA is used in the pharmaceutical and the food and beverage industry. In the pharmaceutical industry, it is often used as a coating component, gel and emulsion stabilizing, and polymer film-forming excipient. The listed properties make SA suitable to be applied in buccal mucoadhesive films [14–17].

In our previous work, the film-forming properties of HPMC were studied [18]. HPMC is a popular, water-soluble, semisynthetic polymer. It is a white, solid, nontoxic polysaccharide (cellulose ether) molecule. In the literature, many researchers have reported that HPMC has good mucoadhesive properties [19–22]. Due to its large number of methoxy, carboxyl, and hydroxyl groups, it can create stable H-bondings with the mucin of the buccal mucosa. Kumria et al. concluded that the larger HPMC content can raise the mucoadhesion time and mucoadhesion force of films [23]. According to Peh and Wong, HPMC films swelled to a greater extent in simulated saliva solution [24]. This fact proves the great mucoadhesivity of HPMC. HPMC is a polymer with high hydrophilicity for an oral-controlled drug delivery system [20,21,25]. It is used as a film-forming agent, thickener agent, coating agent, and alternative to gelatin, and it is a polymer matrix system in tablets, capsules, gels, and eye drops. In addition, it is applied in agriculture, food, and cosmetics [26].

Glycerol (GLY) is an often-used liquid, which has colorless, viscous, nontoxic (dose-dependent), and sweet-tasting properties. GLY belongs to the family of polysaccharides. In polymer chemistry, GLY is used as a plasticizer, because it can make the film soft, flexible, and elastic [27–30].

Cetirizinedihydrochloride (CTZ), which is a second-generation, nonsedative drug, is a generally used antihistamine [31–33]. It is a member of BCS I classification. CTZ has three ionizable groups, a strong basic amino group, a strong carboxylic acid group, and a weak basic amino group, and it is a zwitterion structure between pH 3.0 and 8.0 [34]. CTZ has two remarkable forms (conformers), a folded and an extended one. The folded conformer has notable lipophobicity, low polarity, and a very low energy form due to the resulting intramolecular ionic bond between the positive and the negative charges. However, the extended form is characterized by high polarity, good lipophilicity, and it can form intramolecular hydrogen bindings, Van der Waals forces, and ionic bonds [35]. CTZ is applied in the case of allergic reactions (urticaria or rhinitis) and asthma bronchial. In addition, it is used intravenously in emergencies (anaphylaxia) by paramedics after the administration of adrenalin and intravenous steroids [36,37].

Our work was focused on preparing buccal mucoadhesive polymer films, which contained SA and CTZ. Many research groups used SA as a polymer film-forming agent to formulate buccal films, but it is not a commonly applied polymer material, unlike cellulose derivatives [15–17]. CTZ is an often-used API. It is available as oral tablets and in liquid forms in the case of an allergic reaction. Patients are able to use it easily, and it can have a fast effect without paramedic assistance; therefore, it is worth formulating and investigating in buccal films. Phalguna et al. and Baniya et al. formulated similar buccal films, but the mechanical properties of the films were not investigated as thoroughly as this

dosage form requires. On the other hand, they did not examine the chemical interactions between the excipients in the film at all, although it is important to investigate them, because interactions may arise between the excipients of the films or the structure of the API may change. The mucoadhesivity of the films was not studied either, despite the fact that it is the criterion of the application. This phenomenon can fundamentally influence the mechanical, chemical, and drug release properties of films [38,39].

Our main aim was to prepare films with different compositions and evaluate the physicochemical investigation of buccal mucoadhesive films containing CTZ and SA by mixed two-level and three-level factorial designs. The interactions between the excipients and the API of the films, which can influence the mechanical and drug release properties of films, were investigated with several methods, and our further aim was to investigate the effect of the GLY content on the API distribution. Statistical analysis (factorial design) was also used to evaluate the data of the films. With this analysis, we are able to predict the properties of certain compositions without measurement, so the efficiency can increase. Moreover, we also aimed to investigate, by using several methods, the possible interactions between the excipients and the API of the films, which can influence the mechanical and drug release properties of the films. Based on these results and our opinion, depending on the composition, CTZ-containing buccal films can be applied in the case of allergic reactions. On the one hand, our goal was to find the optimal structure of the mucoadhesive film; on the other hand, CTZ-containing buccal films, depending on the composition, are well-applicable in the case of allergic reactions.

Therefore, our goal was to prepare films that can have their effect under 2 to 3 min. In the case of our present formulations, the prepared films can be used for the treatment of rhinitis, conjunctivitis, or other general symptoms of allergies.

2. Materials and Methods

2.1. Materials

SA (AppliChem GmbH, Darmstadt, Germany) (10,000–600,000 g/mol) and HPMC (Pharmacoat® 603, Shin Etsu Chemical Co., Ltd., Tokyo, Japan) were used as a film-forming agent in the polymer film. GLY 85% (*w/w* %) was added to the film as a plasticizer [Ph. Eur. 8.], CTZ [Ph. Eur. 8.], which was a gift from ExtractumPharma Pharmaceutical Manufacturing, Marketing and Consulting Inc, Kunfehértó, Hungary was the API in the polymer film. Mucin (Carl Roth GmbH + Co. KG, Karlsruhe, Germany) (10 *w/w* %) dispersion was used in the in vitro mucoadhesion test. Diiodomethane was used in the surface free energy measurement.

2.2. Preparation of Films

The films were prepared at room temperature with the solvent casting method. As the first step of preparation, SA (1, 1.33, 1.5, and 2 *w/w* %) was solved in distilled water and mixed (900× *g* rpm) at room temperature. The solution was heated to 70 °C and mixed (900× *g* rpm), and CTZ was solved in the warm solution (0.5523 g/100 g solution) for 5 h. As the third step, HPMC (0.66:1:1.5 *w/w* %) was added to the solution with mixing without heating. In the fourth step, GLY was added to the solution the following day. Mixing was decreased to 100× *g* rpm for 3 h to make the air bubbles disappear from the solution. The solution was cast on a circular Teflon surface (diameter: 7.6 cm, area: 45.34 cm^2) in rubber rings, with 10 g of solution/ring; then, it was dried at room temperature (24.4 ± 0.5 °C). The dried polymer films were removed from the surface and the ring and were placed in closed containers (24.4 ± 1 °C, 60 ± 2% RH).

The films were prepared according to mixed two-level and three-level factorial designs. The factors were the SA and the GLY concentrations, in both cases, with 2% and 3% total polymer concentration.

The prepared polymer films of different compositions can be seen in Table 1. Every second film composition contains CTZ.

Table 1. Composition of the prepared SA-based films.

Total Polymer (%)	Samples	SA (*w*/*w* %)	HPMC (*w*/*w* %)	GLY (*w*/*w* %)	CTZ (10 mg)
2	1	1	1	1	–
	2	1	1	1	+
	3	1	1	3	–
	4	1	1	3	+
	5	1	1	5	–
	6	1	1	5	+
	7	1.33	0.66	1	–
	8	1.33	0.66	1	+
	9	1.33	0.66	3	–
	10	1.33	0.66	3	+
	11	1.33	0.66	5	–
	12	1.33	0.66	5	+
3	13	1.5	1.5	1	–
	14	1.5	1.5	1	+
	15	1.5	1.5	3	–
	16	1.5	1.5	3	+
	17	1.5	1.5	5	–
	18	1.5	1.5	5	+
	19	2	1	1	–
	20	2	1	1	+
	21	2	1	3	–
	22	2	1	3	+
	23	2	1	5	–
	24	2	1	5	+

2.3. Thickness of Films

The thickness of the films was investigated from 10 randomly selected points of all films (n = 10) with a screw micrometer (Mitutoyo Co. Ltd., Kawasaki, Japan), and the sensibility was 0.001 mm. The means and standard deviations were calculated from these data.

2.4. Tensile Strength (Hardness) of Films

Tensile strength was investigated with a self-developed texture analyzer. The equipment and the software were developed at our institute. It has different sample holders and different probes (needle-like probe and rod-like probe). The equipment has a fixed disc (20 mm in diameter) and a moving sample holder. Depending on the investigation, a different sample holder can be used, and the force (the range was 0–200 N), moving speed (20 mm/min), and time can be registered. The needle-like probe (201 mm^2) was used in the hardness test. The probe was moved downward at constant speed, and the sample was fixed on the bottom part of the equipment. The sampling rate was 50 Hz, and the output was 0–5 V. The probe was passed through the film. The equipment presented in Figure 1 detected the time and force during the investigation. The test was finished when the film was broken. The test was performed ten times (n = 10) for each combination of films. The means and standard deviations were calculated [40,41].

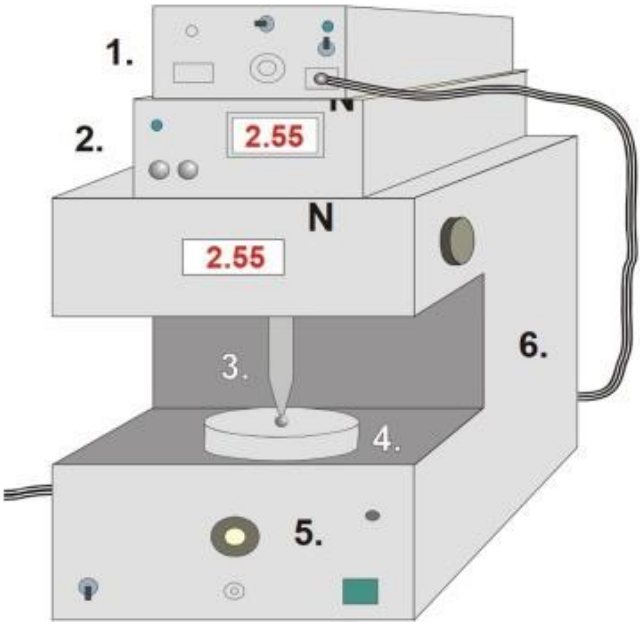

Figure 1. Schematic diagram of the tensile strength and mucoadhesion texture analyzer (**1**—interface, **2**—force display, **3**—rod-like or needle-like probe (jowl), **4**—sample holder, **5**—force measurement unit, and **6**—motor).

2.5. In Vitro Mucoadhesion Test

Mucoadhesion was measured with the same texture analyzer with different settings and assembling modifications. The sample holder was rod-like with a diameter of 5 mm. A double-faced adhesive tape was fixed on the surface of the sample holder, and the polymer film was fixed on the other face of the adhesive tape. A disc with a 35-mm diameter was fixed on the bottom part of the tester, and 40 µL of freshly prepared mucin dispersion (10 *w/w* %) was spread on it. The rod-like sample holder was moved downward and pressed to the mucin-covered, bottom disc with 30 ± 0.1 N for 30 s. This steady-state part can be followed in the force–time curve. After that, the sample holder was moved upwards, and the force was decreased until the sample started to separate from mucin, which can be seen as a well-defined peak in the force–time curve. The peak maximum illustrates the mucoadhesion force. The test was repeated six times (n = 6), and the means and standard deviations were calculated [40,41].

2.6. Contact Angle and Surface Free Energy (SFE) Measurement

Polymer films were placed on the microscope glass slides. One drop of distilled water and diiodomethane was used to measure the contact angle (Θ) of polymer films for 15 s, with the circle fitting method, by using a contact angle apparatus (OCA20-DataPhysics Instrument GmbH, Filderstadt, Germany). One drop of different liquids was applied, the volume of which was 10 µL and 5 µL in the cases of distilled water and diiodomethane, respectively.

The means and standard deviations (SD) were calculated from 6 identical samples of each combination of films (n = 6). The means and standard deviations were used to calculate the surface free energy of films. Surface free energy was calculated with Wu's method. This method defines the amounts of the polar (γ^{p}) and the dispersive (γ^{d}) components of the solids. The SFE of solids can be calculated by using the following connection if the two parameters and the contact angle of the solid are known:

$$(1+\cos\Theta)\cdot\gamma = \frac{4\left(\gamma_s^d\cdot\gamma_l^d\right)}{\gamma_s^d+\gamma_l^d} + \frac{\left(\gamma_s^p\cdot\gamma_l^p\right)}{\gamma_s^p+\gamma_l^p}$$

where Θ is the contact angle of the solid–liquid surface, γ_l is the liquid surface tension, γ_s is the solid surface energy, which is the sum of their polar and dispersive components. According to Wu, the SFE of distilled water is 72.8 mN/m (polar part (γ^p) = 50.2 mN/m; dispersive part (γ^d) = 22.6 mN/m), while the SFE of diiodomethane is 50.8 mN/m (polar part (γ^p) = 1.8 mN/m; dispersive part (γ^d) = 49.0 mN/m) [42].

Knowing the polar and the dispersive parts of the polymer films, the polarity of films can be established by using the following formula:

$$\text{Polarity (\%)} = (\gamma^p \text{ (mN/m)} / \gamma^{tot} \text{ (mN/m)}) \times 100$$

where γ^{tot} (mN/m) = γ^p (mN/m) + γ^d (mN/m).

2.7. FTIR Spectroscopy Measurement

The Fourier-Transform Infrared Spectra of the excipients and the polymer films were investigated by using an Avatar 330 FTIR apparatus (Thermo Fisher Scientific Inc., Waltham, MA, USA) with coupled Zn/Se horizontal attenuated total reflectance (HATR) equipment. Films were laid on a clean crystal of the apparatus. The range of the wavelength was 600 to 4000 cm^{-1} during the investigation. The spectra were obtained from 128 scans, at the spectral resolution of 4 cm^{-1}. CO_2 and H_2O were applied for correction.

2.8. Raman Spectroscopy Measurement

Raman spectroscopy is a promising analytical method to monitor the preparation process and to implement the Process Analytical Technology requirements. In this article, a Dispersive Raman spectrometer was used to confirm the relatively uniform distribution of API in the polymer films. Transmission Raman Spectroscopy is used for noninvasive and fast qualitative investigation of pharmaceutical dosage forms and intermediate products. In our method, the distribution of CTZ was analyzed by Raman surface mapping in CTZ-containing free buccal films.

To investigate the distribution of API, Raman spectra were acquired with a Thermo Fisher DXR Dispersive Raman (Thermo Fisher Scientific Inc., Waltham, MA, USA) equipped with a CCD camera and a diode laser operating at a wavelength of 780 nm. Raman measurements were carried out with a laser power of 24 mW at a 25-µm slit aperture size on a 2-µm spot size. The discrete spectra of the individual substances such as CTZ, HPMC, and SA, and different compositions of polymer films were collected using an exposure time of 6 s, the number of exposures was 20, and the number of background exposures was 512. Smart background was used during the whole investigation. The applied spectral range was 3200–200 cm^{-1} with cosmic ray and fluorescence corrections.

2.9. Dissolution Test

Polymer films of a size of 2 cm × 2 cm (containing 10 mg of CTZ) were investigated in the dissolution test. The dissolution test was made by an Erweka DT700 dissolution basket tester at a mixing speed of 100× *g* rpm. Nine hundred milliliters of phosphate buffer (pH = 6.8) was used as the dissolution medium, and its temperature was 37 °C [43]. Aliquots of 5 mL were analyzed in 5, 10, 15, 20, 30, 40, 50, 60, 90, and 120 min with Genesys 10S UV-VIS (Thermo Fisher Scientific Inc., Waltham, MA, USA) UV-spectrophotometry at λ = 207 nm.

2.10. Statistical Analysis

The collected data were analyzed with the factorial ANOVA method by Tibco Statistica v13.4.0.14 (Statsoft Inc., Tulsa, OK, USA) software. The results were evaluated by being mixed two-level and three-level factorial designs. The equations describe the relationship between the two factors (x_1-concentration of SA and x_2-concentration of GLY) and the four optimalization parameters ($y_1$tensile strength, y_2–mucoadhesion force, y_3–surface free energy, and y_4–dissolution). The low, zero and high levels of the factors are shown in Table 2.

Table 2. The values of factors for mixed two-level and three-level factorial designs.

Total Polymer Concentration (%)	Factors	Low Level	Zero Level	High Level
2%	Concentration of SA (x_1)	1	-	1.33
	Concentration of GLY (x_2)	1	3	5
3%	Concentration of SA (x_1)	1.5	-	2
	Concentration of GLY (x_2)	1	3	5

3. Results

3.1. Thickness and Tensile Strength of the Films

In Figure 2, it can be seen that the thickness (y_1) of different compositions of film increases depends on the polymer and GLY concentration. The 3% polymer films are thicker than the 2% ones; therefore, the polymer concentration can increase the thickness of the films due to the higher amount of polymer (Equations (1)–(4)). The type of polymer does not influence the thickness notably; there is no difference between the 1:1 SA and HPMC (samples 1–6 and 13–18) and 2:1 SA and HPMC films (samples 7–12 and 19–24). It can be seen the C_{SA} (x_1) coefficients were very low in all cases, and they were not significant. C_{GLY} (x_2) can also influence thickness, and these were statistically significant ($p < 0.05$) in all cases. According to Gao and et al., GLY has a water retention effect, so GLY can increase the distance of bonding; therefore, the thickness of the films can be increased [30]. CTZ can also enhance the thickness, which can be explained by the fact that CTZ raises the dry matter content of the films.

$$y_1 = 138.9 + 40.53 \cdot x_2 + 3.94 \cdot x_2^2 + 5.69 \cdot x_1 \cdot x_2 \text{ (2\% polymer films containing CTZ)} \quad R^2 = 0.9218 \tag{1}$$

$$y_1 = 168.02 + 4.59 \cdot x_1 + 54.89 \cdot x_2 + 17.43 \cdot x_1 \cdot x_2^2 \text{ (3\% polymer films containing CTZ)} \quad R^2 = 0.9784 \tag{2}$$

$$y_1 = 116.12 + 1.66 \cdot x_1 + 46.98 \cdot x_2 - 4.47 \cdot x_1 \cdot x_2 \text{ (2\% polymer films without CTZ)} \quad R^2 = 0.9461 \tag{3}$$

$$y_1 = 145.45 + 2.85 \cdot x_1 + 54.95 \cdot x_2 + 7.7 \cdot x_1 \cdot x_2 \text{ (3\% polymer films without CTZ)} \quad R^2 = 0.9972 \tag{4}$$

The mechanical properties of the different polymer films, such as film thickness, tensile strength, mucoadhesion, are summarized numerically in Table 3.

According to Paolicelli et al., GLY can make the film soft, elastic, and flexible. In our research, it can be seen that GLY decreases the tensile strength (y_2) of films [28]. This observation is due to the fact that GLY interacts with other components (CTZ, SA, and HPMC); typically forms H-bonds; and retains water. In addition, GLY can increase the bonding distance, so films with a high GLY concentration can break more easily.

It can be seen that the average values (14.82 and 9.55) were lower in the case of 2% polymer concentration than in the case of 3% (25.32 and 13.81). The total polymer increases the tensile strength, because it can form a cohesive, strong, stable structure in the films due to the bonding of polymer chains. On the other hand, our results show that a higher amount of SA (x_1) (samples 7–12 and 19–24) can result in a stronger structure compared to an equal amount of the polymer. This is shown by the value of the coefficients x_1 shown in (Equations (5)–(8)), which is positive in all cases and statistically significant in two cases (Equations (7) and (8)). It is possible that SA can create stronger and a larger number of bonds with CTZ than HPMC can with CTZ and itself. Another finding is that 3% polymer films have larger strengths than 2% polymer films.

Finally, it can be concluded that 2% polymer films with lower c_{SA} (samples 1–6) have low tensile strengths (less than 10 N), and these films are very breakable. This property is not appropriate from the aspect of application. The other film compositions have high

tensile strength and can be used properly for buccal application, because they do not break from the force of the finger.

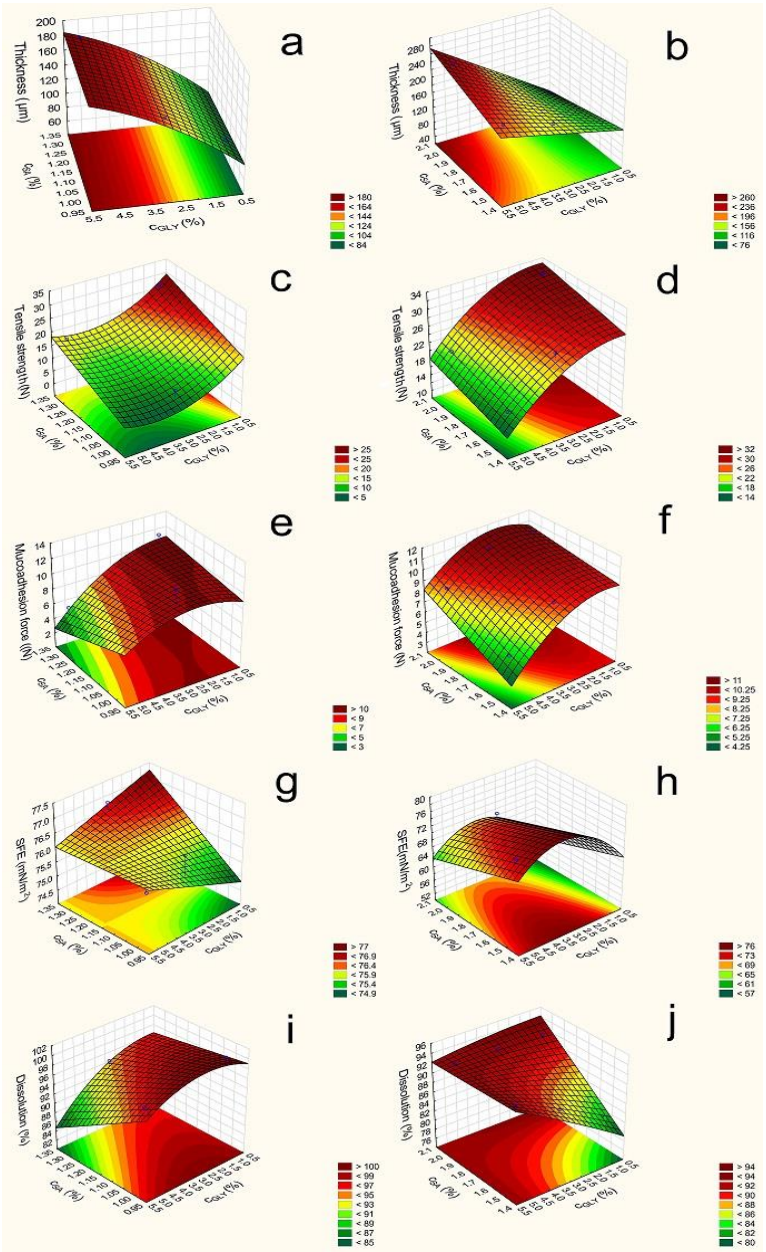

Figure 2. Response surface of polymer films containing CTZ (**left side**—2% polymer films; **right side**—3% polymer films; (**a**,**b**): Film thickness (2%: F (x_2): 259.43; F (x_2^2): 3.27; F (x_1x_2): 5.12; 3%: F (x_1): 12.48; F (x_2): 1189.26; F (x_1x_2): 119.9) (**c**,**d**): Tensile strength (2%: F (x_1): 13.61; F (x_2): 8.0; F (x_2^2): 2.0; 3%: F (x_1): 9.52; F (x_2): 75.7; F (x_2^2): 4.97); (**e**,**f**): Mucoadhesion force (2%: F (x_2): 3.03; F (x_1x_2): 0.7; 3%: F (x_1): 153.54; F (x_2): 280.33; F (x_2^2): 54.94; F (x_1x_2): 18.63); (**g**,**h**): Surface free energy (2%: F (x_2): 0.008; F (x_2^2): 14.35; 3%: F (x_1): 8.92; F(x_2): 3.4; F (x_2^2): 6.82); (**i**,**j**): Dissolution (2%: F (x_1): 15.98; F (x_2): 9.3; F (x_2^2): 1.38; F(x_1x_2): 2.68; 3%: F (x_1): 12.9; F (x_2): 764.8; F (x_2^2): 2.68; F(x_1x_2): 699.21).

Table 3. Mechanical properties of the various polymer films.

Samples	Thickness (μm)	Tensile Strength (N)	Mucoadhesion (N)
1	56.25 ± 8.54	5.61 ± 0.01	16.94 ± 1.20
2	104.75 ± 7.27	13.89 ± 0.92	8.56 ± 1.52
3	128.00 + 7.7	6.07 ± 1.07	15.70 ± 1.32
4	142.32 ± 8.52	9.90 ± 1.19	11.94 ± 1.31
5	159.14 ± 6.32	5.50 ± 1.95	7.13 ± 2.04
6	174.43 ± 6.02	6.33 ± 0.75	6.38 ± 1.59
7	81.50 ± 6.66	18.15 ± 1.45	16.02 ± 2.20
8	86.74 ± 6.34	27.37 ± 0.28	11.57 ± 1.45
9	105.31 ± 8.18	12.85 ± 2.37	8.54 ± 1.10
10	146.00 ± 6.06	14.56 ± 2.18	6.63 ± 1.25
11	166.52 ± 3.87	9.10 ± 1.91	7.97 ± 2.23
12	179.19 ± 4.99	16.92 ± 1.46	5.37 ± 1.64
13	93.53 ± 6.35	8.53 ± 0.57	22.12 ± 2.11
14	125.29 ± 5.56	28.06 ± 3.76	9.66 ± 0.70
15	146.22 ± 5.91	11.39 ± 0.91	17.59 ± 0.63
16	164.79 ± 5.88	26.47 ± 1.42	9.07 ± 1.95
17	188.03 ± 2.71	4.58 ± 0.37	15.64 ± 1.41
18	200.22 ± 8.14	16.28 ± 2.92	5.83 ± 2.11
19	87.23 ± 1.26	17.96 ± 1.52	17.32 ± 2.74
20	102.00 ± 2.71	32.68 ± 3.03	10.82 ± 1.99
21	145.12 ± 3.46	23.47 ± 2.49	16.87 ± 1.51
22	169.20 ± 2.49	27.68 ± 3.65	10,7 ± 2.33
23	212.55 ± 9.98	16.96 ± 1.95	11.95 ± 0.30
24	246.65 ± 5.51	20.75 ± 0.22	8.56 ± 1.87

The different optimalization parameters were determined by a statistical analysis. In the first step, the tensile strength was investigated. The data and Figure 2 reveal that, in the 2% polymer films, SA and GLY have a significant effect. The SA concentration can increase the tensile strength, but GLY has a reverse effect on the tensile strength; it can decrease the tensile strength of the films. In the 3% polymer films, we can see a similar effect, but the effect of GLY is not significant. Equations (Equations (5)–(8)) can be seen below in the case of the different compositions. The significant parameters are marked with red letters.

Tensile strength:

$$y_2 = 14.82 + 4.79 \cdot x_1 - 4.50 \cdot x_2 - 1.95 \cdot x_2^2$$
(2% polymer films containing CTZ)
$$R^2 = 0.9218 \quad (5)$$

$$y_2 = 25.32 + 1.72 \cdot x_1 - 5.93 \cdot x_2 + 1.32 \cdot x_2^2$$
(3% polymer films containing CTZ)
$$R^2 = 0.9784 \quad (6)$$

$$y_2 = 9.55 + 3.81 \cdot x_1 - 2.29 \cdot x_2 - 2.24 \cdot x_1 \cdot x_2$$
(2% polymer films without CTZ)
$$R^2 = 0.9955 \quad (7)$$

$$y_2 = 13.81 + 5.66 \cdot x_1 - 1.24 \cdot x_2 + 2.70 \cdot x_2^2 + 0.73 \cdot x_1 \cdot x_2$$
(3% polymer films without CTZ)
$$R^2 = 0.9979 \quad (8)$$

3.2. In Vitro Mucoadhesion Test

The results of the mucoadhesion of the prepared films are presented in Figure 2. The CTZ-free films had high mucoadhesion force (y_3) values, and the average values were 18.96 (Equation (11)) and 23.82 (Equation (12)). The CTZ-containing samples had significantly

lower mucoadhesion force (average value: 8.41 and 9.1 (Equations (9) and (10)), so CTZ decreases the mucoadhesion of polymer films, possibly due to the interaction between the carboxylic groups of SA, HPMC, and CTZ molecules; thus, fewer groups are able to bind to the mucin. In the case of these samples, mucoadhesion is moderate, but they can be used for the buccal drug delivery system, because this lower force is enough for buccal mucoadhesion. The increasing total amount of polymers increased the mucoadhesion due to the higher number of free binding groups in the system, which can bind to the mucin of the buccal mucous.

GLY (x_2) can influence the mucoadhesion force. The increasing amount of GLY decreased the mucoadhesion force, probably because of the hydrogen bond, which can be formed between GLY and the film-forming polymers and, also, due to the fact that no binding is formed with the chains of mucin because of the lower number of free chains in the polymer.

During the statistical analysis, the mucoadhesion force of the films of all compositions (CTZ-free and CTZ containing) was found to be decreased by GLY (x_2), and in the case of films prepared with 3% polymer concentrations, it is statistically significant. The c_{SA} (x_1) slightly decreased or did not affect it, because SA has a moderate mucoadhesion force, while HPMC has a higher one, so a greater HPMC concentration can cause higher mucoadhesion in the films, but this effect was not statistically significant.

Mucoadhesion force:

$$y_3 = 8.41 - 2.09 \cdot x_2 - 1.01 \cdot x_1 \cdot x_2 \quad (2\% \text{ polymer films containing CTZ}) \quad R^2 = 0.6133 \tag{9}$$

$$y_3 = 9.10 + 0.92 \cdot x_1 - 1.53 \cdot x_2 + 0.58 \cdot x_2^2 + 0.39 \cdot x_1 \cdot x_2 \quad (3\% \text{ polymer films containing CTZ}) \quad R^2 = 0.9981 \tag{10}$$

$$y_3 = 18.96 - 1.21 \cdot x_1 - 4.47 \cdot x_2 + 0.44 \cdot x_1 \cdot x_2 \quad (2\% \text{ polymer films without CTZ}) \quad R^2 = 0.8408 \tag{11}$$

$$y_3 = 23.82 - 1.53 \cdot x_1 - 2.96 \cdot x_2 \quad (3\% \text{ polymer films without CTZ}) \quad R^2 = 0.9120 \tag{12}$$

3.3. Contact Angle and Surface Free Energy (SFE) Measurement

The SFEs (y_4) of the prepared films are shown in Table 4. This measurement is very important from the aspect of applying this pharmaceutical form, because the saliva has to spread on the surface of the films extensively in order for mucoadhesion to develop. The CTZ-free films exhibited medium SFE 51.99 and 57.81 average values (Equations (15) and (16)), while the CTZ-containing films have significantly higher SFE, the average value was 69 and 76.11 (Equations (13) and (14)), so CTZ can increase the SFE of films, particularly the polar part of SFE. CTZ films also demonstrated significantly higher polarity, which may be caused by the carboxylic group of the CTZ molecule. From these results, it seems to be an extended conformer of CTZ can be found in the prepared films [34]. Contact angle showed lower values in the CTZ containing films. The SFE of CTZ-free films changed particularly as a function of increasing GLY concentration (x_2) and only slightly as a function of the SA concentration (x_1). This observation was not true for the CTZ films, because in those films, the SFEs had roughly constant values independently of the concentration of GLY and polymer concentration (Figure 2).

Table 4. Surface free energy (γ^{tot}), dispersive (γ^{d}), and polar part (γ^{p}) of SFE and the polarity (%) of prepared films.

Samples	γ^{tot} (mN/m)	γ^{d} (mN/m)	γ^{p} (mN/m)	Polarity (%)
1	49.59	32.54	17.05	34.38
2	74.88	38.85	36.03	48.12
3	51.65	36.34	15.31	29.64
4	76.33	37.44	38.89	50.95
5	62.60	36.35	26.25	41.93
6	75.72	35.60	40.12	52.98
7	53.56	32.28	21.29	39.75
8	76.86	39.17	37.69	49.04
9	66.21	31.85	34.36	51.90
10	76.89	40.57	36.32	47.24
11	63.23	28.15	35.08	55.48
12	75.98	38.26	37.73	49.66
13	54.32	33.12	21.20	39.03
14	68.61	38.80	29.87	43.54
15	57.36	36.21	21.15	36.87
16	73.78	35.14	38.65	52.39
17	50.84	33.59	17.25	33.93
18	73.72	36.07	37.65	51.07
19	47.99	33.56	14.43	30.07
20	61.05	35.11	25.93	42.47
21	48.72	31.61	17.11	35.12
22	71.73	37.12	34.61	48.25
23	52.68	36.01	16.67	31.64
24	65.12	38.40	26.72	41.03

During the next step of the statistical analysis, SFE was determined in the different compositions of films. In the films, containing CTZ, SA, and GLY can increase SFE in the 2% polymer films, while in the 3% CTZ-free films SA decreases SFE. See Equations (13)–(16) below.

Surface free energy:

$$y_4 = 76.11 + 0.46 \cdot x_1 + 0.375 \cdot {x_2}^2 - 0.43 \cdot x_1 \cdot x_2$$
(2% polymer films containing CTZ) (13)
$$R^2 = 0.9638$$

$$y_4 = 69.00 - 3.04 \cdot x_1 + 2.30 \cdot x_2 + 2.82 \cdot {x_2}^2$$
(3% polymer films containing CTZ) (14)
$$R^2 = 0.9054$$

$$y_4 = 57.81 + 3.19 \cdot x_1 + 5.67 \cdot x_2 + 0.84 \cdot {x_2}^2$$
(2% polymer films without CTZ) (15)
$$R^2 = 0.7854$$

$$y_4 = 51.99 - 2.19 \cdot x_1 + 2.04 \cdot x_1 \cdot x_2$$
(3% polymer films without CTZ) (16)
$$R^2 = 0.7237$$

3.4. FTIR Measurement

The prepared films were investigated with FTIR spectroscopy to determine the interactions between the components of the films. According to Paczkowsa et al., the carboxyl group of CTZ can be explored at 1739 cm^{-1} in FTIR spectra (Figure 3) [44]. In the spectra of CTZ, this peak can be separated sharply. However, in the films, this peak is shifted and disappears, depending on the concentration of the polymer. In the 2% polymer films, the CTZ peak is shifted towards the larger wavenumber, but the intensity of the peak is

smaller than in the case of the raw material. As for 3% polymer films, the peak disappears completely, which proves that interactions can develop between CTZ and the polymers in the films. The carboxyl group of CTZ can be found at 1739 cm^{-1}, so it can be asserted that hydrogen bondings are created between SA, HPMC, and the carboxylic group of CTZ. Due to the small polymer concentration, the films have fewer OH groups of SA and HPMC, which can create hydrogen bonding, so, in this case, the peak only just shifted. However, the 3% polymer films have more OH groups, thus more hydrogen bonds can be created, which can cause a more remarkable structure change, so the peak can disappear completely.

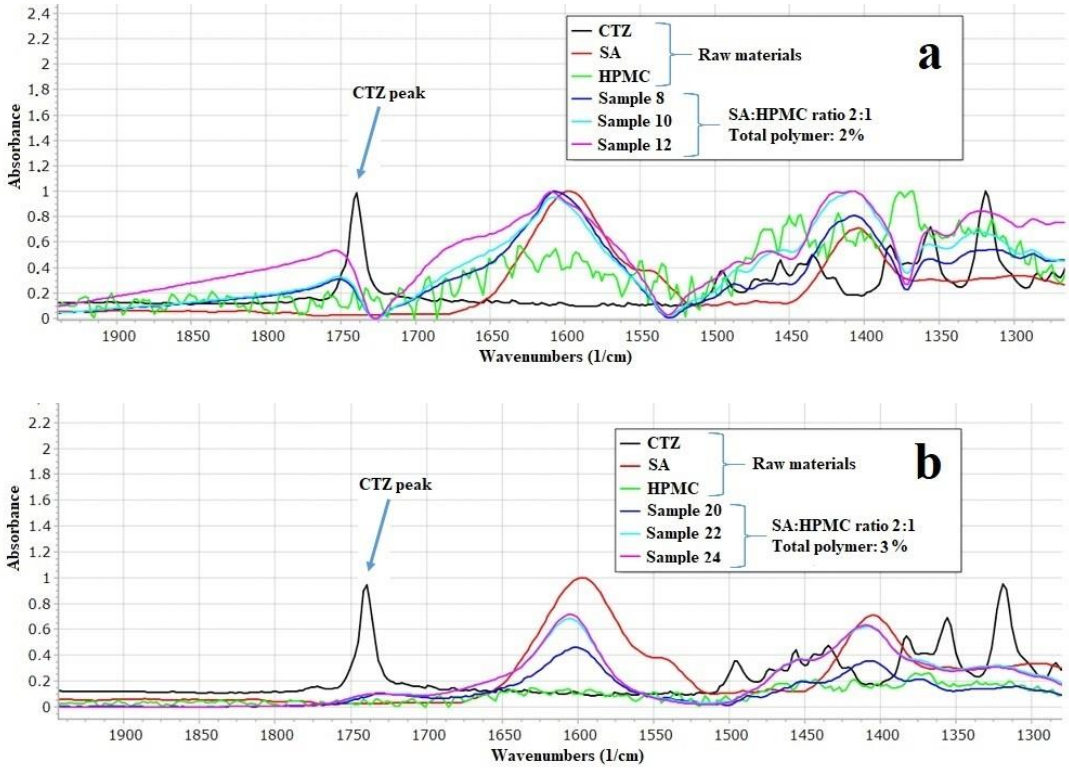

Figure 3. Individual FTIR spectra of SA, HPMC, CTZ, and prepared films (**a**): 2% polymer films and (**b**): 3% polymer films.

Indeed, there are important bands in the higher wavenumber region. A spectral peak is manifested at 2384 cm^{-1}; this is the stretching vibration of the N-H group of CTZ [45]. In both 2% and 3% concentration polymer films, this peak disappears regardless of the GLY concentration. This observation can suggest that, in the films interaction develop between the N-H-group of CTZ and the other components of films. A peak of SA can be detected at 2937 cm^{-1} [46]. This peak is assigned to the C-H stretching vibration. In the polymer films, this peak is shifted to a larger wavenumber and merges with the peak of GLY. The band at 3300 cm^{-1} shows the C-O stretching vibration. The intensity of this peak can increase as a function of GLY concentration and is shifted to a smaller wavenumber. With these findings, we believe we have sufficiently demonstrated the interactions that can occur in the films.

As it can be seen, the dissolution of the API is faster from the 2% polymer films, which contain the two different polymer materials in equal amounts than from those films that contain SA and HPMC in the ratio of 2:1 (it can be found in Figure 3 in Section 3.4, in the dissolution test part of the article). This observation can be explained by the interaction between SA and GLY and other components at 2937^{-1} cm^{-1}. The dependence of the GLY concentration of the drug release is related to the interaction at 3300 cm^{-1}. The high GLY concentration can result in a stronger interaction between the components of the films, as can be seen in the region from 3000 cm^{-1} to 2800 cm^{-1} and in the region 1750 cm^{-1} and 1550 cm^{-1}. The results of Raman spectroscopy also confirm these interactions.

3.5. Raman Spectroscopy Measurement

The individual Raman spectra of SA, HPMC, and CTZ are shown in Figure 4. Based on the comparison of the spectra of the components, a CTZ peak was chosen at 1598.15 cm^{-1}. It belongs to the C-C stretchings in the phenyl and chlorophenyl groups in the chemical structure of CTZ [44]. This distinct peak was chosen for the chemical mapping profile, because it characterizes the API individually.

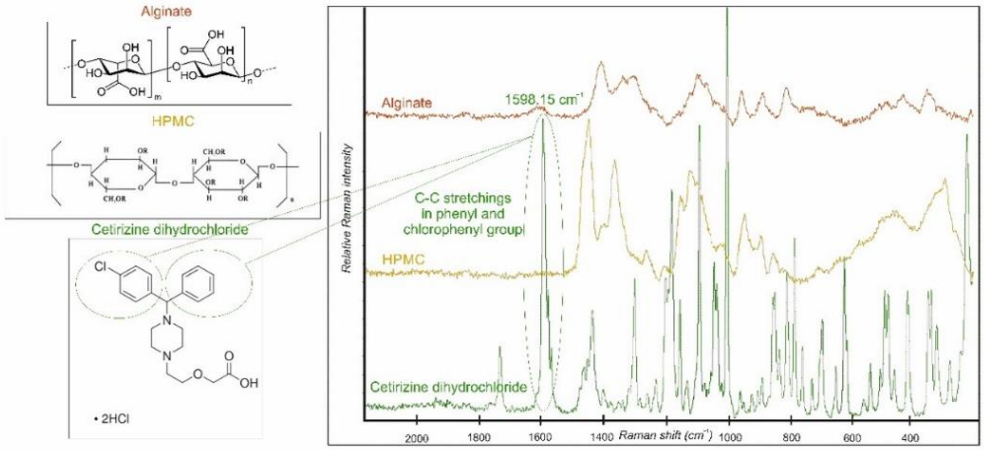

Figure 4. Individual Raman spectra of SA, HPMC, and CTZ.

Chemical maps are presented in Figure 5. The CTZ distributions of samples with different GLY content are homogenous. The warm (red and orange) colors mean a greater API content in the samples. In the film with 1% GLY content the API can be in crystalline agglomerates (yellow, orange spots) in the preparation. In the two other cases, especially in the case of the sample containing 3% GLY, the color distribution of the maps is very smooth. It suggests a possible molecular disperse distribution of the API in the film. It can be concluded that the water-soluble API is in a dissolved form in the films because the larger GLY concentration also means larger water content because of the moisturizing property of GLY. This property of the films can be disadvantageous, because it can cause the physical instability of the samples. Besides, the larger GLY concentration can be harmful during the mucoadhesion of buccal films because GLY reduces the amount of mucoadhesive polymer chains, which are able to evolve binding.

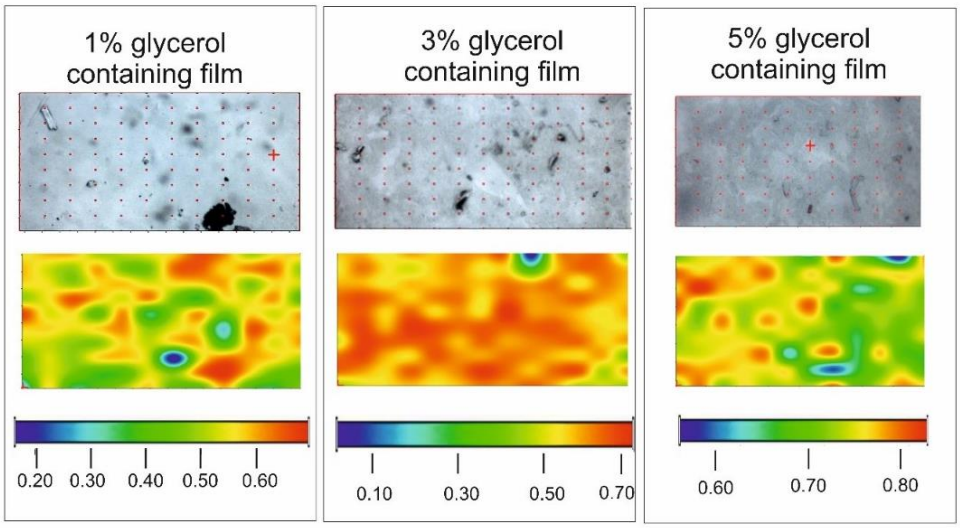

Figure 5. Chemical mapping of films with different GLY contents.

3.6. Dissolution Test

The entire amount of the API can be dissolved from the various films within 120 min. In the first 20 min, almost 100% of the API can be dissolved from the films with 2% polymer concentration (Figure 6). Centkowska et al. found that the thickness of the HPMC films can influence the release of API from the film [47]. CTZ can dissolve from the thinner polymer layer faster than from thicker films, and on the other hand, in the case of thinner films, HPMC is able to dissolve more easily. Films with a lower SA concentration have faster API dissolution, which can be slowed down by GLY. When the SA and GLY concentrations were increased, dissolution became slower in the case of 2% polymer concentration.

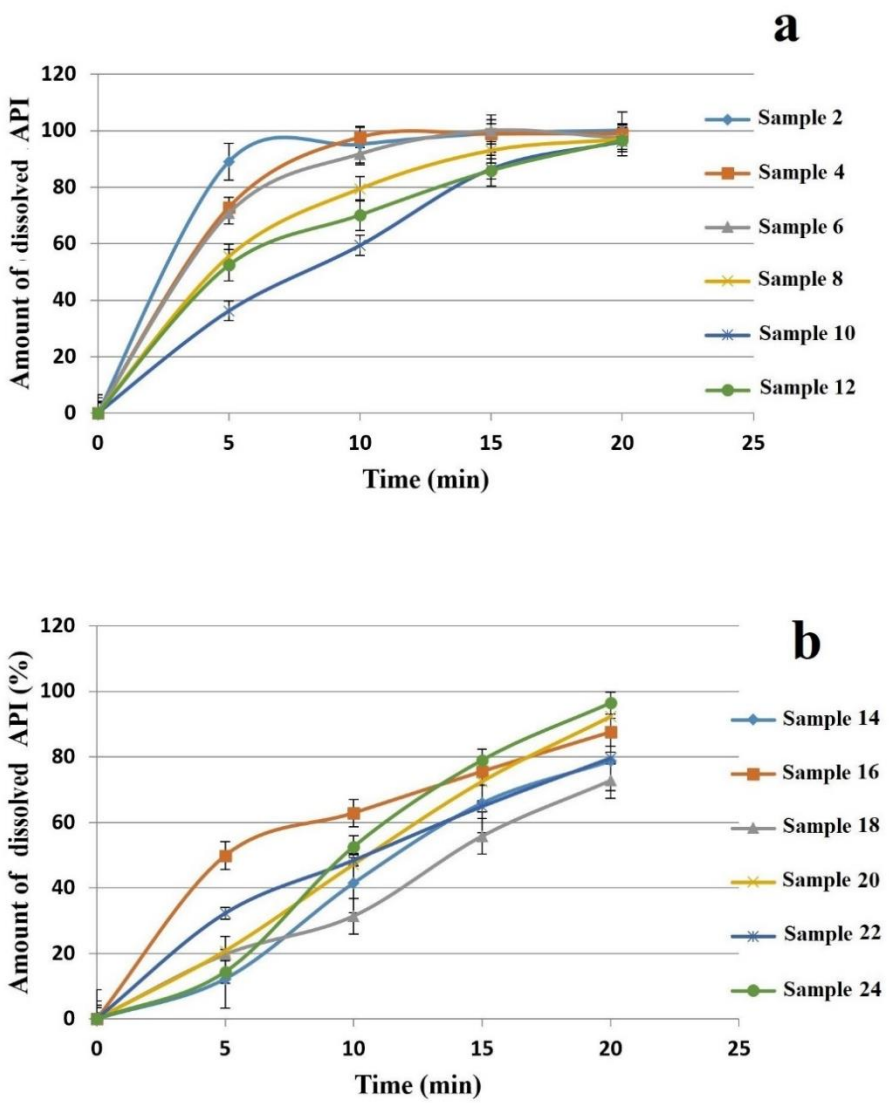

Figure 6. Dissolution curves of prepared polymer films in the first 20 min (**a**): 2% polymer films, and (**b**): 3% polymer films.

The dissolution curve of 3% polymer films is shown in Figure 6, which reveals a connection between the SA concentration and dissolution rates. In about 120 min, the entire amount of the API can be dissolved completely, but in the first 20 min, the API cannot be released fully; 65% to 96% of the API was dissolved from the different composition films. It is noteworthy in the figure that, at the beginning of the test (first 5 min), the API was dissolved faster from the films with equal polymer concentration. The reason for this is that in the case of 3% polymer concentration a stable, cohesive structure is formed between the chains of the polymers, GLY and API, as visible from the thickness and hardness tests;

therefore, GLY cannot affect the dissolution significantly. Compared to 2% films, the effect of GLY is less than expected in 3% films.

When the dissolved drug was investigated after 20 min with a statistical analysis, it can be seen that, in the 2% polymer films c_{SA} (x_1) can decrease it, while in the 3% films $c_{SA,}$ can enhance it. c_{GLY} (x_2) can raise the dissolution rate when high SA concentration is applied (Figure 2). Equations (17) and (18) can be observed below.

Dissolution:

$$y_5 = 95.66 - 3.1 \cdot x_1 - 2.89 \cdot x_2 + 0.97 \cdot x_2^2 - 1.55 \cdot x_1 \cdot x_2$$
(2% polymer films containing CTZ) (17)
$$R^2 = 0.9671$$

$$y_5 = 89.85 + 2.54 \cdot x_1 + 2.40 \cdot x_2 + 0.12 \cdot x_2^2 - 2.29 \cdot x_1 \cdot x_2$$
(3% polymer films containing CTZ) (18)
$$R^2 = 0.9996$$

4. Conclusions

In this present study we successfully formulated mucoadhesive polymer films, which contained CTZ as API. The physical properties of the films, which are of great importance in the formulation of polymer films, were investigated. We can conclude that the physical properties of the polymer films, such as thickness and tensile strength, change considerably depending on the composition of films. These are critical parameters of the formulation because buccal films have to be elastic, flexible, and able to exert satisfactory mucoadhesive force at the same time. The $_{GLY}$ was a statistically significant factor in the case of film thickness and tensile strength for 3% total polymer film but the coefficient also had a high value in the case of 2% total polymer. In the mucoadhesion test, c_{GLY} was found to be a significant factor with the inverse relationship. It can decrease mucoadhesion force; therefore, only 1% GLY concentration is recommended.

CZT-containing films had lower contact angle values, the fluid could spread on the surface of the film. It proves that CTZ-containing films have a hydrophilic surface. CTZ can also increase SFEs, because it has hydrophilic molecule groups, and it can increase the hydrophilicity of the polymer film system. In these cases, no statistically significant factor was found.

During the interaction study, interactions could be observed between the polymer components and the CTZ molecules, which depended on the polymer concentration. In the 3% polymer films, the development of hydrogen bonds is remarkable.

The distribution of CTZ is homogeneous in the films, so the preparation of the films can be considered appropriate. GLY can influence the form of CTZ in the films. In the films with 1% GLY concentration CTZ is crystalline, while in the films with 3% and 5% GLY concentration the API is molecular disperse.

In 20 min, a higher amount of API can dissolve from the thicker and lower polymer concentration polymer film samples, because they are not able to form a stable, strong structure, so the dissolution of the API is faster and easier. In the film samples with a higher polymer concentration, the polymer molecules and GLY and CTZ can create strong bonds, so CTZ can be dissolved more slowly. GLY can decrease the dissolution rate of CTZ.

As a conclusion, samples with 1% of GLY were found to be appropriate for the application on the buccal mucosa. Sample 8 was found as the optimal composition.

We are planning to continue to investigate the films with in vitro permeation tests on buccal cell lines, with ex vivo permeation tests across porcine buccal mucosa in the future. We would like to publish these results in another article together with the results of the accelerated stability test.

Author Contributions: Conceptualization, K.K. and G.R.J.; Data curation, K.P. and O.J.-L.; Formal analysis, K.P., K.K. and O.J.-L.; Funding acquisition, K.P. and G.R.J.; Investigation, K.P. and O.J.-L.; Methodology, K.P.; Project administration, K.K. and G.R.J.; Resources, G.R.J.; Supervision, K.K.

and G.R.J.; Visualization, K.K. and G.R.J.; Writing—original draft, K.P., K.K. and O.J.-L.; Writing—review & editing, K.K. and G.R.J. All authors have read and agreed to the published version of the manuscript.

Funding: The publication was funded by The University of Szeged Open Access Fund (FundRef, Grant No. 5239).

Institutional Review Board Statement: Not applicable.

Informed Consent Statement: Not applicable.

Data Availability Statement: Data sharing not applicable.

Acknowledgments: We thank ExtractumPharma Zrt for providing the API (CTZ) for us. Our work was supported by the Richter Gedeon Talentum Foundation to help me participate in the PhD program and was supported also by EFOP 3.6.3-VEKOP-16-2017-00009 project.

Conflicts of Interest: The authors declare no conflict of interest.

Abbreviations

Sodium alginate, SA; glycerol, GLY; hydroxypropyl methylcellulose, HPMC; cetirizine dihydrochloride, CTZ; surface free energy, active pharmaceutical ingredient, API; surface free energy, SFE; Fourier-Transform Infrared Spectra, FTIR; standard deviation, SD.

References

1. Eleftheriadis, G.K.; Monou, P.K.; Bouropoulos, N.; Boetker, J.; Rantanen, J.; Jacobsen, J.; Vizirianakis, I.S.; Fatouros, D.G. Fabrication of Mucoadhesive Buccal Films for Local Administration of Ketoprofen and Lidocaine Hydrochloride by Combining Fused Deposition Modeling and Inkjet Printing. *J. Pharm. Sci.* **2020**, *109*, 2757–2766. [CrossRef] [PubMed]
2. Koradia, H.; Chaudhari, K. Formulation of unidirectional buccal tablet of Mirtazapine: An in vitro and ex vivo evaluation. *J. Drug Deliv. Sci. Technol.* **2018**, *43*, 233–242. [CrossRef]
3. Marques, A.C.; Rocha, A.I.; Leal, P.; Estanqueiro, M.; Lobo, J.M.S. Development and characterization of mucoadhesive buccal gels containing lipid nanoparticles of ibuprofen. *Int. J. Pharm.* **2017**, *533*, 455–462. [CrossRef] [PubMed]
4. Al-Dhubiab, B.E.; Nair, A.; Kumria, R.; Attimarad, M.; Harsha, S. Development and evaluation of buccal films impregnated with selegiline-loaded nanospheres. *Drug Deliv.* **2014**, *23*, 2154–2162. [CrossRef] [PubMed]
5. Itin, C.; Komargodski, R.; Domb, A.J.; Hoffman, A. Controlled Delivery of Apomorphine Through Buccal Mucosa, Towards a Noninvasive Administration Method in Parkinson's Disease: A Preclinical Mechanistic Study. *J. Pharm. Sci.* **2020**, *109*, 2729–2734. [CrossRef] [PubMed]
6. Orlu, M.; Ranmal, S.R.; Sheng, Y.; Tuleu, C.; Seddon, P. Acceptability of orodispersible films for delivery of medicines to infants and preschool children. *Drug Deliv.* **2017**, *24*, 1243–1248. [CrossRef] [PubMed]
7. Chachlioutaki, K.; Tzimtzimis, E.K.; Tzetzis, D.; Chang, M.-W.; Ahmad, Z.; Karavasili, C.; Fatouros, D.G. Electrospun Orodispersible Films of Isoniazid for Pediatric Tuberculosis Treatment. *Pharmacy* **2020**, *12*, 470. [CrossRef]
8. Macedo, A.S.; Castro, P.M.; Roque, L.; Thomé, N.G.; Reis, C.P.; Pintado, M.E.; Fonte, P. Novel and revisited approaches in nanoparticle systems for buccal drug delivery. *J. Control. Release* **2020**, *320*, 125–141. [CrossRef]
9. Patel, V.F.; Liu, F.; Brown, M.B. Advances in oral transmucosal drug delivery. *J. Control. Release* **2011**, *153*, 106–116. [CrossRef]
10. Serrano, D.R.; Fernandez-Garcia, R.; Mele, M.; Healy, A.M.; Lalatsa, A. Designing Fast-Dissolving Orodispersible Films of Amphotericin B for Oropharyngeal Candidiasis. *Pharmaceutics* **2019**, *11*, 369. [CrossRef] [PubMed]
11. Karagianni, A.; Peltonen, L. Production of Itraconazole Nanocrystal-Based Polymeric Film Formulations for Immediate Drug Release. *Pharmaceutics* **2020**, *12*, 960. [CrossRef]
12. Kumria, R.; Nair, A.B.; Goomber, G.; Gupta, S. Buccal films of prednisolone with enhanced bioavailability. *Drug Deliv.* **2014**, *23*, 471–478. [CrossRef] [PubMed]
13. Xiao, C.; Liu, H.; Lu, Y.; Zhang, L. Blend Films from Sodium Alginate and Gelatin Solutions. *J. Macromol. Sci. Part A* **2001**, *38*, 317–328. [CrossRef]
14. Galus, S.; Lenart, A. Development and characterization of composite edible films based on sodium alginate and pectin. *J. Food Eng.* **2013**, *115*, 459–465. [CrossRef]
15. Khan, S.; Boateng, J.S.; Mitchell, J.; Trivedi, V. Formulation, Characterisation and Stabilisation of Buccal Films for Paediatric Drug Delivery of Omeprazole. *AAPS PharmSciTech* **2015**, *16*, 800–810. [CrossRef] [PubMed]
16. Okeke, O.C.; Boateng, J.S. Nicotine stabilization in composite sodium alginate based wafers and films for nicotine replacement therapy. *Carbohydr. Polym.* **2017**, *155*, 78–88. [CrossRef] [PubMed]
17. Juliano, C.C.A.; Cossu, M.; Pigozzi, P.; Rassu, G.; Giunchedi, P. Preparation, In Vitro Characterization and Preliminary In Vivo Evaluation of Buccal Polymeric Films Containing Chlorhexidine. *AAPS PharmSciTech* **2008**, *9*, 1153–1158. [CrossRef] [PubMed]

18. Kelemen, A.; Katona, B.; Módra, S.; Aigner, Z.; Sebe, I.; Pintye-Hódi, K.; Zelkó, R.; Regdon, J.G.; Kristó, K. Effects of Sucrose Palmitate on the Physico-Chemical and Mucoadhesive Properties of Buccal Films. *Molecules* **2020**, *25*, 5248. [CrossRef] [PubMed]
19. Tagami, T.; Ando, M.; Nagata, N.; Goto, E.; Yoshimura, N.; Takeuchi, T.; Noda, T.; Ozeki, T. Fabrication of Naftopidil-Loaded Tablets Using a Semisolid Extrusion-Type 3D Printer and the Characteristics of the Printed Hydrogel and Resulting Tablets. *J. Pharm. Sci.* **2019**, *108*, 907–913. [CrossRef] [PubMed]
20. Fu, X.; Wang, G.; Liang, W.; Chow, M. Prediction of drug release from HPMC matrices: Effect of physicochemical properties of drug and polymer concentration. *J. Control. Release* **2004**, *95*, 209–216. [CrossRef] [PubMed]
21. Viridén, A.; Wittgren, B.; Larsson, A. Investigation of critical polymer properties for polymer release and swelling of HPMC matrix tablets. *Eur. J. Pharm. Sci.* **2009**, *36*, 297–309. [CrossRef] [PubMed]
22. Sosnik, A.; das Neves, J.; Sarmento, B. Mucoadhesive polymers in the design of nano-drug delivery systems for administration by non-parenteral routes: A review. *Prog. Polym. Sci.* **2014**, *39*, 2030–2075. [CrossRef]
23. Kumria, R.; Nair, A.; Al-Dhubiab, B.E. Loratidine buccal films for allergic rhinitis: Development and evaluation. *Drug Dev. Ind. Pharm.* **2014**, *40*, 625–631. [CrossRef]
24. Peh, K.K.; Wong, C.F. Polymeric films as vehicle for buccal delivery: Swelling, mechanical, and bioadhesive properties. *J. Pharm. Pharm. Sci.* **2000**, *2*, 53–61.
25. Castán, H.; Ruiz, M.; Clares, B.; Morales, M. Design, development and characterization of buccal bioadhesive films of Doxepin for treatment of odontalgia. *Drug Deliv.* **2015**, *22*, 869–876. [CrossRef] [PubMed]
26. Deshmukh, K.; Basheer Ahamed, M.; Deshmukh, R.R.; Khadheer Pasha, S.K.; Bhagat, P.R.; Chidambaram, K. 3-Biopolymer composites with high dielectric performance: Interface engineering. In *Biopolymer Composites in Electronics*; Sadasivuni, K.K., Ponnamma, D., Kim, J., Cabibihan, J.-J., AlMaadeed, M.A., Eds.; Elsevier: Amsterdam, The Netherlands, 2017; pp. 27–128. [CrossRef]
27. Ghavami-Lahiji, M.; Shafiei, F.; Najafi, F.; Erfan, M. Drug-loaded polymeric films as a promising tool for the treatment of periodontitis. *J. Drug Deliv. Sci. Technol.* **2019**, *52*, 122–129. [CrossRef]
28. Paolicelli, P.; Petralito, S.; Varani, G.; Nardoni, M.; Pacelli, S.; Di Muzio, L.; Tirillò, J.; Bartuli, C.; Cesa, S.; Casadei, M.A.; et al. Effect of glycerol on the physical and mechanical properties of thin gellan gum films for oral drug delivery. *Int. J. Pharm.* **2018**, *547*, 226–234. [CrossRef] [PubMed]
29. Cazón, P.; Velazquez, G.; Vázquez, M. Novel composite films from regenerated cellulose-glycerol-polyvinyl alcohol: Mechanical and barrier properties. *Food Hydrocoll.* **2019**, *89*, 481–491. [CrossRef]
30. Gao, W.; Liu, P.; Li, X.; Qiu, L.; Hou, H.; Cui, B. The co-plasticization effects of glycerol and small molecular sugars on starch-based nanocomposite films prepared by extrusion blowing. *Int. J. Biol. Macromol.* **2019**, *133*, 1175–1181. [CrossRef]
31. Schmid, Y.; Navarini, A.; Thomas, Z.-R.M.; Pfleiderer, B.; Krähenbühl, S.; Mueller, S.M. Sex differences in the pharmacology of itch therapies—a narrative review. *Curr. Opin. Pharmacol.* **2019**, *46*, 122–142. [CrossRef] [PubMed]
32. He, A.; Feldman, S.R.; Fleischer, A.B. An assessment of the use of antihistamines in the management of atopic dermatitis. *J. Am. Acad. Dermatol.* **2018**, *79*, 92–96. [CrossRef] [PubMed]
33. Ijaz, M.; Ahmad, M.; Akhtar, N.; Laffleur, F.; Bernkop-Schnürch, A. Thiolated α-Cyclodextrin: The Invisible Choice to Prolong Ocular Drug Residence Time. *J. Pharm. Sci.* **2016**, *105*, 2848–2854. [CrossRef] [PubMed]
34. Van Balen, G.P.; Caron, G.; Ermondi, G.; Pagliara, A.; Grandi, T.; Bouchard, G.; Fruttero, R.; Carrupt, P.; Testa, B. Lipophilicity Behaviour of the Zwitterionic Antihistamine Cetirizine in Phosphatidylcholine Liposomes/Water Systems. *Pharm. Res.* **2001**, *18*, 694–701. [CrossRef] [PubMed]
35. Testa, B.; Pagliara, A.; Carrupt, P.A. The molecular behaviour of cetirizine. *Clin. Exp. Allergy* **1997**, *27*, 13–18. [CrossRef] [PubMed]
36. Alrasbi, M.; Sheikh, A. Comparison of international guidelines for the emergency medical management of anaphylaxis. *Allergy* **2007**, *62*, 838–841. [CrossRef]
37. Soar, J.; Pumphrey, R.; Cant, A.; Clarke, S.; Corbett, A.; Dawson, P.; Ewan, P.; Foëx, B.; Gabbott, D.; Griffiths, M.; et al. Emergency treatment of anaphylactic reactions—Guidelines for healthcare providers. *Resuscitation* **2008**, *77*, 157–169. [CrossRef] [PubMed]
38. Phalguna, Y.; Pasupulati, H.; Rudra, S. Formulation, Characterization and In-Vitro Evaluation of Fast Dissolving Oral Films of Cetirizine HCL. *J. Drug Deliv. Ther.* **2019**, *9*, 122–125. [CrossRef]
39. Baniya, D.P.; Pandey, G.; Bajaracharya, M.; Dhungana, B.R. Formulation and Evaluation of Fast Dissolving Oral Films of Cetirizine Hydrochloride. *Eur. J. Med. Sci.* **2020**, *2*, 23–29. [CrossRef]
40. Ibrahim, Y.H.-E.; Regdon, G.; Kristó, K.; Kelemen, A.; Adam, M.E.; Hamedelniel, E.I.; Sovány, T. Design and characterization of chitosan/citrate films as carrier for oral macromolecule delivery. *Eur. J. Pharm. Sci.* **2020**, *146*, 105270. [CrossRef] [PubMed]
41. Kelemen, A.; Gottnek, M.; Regdon, G.; Pintye-Hódi, K.; Regdon, J.G. New equipment for measurement of the force of adhesion of mucoadhesive films. *J. Adhes. Sci. Technol.* **2015**, *29*, 1360–1367. [CrossRef]
42. Gottnek, M.; Süvegh, K.; Pintye-Hódi, K.; Regdon, G.; Regdon, J.G. Effects of excipients on the tensile strength, surface properties and free volume of Klucel® free films of pharmaceutical importance. *Radiat. Phys. Chem.* **2013**, *89*, 57–63. [CrossRef]
43. Patel, V.F.; Liu, F.; Brown, M.B. Modeling the oral cavity: In vitro and in vivo evaluations of buccal drug delivery systems. *J. Control. Release* **2012**, *161*, 746–756. [CrossRef] [PubMed]
44. Paczkowska, M.; Mizera, M.; Lewandowska, K.; Kozak, M.; Miklaszewski, A.; Cielecka-Piontek, J. Effects of inclusion of cetirizine hydrochloride in β-cyclodextrin. *J. Incl. Phenom. Macrocycl. Chem.* **2018**, *91*, 149–159. [CrossRef] [PubMed]

45. Arshad, M.S.; Hassan, S.; Hussain, A.; Abbas, N.; Kucuk, I.; Nazari, K.; Ali, R.; Ramzan, S.; Alqahtani, A.; Andriotis, E.G.; et al. Improved transdermal delivery of cetirizine hydrochloride using polymeric microneedles. *DARU J. Pharm. Sci.* **2019**, *27*, 673–681. [CrossRef] [PubMed]
46. Sellimi, S.; Younes, I.; Ben Ayed, H.; Maalej, H.; Montero, V.; Rinaudo, M.; Dahia, M.; Mechichi, T.; Hajji, M.; Nasri, M. Structural, physicochemical and antioxidant properties of sodium alginate isolated from a Tunisian brown seaweed. *Int. J. Biol. Macromol.* **2015**, *72*, 1358–1367. [CrossRef] [PubMed]
47. Centkowska, K.; Ławrecka, E.; Sznitowska, M. Technology of Orodispersible Polymer Films with Micronized Loratadine—Influence of Different Drug Loadings on Film Properties. *Pharmaceutics* **2020**, *12*, 250. [CrossRef] [PubMed]

II.

pharmaceutics

MDPI

Article

Stability, Permeability and Cytotoxicity of Buccal Films in Allergy Treatment

Krisztián Pamlényi [1], Géza Regdon, Jr. [1], Dániel Nemes [2], Ferenc Fenyvesi [2], Ildikó Bácskay [2] and Katalin Kristó [1,*]

[1] Institute of Pharmaceutical Technology and Regulatory Affairs, University of Szeged, H-6720 Szeged, Hungary
[2] Department of Pharmaceutical Technology, University of Debrecen, H-4032 Debrecen, Hungary
* Correspondence: kristo.katalin@szte.hu; Tel.: +36-62-545574; Fax: +36-62-545571

Abstract: Oral mucoadhesive systems, such as polymer films, are among innovative pharmaceutical products. These systems can be applied in swallowing problems and can also be used in geriatrics and paediatrics. In our earlier work, we successfully formulated buccal mucoadhesive polymer films, which contained cetirizine-hydrochloride (CTZ) as the API. The present study focused on investigating the stability and permeability of the prepared films. The stability of the films was studied with an accelerated stability test. During the stability test, thickness, breaking hardness and in vitro mucoadhesivity were analysed. Furthermore, the interactions were studied with FT-IR spectroscopy, and the changes in the amount of the API were also monitored. Cytotoxicity and cell line permeability studies were carried out on TR 146 buccal cells. Compositions that can preserve more than 85% of the API after 6 months were found. Most of the compositions had a high cell viability of more than 50%. Citric acid (CA) decreased the stability and reduced every physical parameter of the films. However, cell line studies showed that the permeability of the films was enhanced. In our work, we successfully formulated CTZ-containing buccal films with adequate stability, high cell viability and appropriate absorption properties.

Keywords: mucoadhesive; buccal films; drug delivery; alginate; cetirizine; antihistamine; stability; permeability; cytotoxicity

Citation: Pamlényi, K.; Regdon, G., Jr.; Nemes, D.; Fenyvesi, F.; Bácskay, I.; Kristó, K. Stability, Permeability and Cytotoxicity of Buccal Films in Allergy Treatment. *Pharmaceutics* **2022**, *14*, 1633. https://doi.org/10.3390/pharmaceutics14081633

Academic Editors: Sonia M. Iurian, Ioan Tomuta, Catalina Bogdan, Tibor Casian and Marzia Cirri

Received: 10 June 2022
Accepted: 3 August 2022
Published: 5 August 2022

1. Introduction

An allergy is a condition caused by the hypersensitivity of the immune system, an increased sensitivity that results from a harmful substance triggering an immunological response [1]; it is also known as allergic disease. Allergies affect more and more people all around the world [2]. The symptoms of allergic diseases may include red skin, red eyes, a runny nose, sneezing, shortness of breath or swallowing problems. Medications can be used to improve allergy symptoms [1,3,4].

The most commonly applied medications in the treatment of allergies are antihistamines, which can block the H1 receptor [4]. Cetirizine dihydrochloride (CTZ) is a second-generation, non-sedative antihistamine [5,6]; it is the active metabolite of the first-generation H1 receptor blocker, hydroxyzine [7]. Due to its antihistamine properties, it can be used effectively in the treatment of seasonal or chronic allergic rhinitis and urticaria [7,8]. Some studies reported that it can reduce bronchoconstriction and swallowing problems. CTZ is available on the market in tablets and solution dosage forms [9]. The patient must always swallow the dosage form, but it is impossible if there is a swallowing problem due to laryngeal oedema. In this case, the patient has to apply an injection or wait for medical help.

Buccal polymer films offer an alternative and innovative way to deliver an active pharmaceutical ingredient (API) to the systemic circulation without swallowing the dosage

form [10]. The application of buccal films is easy and not painful, and patients do not feel a foreign body sensation. Therefore, in geriatrics and paediatrics, they could offer great advantages over per os tablets and suppositories [11,12]. At the same time, a lower dose of the API can be used compared with the listed dosage forms. The first-pass effect of the liver is avoided, and the API can enter the systemic circulation directly from the buccal mucosa. The API and gastric acid do not contact each other in the case of buccal drug administration, so the stomach can be protected from the API and vice versa [13–15]. Buccal films as a dosage form are not official in the Pharmacopoeias [16]. However, the pharmaceutical industry has already started to focus on buccal films and recognized them as a potential drug delivery system [17], as evidenced by the availability on the market of a buccal film called Breakyl®, containing fentanyl [18]. Many research groups have tried to formulate buccal polymers films with different APIs, such as omeprazole, miconazole, ondansetron and prednisolone [19–22]. Transcellular and paracellular drug delivery across the lipid membrane of the buccal mucosa is equally good, which can result in good transport for hydrophilic and lipophilic APIs [23]. The bioavailability of the API can be enhanced with films; the API bypasses the liver, so the first-pass effect of the liver does not influence the pre-metabolization of the API [24]. At the same time, the API can be protected from the degradation of the gastrointestinal tract [25]. Therefore, the entire amount of the permeated API can have an effect. In our case, CTZ can act immediately after permeation, so it can quickly reduce serious symptoms without medical help. Further advantages of buccal films are that they are painless and easy to apply; patients can use them easily compared with an injection [26]. Summarizing these facts, buccal films containing CTZ are able to reduce and moderate allergic symptoms in a short time, and depending on the formulation, they are also capable of protecting allergic patients from a life-threatening condition.

In our earlier work, we formulated buccal films with sodium alginate (SA), HPMC and glycerol (GLY), partly with the composition that appears in this research [15]. In that work, the physical properties of the prepared films were studied, such as thickness, tensile strength and in vitro mucoadhesion. Statistical analysis was applied to predict the optimal composition. In addition, the chemical interactions were studied, and the homogeneity of the API was also investigated in the different compositions. Finally, the API content was measured [15]. Most of the compositions were found to be promising, so we found them worthwhile to investigate further.

Sodium alginate (SA) is a linear polysaccharide from a natural source, extracted from brown seeds. SA has hydroxyl and carboxyl groups, which can bind to the mucin of the buccal mucosa, so it is a mucoadhesive polymer [19]. In pharmaceutical technology, it can be used as a polymer film-forming agent to develop buccal films [15,19]. In addition, it is used as a coating agent as well [27]. HPMC is an old conventional material in the pharmaceutical industry. It is a water-soluble polymer. It has a larger number of functional groups (methoxy, carboxyl, hydroxyl), so it can form stable H-bonds with the mucin [28,29]. It is applied as a film-forming agent and a coating agent, and it is often the base of the matrix system in tablets, gels and eye drops [30]. Glycerol (GLY) is a well-known, colourless, viscous, cytocompatible liquid. GLY is widely used in various fields. In pharmaceutical technology and polymer chemistry, it is applied as a plasticizer because it can increase the flexibility and elasticity of film and the coating [31].

The aim of our current research is to investigate the physical and physicochemical stability of the prepared films, which had a promising composition based on our earlier research work [15]. The investigation of the stability of oral films is a less explored area of buccal film research, so it can be stated that it is definitely the novelty of our article. During this period, many processes may take place in the film, and we aimed to examine them. Based on data from the literature, citric acid (CA) enhances permeation [32,33]; therefore, it was incorporated into the films to enhance permeation. Moreover, we also examined the permeation of CTZ from buccal films across an artificial membrane and the TR 146 buccal cell line as well, which are also novelties in our work. The dissolution test is extremely important, but the knowledge of cell permeation is essential for the effect to occur; therefore,

we set a goal to investigate it. Cytotoxicity is also an important investigation because it may influence the outcome of the further development of the dosage form. Finally, based on our results, we aimed to select the best composition with good stability, high permeability and appropriate cytotoxicity.

2. Materials and Methods

2.1. Materials

Sodium alginate (SA) (Biochemica GmbH, Darmstadt, Germany) (10,000–600,000 g/mol) and hydroxy methylcellulose (HPMC) (Pharmacoat® 603, Shin Etsu Chemical Co., Ltd., Tokyo, Japan) were used as film-forming agents in the polymer film. Glycerol (GLY) 85% (*w*/*w* %) was added to the film as a plasticizer (Ph. Eur.8.). Citric acid (CA) (Ph. Eur. 8.) was incorporated in the polymer film system as a permeation enhancer. Cetirizine dihydrochloride (CTZ) (Ph. Eur. 8.) was the API, which was a gift from ExtractumPharma Pharmaceutical Manufacturing, Marketing and Consulting Inc., Kunfehértó, Hungary. Mucin (Carl Roth GmbH + Co. KG, Karlsruhe, Germany) (10 *w*/*w* %) dispersion was used in the in vitro mucoadhesion test.

2.2. Preparation of Buccal Films

Samples 5, 7, 9 and 11 (Table 1) were prepared and tested for their physical and physicochemical parameters in our previous work [15]. Based on this study, these samples proved to be promising compositions during the optimization process; therefore, we continued to work with these compositions in our present work. In this work, the CA-free samples and CA-containing films were also reproduced so that the effect of CA could be examined during the comparison. In addition, we studied how the parameters change in the case of purely SA-based films without HPMC (Samples 1–4).

Table 1. Composition of different SA- and HPMC-based films.

Samples	SA (*w*/*w* %)	HPMC (*w*/*w* %)	GLY (*w*/*w* %)	CA (*w*/*w* %)	CTZ (10 mg)
1	3	0	1	−	+
2	3	0	1	+	+
3	3	0	3	−	+
4	3	0	3	+	+
5	1.5	1.5	1	−	+
6	1.5	1.5	1	+	+
7	1.5	1.5	3	−	+
8	1.5	1.5	3	+	+
9	2	1	1	−	+
10	2	1	1	+	+
11	2	1	3	−	+
12	2	1	3	+	+

The films were prepared at room temperature with the solvent casting method. As the first step of preparation, SA (1.5, 2, 3 *w*/*w* %) was dissolved in distilled water and mixed (900 rpm) at room temperature. The solution was heated to 70 °C and mixed (900 rpm), and CTZ was then incorporated in the warm solution (70 °C, 0.5523 g/100 g solution), and the mixing was continued for 5 h. As the third step, HPMC (0, 1, 1.5 *w*/*w* %) and CA were added to the solution with mixing without heating. In the fourth step, GLY was added to the solution the following day. Mixing was decreased to 100 rpm for 3 h to help the air bubbles disappear from the solution. The solution was cast on a glass surface in Petri dishes, with 10 g of solution/dish; then, it was dried at room temperature (24.4 ± 0.5 °C). The dried polymer films were removed from the surface and were placed in closed containers (24.4 ± 1 °C, 60 ± 2% RH), and the other part of the prepared films was also placed in closed containers, but at 40 °C ± 2 °C, 75% RH ± 5% RH. The prepared films contained 10 mg of CTZ on an area of 4 cm^2, which is the therapeutic dose of this API.

Table 1 shows the different compositions of the prepared polymer films. Every film composition contains CTZ, and every second film composition contains CA.

2.3. Stability Test

During product development, it is essential and unavoidable to assess the stability of the drug and the drug delivery system. In our research work, stability studies were done according to ICH guidelines. The prepared films were placed in closed containers and stored at 40 °C ± 2 °C, 75% RH ± 5% RH for a period of 6 months. Different methods were applied to obtain information about the changes in the properties of the films. During the stability test, thickness, breaking hardness, in vitro mucoadhesivity and permeability were analysed to determine changes in the physical properties of the films. Furthermore, the interactions were also examined with FT-IR spectroscopy, and the drug content was also detected during the 6-month period.

2.3.1. Breaking Hardness of Films

Breaking hardness was measured with a texture analyser developed in our department [34]. The equipment has different sample holders and two different probes (needle-like probe, rod-like probe). The equipment has two parts, a fixed disc and a moving sample holder. Depending on the measurement, a different sample holder can be applied, and during the investigation, the force, moving speed and time can be registered and followed. The needle-like probe was applied in the breaking hardness test. The probe went to the sample, which was fixed on the bottom part of the equipment. The probe went through the film, and the equipment detected the time and force during the investigation. The test was finished when the film was broken. The test was done six times (n = 6) for each combination of films. The means and standard deviations were calculated. The equipment was presented in our earlier research papers [15,33,34].

2.3.2. In Vitro Mucoadhesivity of Films

Mucoadhesion was investigated with the same texture analyser with different settings and parameter modifications [15,35]. In this study, a rod-like sample holder with a diameter of 5 mm was used. A double-faced adhesive tape was fixed on the surface of the sample holder, and the polymer film was fixed to the other face of the adhesive tape. On the bottom part of the tester, a fixed disc with a diameter of 35 mm was applied, and 40 µL of freshly prepared mucin dispersion (10 w/w %) was spread on it. The rod-like sample holder went to the fixed, bottom disc and pressed the polymer film to the mucin-covered bottom disc with 30 ± 0.1 N for 30 s. This steady-state part can be found in the force–time curve. Thereafter, the sample holder went back to the original place, and the force was decreased until the sample started to separate from the mucin, which can be seen as a well-defined, sharp peak in the force–time curve, indicating the in vitro mucoadhesion force of the films. The test was done six times (n = 6), and the means and standard deviations were calculated.

2.3.3. Active Agent Content

In the determination of API content, 4 cm^2 polymer films (containing 10 mg of CTZ) were studied. The test was carried out by an Erweka DT700 dissolution basket tester at a mixing speed of 100 rpm. An amount of 900 mL of phosphate buffer (pH = 6.8) was used as dissolution medium; its temperature was 37 °C [36]. Six parallel measurements were performed. Aliquots of 5 mL were analysed at 120 min with Genesys 10S UV–VIS (Thermo Fisher Scientific, Waltham, MA, USA) UV-spectrophotometry at λ = 207 nm wavelength.

2.3.4. FT-IR Spectroscopy

An Avatar 330 FT-IR apparatus (Thermo-Scientific, Waltham, MA, USA) was used to analyse the Fourier-Transform Infrared Spectra of the raw materials and the prepared polymer films. The apparatus was equipped with a coupled Zn/Se horizontal attenuated total reflectance (HATR) unit. The films were put on a clean crystal of the apparatus.

The range of wavelength was 600 to 4000 cm^{-1} during the investigation. The spectra were collected from 128 scans at the spectral resolution of 4 cm^{-1} with CO_2 and H_2O for correction.

2.4. Permeation Test

The permeation property of CTZ was investigated with two different permeation methods. As the first step, in the Enhancer Cell, the permeation of the API was examined from the polymer films across an artificial cellulose acetate membrane. In the next step, the permeation of the API was measured on the TR146 buccal cell line under in vitro conditions [37–39].

2.4.1. Permeation Test across Artificial Membrane

The permeation of CTZ was studied in the Enhancer Cell across an artificial cellulose acetate membrane (Whatman®, SN:WHA10404106, pore size 0.2 μm, surface 2.54 cm^2) [40]. The size of the measured films was 1 × 1 cm. The films were put on the surface of the membrane and placed into the donor phase, which was 2 mL phosphate buffer (pH = 6.8), modelling saliva. The acceptor phase was also phosphate buffer (pH = 7.4, 300 mL), which simulated the pH of blood. The test was run in an Erweka DT700 dissolution basket tester at a mixing speed of 100 rpm. Aliquots of 5 mL were analysed at 15, 30, 60, 90, 120, 180 and 240 min with Genesys 10S UV–VIS (Thermo Fisher Scientific, Waltham, MA, USA) UV-spectrophotometry at λ = 207 nm wavelength.

2.4.2. Cell Culturing

TR-146 cells (European Collection of Authenticated Cell Cultures Catalogue No: 10032305) were cultured in Dulbecco's modified Eagle's medium with L-glutamine and D-glucose supplemented with 10% (*v*/*v*) FBS, 3.7 g/L sodium hydrogen carbonate, 1% (*v*/*v*) non-essential amino acid solution and 100 IU/mL penicillin K, with 100 μg/mL streptomycin sulfate at 37 °C in an atmosphere of 5% CO_2 in plastic cell culture flasks. The cells were routinely maintained by regular passaging. Cells used for our experiments were between passage numbers 20 and 28.

2.4.3. In Vitro Permeation Test

For the permeation test, 1 × 10^5 cells were seeded on ThinCert® PET cell culture inserts with a pore size of 0.4 μm, a pore density of 2 × 10^6/cm^2 and a culturing surface of 33.6 mm^2 (Greiner BioOne, Mosonmagyaróvár, Hungary). The culture medium was changed twice per week on the inserts, and the cells were grown for 2 weeks in 24-well plates. A Millicell ERS 1 device was used to measure transepithelial electrical resistance (Merck, Budapest, Hungary). After 2 weeks, only inserts with a resistance value over 130 Ω·cm^2 were used, which correlates well with previous reports [41]. The films were cut to equal weight with an overall CTZ content of 0.35 mg. Each film was dissolved in Hank's balanced salt solution (HBSS) with pH = 7.2 before the experiment. The cell culture medium was removed from the inserts, and 400 μL of the dissolved films was added to the apical compartment (AC) and 1000 μL to the basolateral compartment (BC). After 30, 60 and 90 min, 2 × 100 μL of solution was removed from the wells after gentle mixing. The removed volume was replaced with HBSS. The samples were placed into UV-Star 96-well plates (Greiner BioOne, Mosonmagyaróvár, Hungary), and their absorbance was measured at 248 nm with a Multiskan Go microplate reader (Thermo-Fisher, Waltham, MA, USA). Apparent permeability (Papp) was calculated as: $(\Delta Q/\Delta t) \times (1/(0.336\ cm^2 \times C_0))$, where C_0 is the concentration of the tested compound (mg/mL); $\Delta Q/\Delta t$ is the rate of permeability of the tested compound ((mg/mL)·s^{-1}) between 60 and 90 min.

2.5. Cytotoxicity Test

In order to study the cytotoxicity of CTZ films, a Guava® easyCyte™ 5HT (Luminex, Austin, TX, USA) flow cytometer was used for our experiments. TR-146 cells were collected

from cell culture flasks with a trypsin–EDTA solution and redistributed into separate tubes, and 1 million cells were treated with 1 mL of CTZ solution (CTZ films dissolved in HBSS in equal concentration as in the case of the permeation tests). After 30 min of incubation, the cells were centrifuged, the test solutions were removed, and the cells were gently washed with cold HBSS and centrifuged again. The supernatant was removed, and a 1 million cells/mL cell suspension was prepared with HBSS and then stained with 1 µL of 100 µg/mL propidium iodide solution. After 15 min, the suspensions were distributed on 96-well microplates in a volume of 200 µL (3 wells/group) and analysed. Propidium iodide was excited with a 488 nm laser and detected at the 525/30 nm channel (green parameter). On the Forward and Side Scatter Patterns (FSC-SSC) scatterplot, the non-cellular events were excluded. The remaining events (8000–10,000) were analysed on a scatterplot, and gates were created to determine stained (necrotic) and non-stained (living) cells [42]. The experiment was carried out in triplicate. As negative control, HBSS was used, and cells treated with HBSS instead of the dissolved films were considered 100%, to which all treated groups were compared. As positive control, cells were treated with 1% Triton-X 100.

2.6. Statistical Analyses

The significance tests for breaking hardness and in vitro mucoadhesivity were performed with Microsoft Excel (version 15, Redmond, Washington, DC, USA) software. A Two-Sample T-Test was applied. The test was done six times for each sample. In all cases, the samples were compared to the freshly prepared sample (0 months). The apparent permeability values of the films were analysed with the Kruskal–Wallis test with Dunn's test as post hoc test. In each case, we used a significance level of $p < 0.05$. Significance is labelled as ns = $p \geq 0.05$; * = $p < 0.05$ ** = $p < 0.01$.

3. Results

3.1. Stability Test

3.1.1. Breaking Hardness of Films

The results of the breaking hardness measurements are presented in Figure 1. The significance results are marked with * (*: $p < 0.05$). The changes in the extent of the breaking hardness of the films during the 6-month period are marked in different colours. Breaking hardness decreased for every composition during the period. At the beginning of the investigation, the breaking hardness of the films containing CA was higher than that of the films without CA. This observation could be explained by the fact that CA can form cross-linking and hydrogen bonds with the other components of the films; therefore, CA-containing films have a stronger, cohesive structure [43]. On the other hand, Uranga et al. found that CA can have a plasticizer effect in the polymer film, which can confirm the higher force in the freshly prepared sample; therefore, these films are flexible [44]. At the same time, in the case of CA-containing films (Samples 2, 4, 6, 8, 10, 12), the decrease in breaking hardness was higher than without CA (Samples 1, 3, 5, 7, 9, 11). As the GLY concentration increased, the tensile strength of the films decreased, which correlates with data from the literature for films with a similar composition [27,45]. During storage, GLY can decompose, which can cause the decrease in the breaking hardness of the films, and due to this fact, the water content of the films also decreases. For films with a higher GLY concentration, the decrease in breaking hardness is higher, so these films can become more breakable over time. As we can see, the reduction in breaking hardness was outstanding when comparing the freshly prepared samples and the 3-month samples. As for the 3-month and the 6-month samples, the changes in the breaking hardness values were very low, presumably because most of the chemical decomposition process may take place by the third month. This assumption is also supported by the results of the FT-IR measurements. Because of these facts, it can be said that the films that do not contain CA and contain a low GLY amount have adequate stability in terms of breaking hardness (Samples 1, 5, 9).

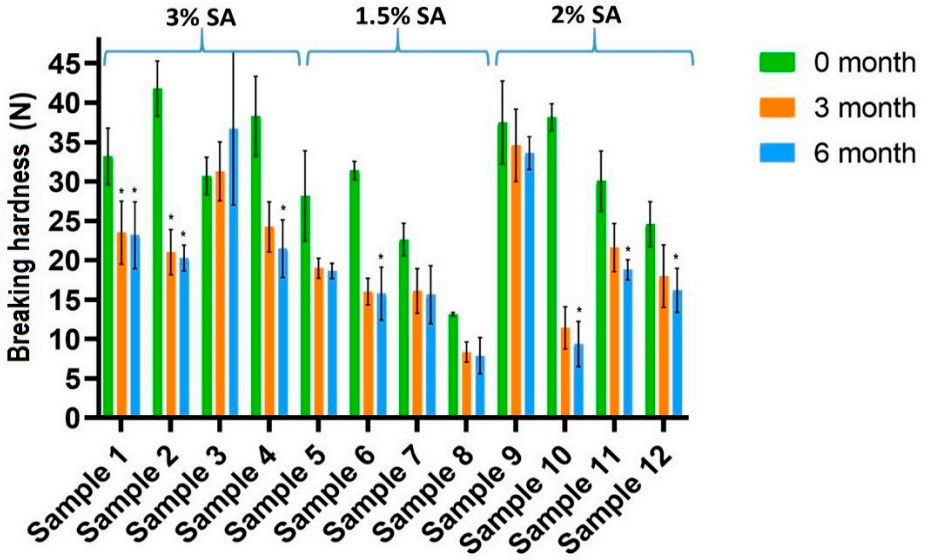

Figure 1. Breaking hardness of the prepared films (Samples 2, 4, 6, 8, 10, 12 contain CA) (* $p < 0.05$; $n = 6$). The samples were compared to the freshly prepared sample (0 months).

3.1.2. In Vitro Mucoadhesivity of Films

Figure 2 shows the mucoadhesivity of the films, with different colours at different times. The significance results are marked with * (*: $p < 0.05$). As can be seen, mucoadhesion force increased for almost every sample during the 6-month period. This is a positive fact because it means that the films can connect to the buccal mucosa in a stronger way after storage time. This phenomenon can probably be explained by the fact that more free chains are formed during storage, so carboxyl and hydroxyl groups can connect to the oligosaccharide chain of mucin on the buccal mucosa. This observation is also supported by the results of the breaking hardness of the films because breaking hardness can decrease in every sample during storage, which means the cohesive structure can be destroyed by the forced condition.

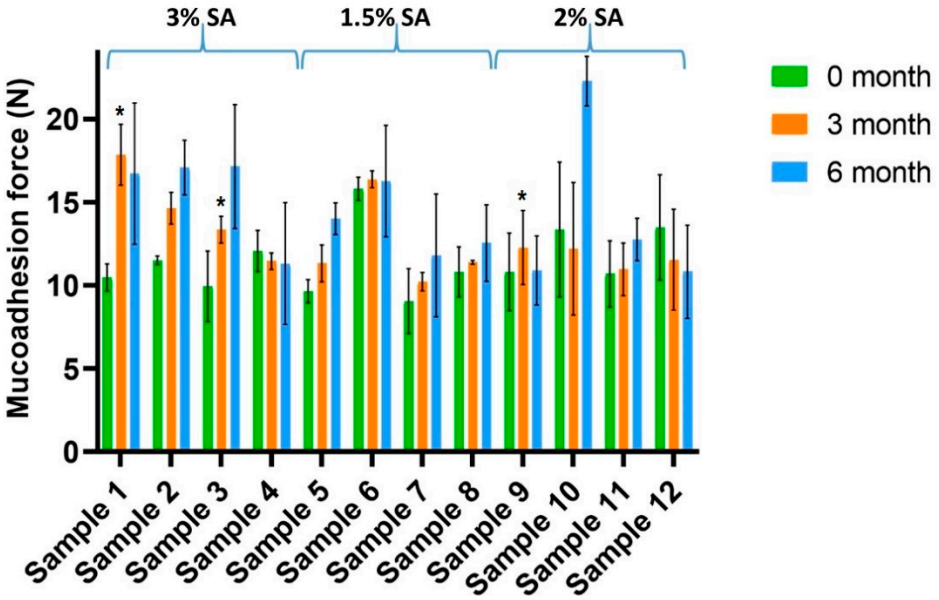

Figure 2. Mucoadhesivity of the prepared films (Samples 2, 4, 6, 8, 10, 12 contain CA) (* $p < 0.05$; $n = 6$). The samples were compared to the freshly prepared sample (0 months).

Based on our results, SA showed excellent mucoadhesion properties, which correlates with data from the literature [46,47]. Films without HPMC showed a higher rise in

mucoadhesion force compared with the films without HPMC (Samples 1–4), so it can be said that HPMC can enhance the stability of the structure formed during the investigated period because the changes of mucoadhesion force in the films containing HPMC are smaller than in the case of the films without HPMC. Moreover, these results suggest that the films containing CA have higher in vitro mucoadhesion force, especially in the case of the 6-month samples, than the films without CA. The GLY concentration can also influence the mucoadhesivity of films. Films with a higher GLY concentration may cause lower growth and growth rate in mucoadhesivity. This observation may be due to the fact that high amounts of GLY can build better in the polymer film structure; therefore, during storage, fewer chains are free that are able to bind to the mucin of the buccal mucosa.

3.1.3. Active Agent Content

Figure 3 shows the results of the change in content during 6 months of storage. The results are marked in different colours for the different times of the investigation. In Figure 3, the results appear numerically for the compositions that can preserve more than 85% of the API after 3 or 6 months, according to pharmacopeia expectations. As expected, a decrease can be observed for each sample under the forced condition during storage. The reductions in the amount of the API were higher at the beginning of the investigation, while later, the changes were smaller. The changes were larger for films containing CA, so it can be concluded that CA can decrease the stability of films. GLY can also enhance the decomposition of the API. It was found that films with a larger amount of GLY had a lower amount of API after 6 months than films with a low amount of GLY, so higher GLY concentrations in the films can also reduce film stability. The reason for this is that films with a high GLY concentration have a higher water content because of the water-retention effect of GLY, and a higher water content can increase decomposition. As can be seen, Sample 1 and Sample 5 can preserve the required amount of the API after 6 months, while Sample 6, Sample 9 and Sample 10 can preserve it after 3 months.

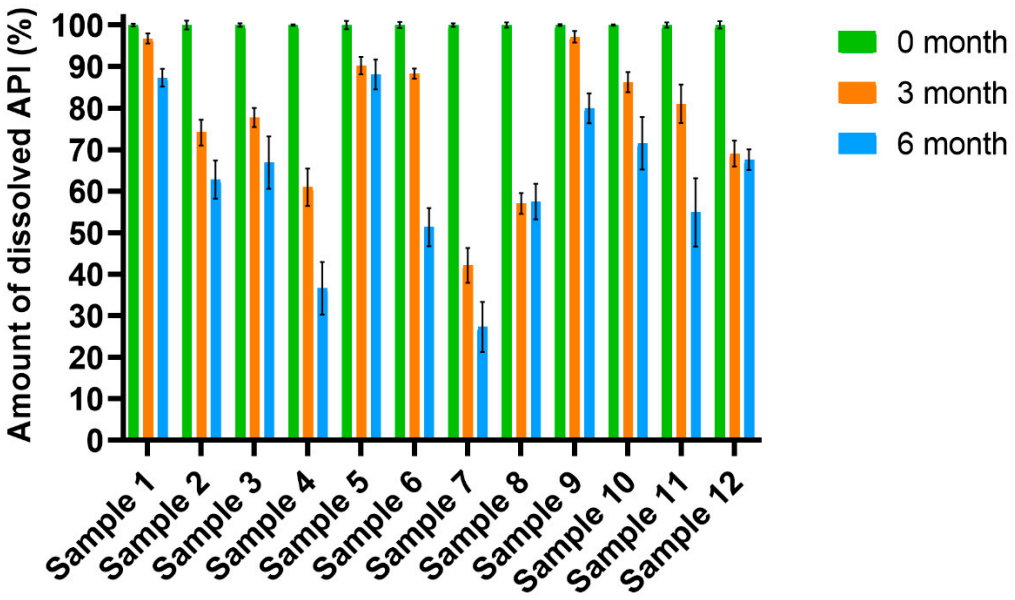

Figure 3. API content for different films during accelerated stability study (Samples 2, 4, 6, 8, 10, 12 contain CA) (n = 6).

3.1.4. FT-IR Spectroscopy

The prepared films were investigated with FT-IR spectroscopy to determine the interactions between the components of the films. In Figure 4, the FT-IR spectra of the films can be seen. Part "A" of Figure 4 shows the film composition with the largest amount of API (Sample 1) after 6 months, while in the bottom figure, the film composition with

the least amount of API is presented (Sample 8). As can be seen, the carboxyl group of CTZ can be detected at 1739 cm^{-1} in the FT-IR spectrum. In the spectrum of CTZ as a raw material, this peak can be sharply distinguished. However, in the films, this peak was shifted to the higher wavenumbers. In Sample 1 (Part "A" of Figure 4), the CTZ peak was shifted towards a higher wavenumber, but the intensity of the peak was smaller than in the case of the raw material. In Part "B" of Figure 4, for Sample 8, the peak disappears completely after 6 months, which shows that the amount of the API decreased because of the forced condition during storage, and hydrogen bonds were formed between SA, HPMC and the carboxylic group of CTZ, which can cause more remarkable structural changes, as seen in the results of the breaking hardness measurement. In addition, there are important bands in the higher wavenumber region. A spectral peak can be found at 2384 cm^{-1}, which shows the stretching vibration of the N-H group of CTZ. This peak disappears in every sample, regardless of the GLY concentration. This observation may suggest that interactions develop in the films between the N-H-group of CTZ and the other components of the films. Overall, it can be stated that the decomposition of the API was greater in CA-containing films than in the ones without CA. Moreover, interactions can occur between the components of the films, mostly in the form of hydrogen bonds, which can greatly affect the breaking hardness of the films.

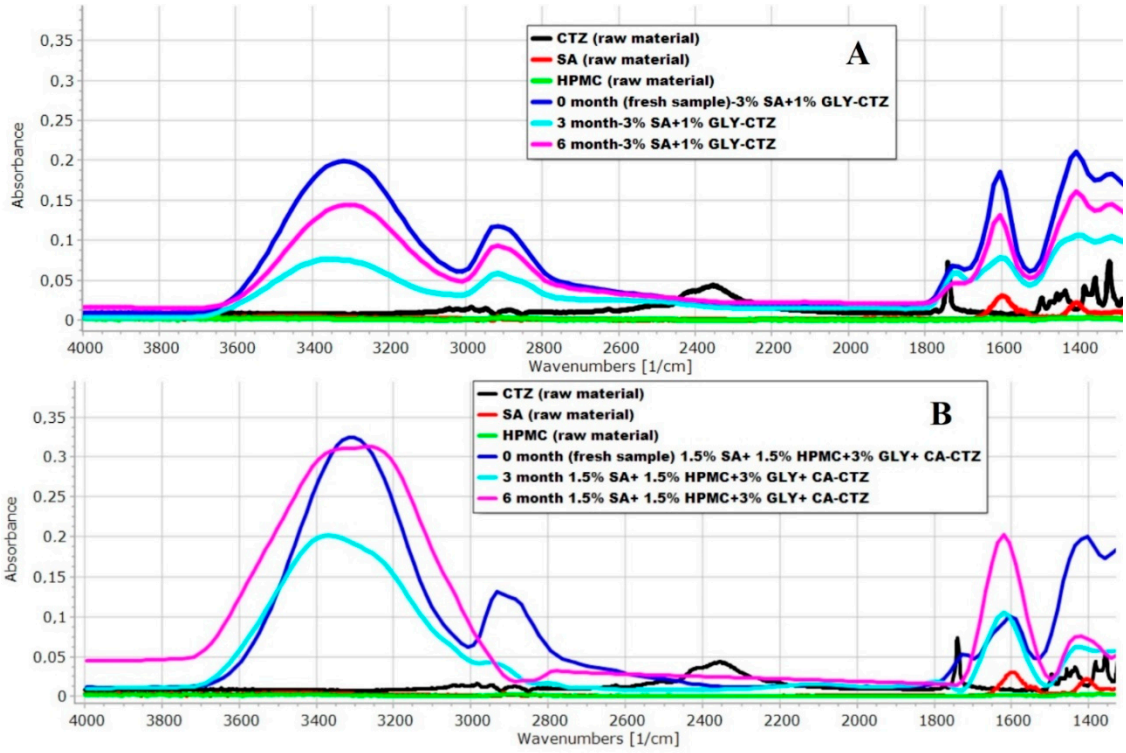

Figure 4. Results of the FT-IR spectra of the prepared films (Part "**A**" Sample 1, Part "**B**" Sample 8).

3.2. Cytotoxicity Test

The TR-146 cells were treated with the dissolved films in a concentration of 0.35 mg/mL CTZ in HBSS as a solvent. Table 2 shows the results of the cytotoxicity test according to flow cytometry stained with propidium iodide. It can be seen that some formulations had a high impact on cell viability. Samples 7 and 10 were below 40%. However, Samples 3, 5 and 12 had almost no cytotoxic effect. The other samples had a cell viability value between 55 and 87%.

Table 2. Cytotoxicity of the prepared films according to flow cytometry. The experiment was carried out in triplicate (Samples 2, 4, 6, 8, 10, 12 contain CA).

Samples	Cell Viability Compared to Control (% ±SD)
1	67.1 ± 2.7
2	78.7 ± 0.6
3	92.8 ± 0.4
4	56.3 ± 1.0
5	99.3 ± 0.8
6	55.9 ± 0.2
7	33.6 ± 0.7
8	87.7 ± 0.1
9	87.2 ± 0.5
10	17.4 ± 0.3
11	56.4 ± 4.6
12	91.3 ± 1.5
Triton X	0.2 ± 0.1

Cellular transport experiments were performed only with Samples 1, 2, 3, 5, 8, 9 and 12, which had cytotoxic values over 60%.

The direct cytotoxicity of cetirizine dihydrochloride is not well-published. Majumder et al. have found that, in a concentration of 400 µM, mouse macrophage RAW 264.7 and mouse myoblast C2C12 cell lines showed only ~50% and ~60% cell viability, respectively [48]. For human lymphocytes, it was found that a concentration of 200 µg/mL decreased cell viability to 50% [49]. In our cytotoxicity and cell viability experiments, the concentration of cetirizine hydrochloride was higher, 744 µM actually.

3.3. Permeation Test

3.3.1. Permeation Test across Artificial Membrane

Figure 5 shows the results of the permeation test across an artificial cellulose membrane. The permeation curves of films of different compositions are shown. From most compositions, more than 40% of the API can permeate to the acceptor compartment. The SA concentration can influence the amount of the permeated API. A higher amount of the API can permeate to the acceptor compartment from the films with a higher SA concentration than from the ones with a lower SA concentration. This correlation is shown in Figure 5, where Sample 1 (brown curve) has a higher permeation rate than the comparable samples (Sample 5—purple curve, Sample 9—green curve). The same correlation can be observed for Sample 3 (yellow curve) and Sample 11 (red curve). Furthermore, it can also be stated that the GLY concentration did not influence the permeation rate and speed of the API.

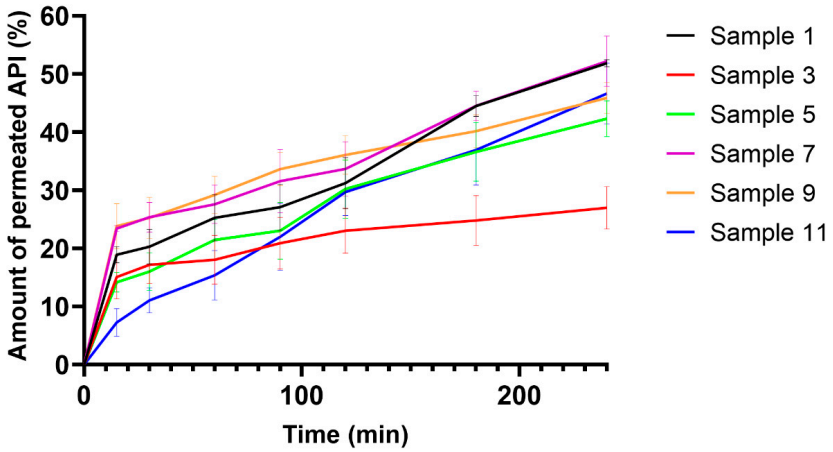

Figure 5. Permeation curves of polymer films on artificial membrane (n = 6).

These results can be considered good because the entire amount of the permeated API can have an effect compared to per os tablets because of the first-pass effect of the liver. At the same time, our results can be improved by a greater volume of the donor phase.

3.3.2. In Vitro Permeation Test

TR-146 cells are an accepted model for the in vitro testing of buccal absorption. The prepared films were dissolved in HBSS, and their cellular transports were observed for 90 minutes. As shown in Figure 6, Sample 2 had exceptionally high permeation, while Sample 12 had the lowest value. The presence of citric acid had no direct effect on cellular transport. Moreover, films with HPMC content had smaller permeability.

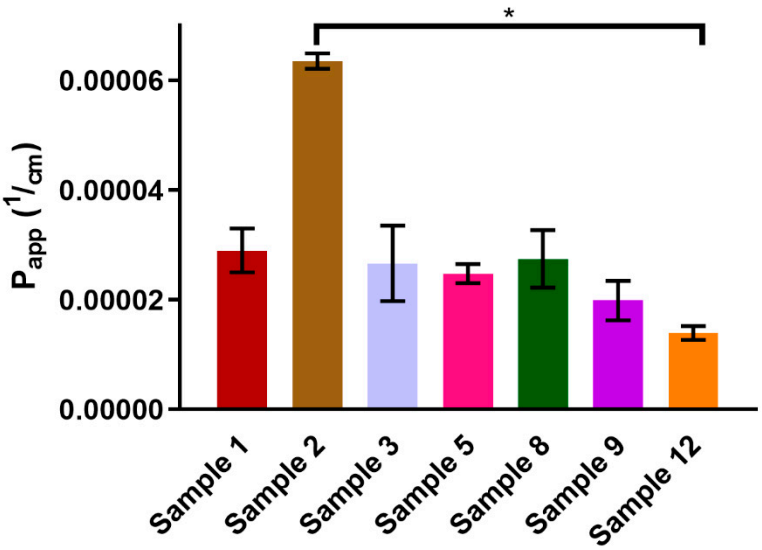

Figure 6. Apparent permeability values of buccal films calculated from the permeability rate of CTZ between 60 and 90 min. Each film was investigated in three separate, parallel cell culture inserts (n = 3). * Significant difference was found only between Sample 2 and Sample 12.

As can be seen in Figure 7, most films had a linear transport rate through the cells between 30 and 90 min. With the exception of Sample 4, all films had a faster transport rate in the first 30 min, after which the transport slowed. The dissolution and the transport of CTZ from all films was stable, with no observed dose dumping [41].

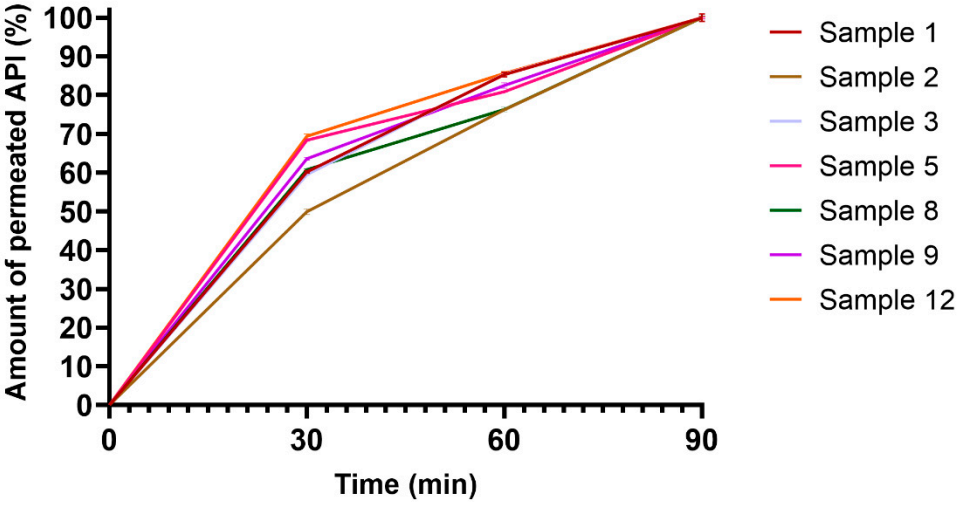

Figure 7. Transported CTZ–time curves of buccal films on the TR-146 cell line. Each film was investigated in three separate, parallel cell culture inserts (Samples 2, 8, 12 contain CA) (n = 3).

4. Discussion

In our earlier work, we prepared buccal films with CTZ-containing films based on SA and HPMC. We found promising results; therefore, we investigated these films further, and we also formulated new compositions.

In our present research work, we focused on the investigation of the stability and permeability of the previously formulated and CA-containing film compositions. However, new compositions were also formulated and investigated. During the stability test, we investigated the physical (mechanical) and chemical stability of the films.

The breaking hardness of all films decreased during storage. The decrease was higher for CA-containing films.

However, during storage, the mucoadhesivity of the films can increase to a great extent, which is a positive fact. CA was able to enhance the mucoadhesion force of the films, and the low GLY concentration may also result in beneficial mucoadhesion properties in the films.

Based on the results of the API content, it can be concluded that the CA-containing films have smaller drug content, and the high GLY concentration can also reduce the amount of the API during storage. Nevertheless, there are compositions that can preserve the API content according to pharmacopeia expectations (Samples 1, 5, 6, 9, 10) after 3 or 6 months.

Through the FT-IR investigation, chemical interactions were found in the buccal films between the N-H-group of CTZ and the other components of films. It can be concluded that the decomposition of CTZ is greater in CA-containing films than in the ones without CA. Furthermore, interactions can occur between the components of the films, mostly in the form of hydrogen bonds, which can greatly affect the breaking hardness and mucoadhesivity of films.

Further research is needed to determine which component of the films exhibits cytoprotective properties to decrease the cytotoxic effect of the API. No direct correlation was found between cell viability and the presence of citric acid. The investigation of cytotoxicity in the course of the development of a new pharmaceutical product is essential and unavoidable in order to prove that the product is safe and non-toxic, so it can be used in humans for further tests in clinical trials. In conclusion, it can be said that Samples 3, 5, 8, 9 and 12 have appropriate and acceptable cytocompatibility because they have high cell viability values, so these samples did not significantly impair the cell viability of the films. However, further research is needed to properly evaluate the cytotoxicity of Samples 1, 2, 4, 6 and 11. Samples 7 and 10 proved to be cytotoxic, so further investigation is not justified.

More than 40% of CTZ was able to permeate to the acceptor compartment from almost all compositions. The SA concentration can influence the amount of the permeated API. A higher amount of the API was able to permeate to the acceptor compartment from the films with a higher SA concentration than from the ones with a lower SA concentration. At the same time, the bioavailability of the API is higher from buccal films than from per os tablets.

The speed of transport of CTZ was nearly constant from all compositions; no excipient caused significantly faster or slower permeation. Apparent permeability was the highest for Sample 2, which was transported across the buccal cell line in a large quantity. CA did not enhance the permeation rate of CTZ in the films, but high alginate content resulted in relatively high permeability. HPMC seemed to decrease apparent permeability. As films with similar compositions were not published before, further investigation is needed to determine how the concentration of each excipient modifies cellular permeability.

Finally, it can be concluded that, from among these compositions, Sample 5 (1.5% SA + 1.5% HPMC + 1% GLY) demonstrated the best stability, cell viability and permeability properties, so this composition is recommended for application on the buccal mucosa.

5. Conclusions

Summarizing our results, it can be said that the breaking hardness of the films decreased during the 6-month period, and the CA reduced it to a greater extent. At the same time, the mucoadhesivity of the films can be increased, especially in case of the CA-containing films. Under storage, the API content decreased, and the CA enhanced the reduction in the API. On the other hand, the high amount of GLY decreased the API content of the films as well. Sample 1 and Sample 5 met the requirements of pharmacopeia after 6 months of stability testing.

Moreover, interactions can be found between the components of the prepared films, mainly in the form of hydrogen bonds.

As a conclusion, it can be said that Samples 3, 5, 8, 9 and 12 have appropriate and acceptable cytocompatibility because these samples have high cell viability values.

Apparent permeability was the highest for Sample 2. CA did not enhance the permeation rate of CTZ in the films, but high alginate concentration resulted in relatively high permeability.

Finally, it can be concluded that Sample 5 (1.5% SA + 1.5% HPMC + 1% GLY) is recommended for application in buccal drug administration because of its great properties.

Author Contributions: Conceptualization, K.K. and G.R.J.; Data curation, K.P., D.N. and F.F.; Formal analysis, K.P., K.K., D.N. and I.B.; Funding acquisition, K.P. and G.R.J.; Investigation, K.P. and D.N.; Methodology, K.P.; D.N. and F.F.; Project administration, K.K. and G.R.J.; Resources, G.R.J.; Supervision, K.K. and G.R.J.; Visualization, K.P.; Writing—original draft, K.P. and D.N.; Writing—review and editing, I.B., K.K. and G.R.J. All authors have read and agreed to the published version of the manuscript.

Funding: The publication was funded by Richter Gedeon Centenarium Foundation (no. 2022/R/26/2526). Project no. TKP2021-EGA-18 has been implemented with the support provided from the National Research, Development and Innovation Fund of Hungary, financed under the TKP2021-EGA funding scheme. The work is supported by the GINOP-2.3.4-15-2020-00008 project. The project is co-financed by the European Union and the European Regional Development Fund.

Institutional Review Board Statement: Not applicable.

Informed Consent Statement: Not applicable.

Data Availability Statement: Not applicable.

Acknowledgments: This research work was supported by the Richter Gedeon Talentum Foundation to help me participate in the Ph.D. program and was also supported by the ÚNKP-21-3 New National Excellence Program of the Ministry for Innovation and Technology from the Source of the National Research, Development and Innovation Fund. The authors thank Richter Gedeon Centenarium Foundation for financial support.

Conflicts of Interest: The authors declare no conflict of interest.

Abbreviations

Sodium alginate, SA; glycerol, GLY; hydroxypropyl methylcellulose, HPMC; citric acid, CA; cetirizine dihydrochloride, CTZ; active pharmaceutical ingredient, API; Fourier-Transform Infrared Spectra, FT-IR; standard deviation, SD; Hank's balanced salt solution, HBSS; apical compartment, AC; basolateral compartment, BC; apparent permeability, Papp; forward and side scatter, FSC-SSC.

References

1. McConnell, T.H. *The Nature of Disease: Pathology for the Health Professions*; Lippincott Williams & Wilkins: Baltimore, MD, USA, 2007; ISBN 978-0-7817-5317-3.
2. Dahl, R.; Stender, A.; Rak, S. Specific Immunotherapy with SQ Standardized Grass Allergen Tablets in Asthmatics with Rhinoconjunctivitis. *Allergy* **2006**, *61*, 185–190. [CrossRef] [PubMed]
3. Wheatley, L.M.; Togias, A. Allergic Rhinitis. *N. Engl. J. Med.* **2015**, *372*, 456–463. [CrossRef]

4. Larsen, J.N.; Broge, L.; Jacobi, H. Allergy Immunotherapy: The Future of Allergy Treatment. *Drug Discov. Today* **2016**, *21*, 26–37. [CrossRef]
5. Holgate, S.T.; Polosa, R. Treatment Strategies for Allergy and Asthma. *Nat. Rev. Immunol.* **2008**, *8*, 218–230. [CrossRef]
6. Sharma, D.; Singh, G.; Kumar, D.; Singh, M. Formulation Development and Evaluation of Fast Disintegrating Tablets of Salbutamol Sulphate, Cetirizine Hydrochloride in Combined Pharmaceutical Dosage Form: A New Era in Novel Drug Delivery for Pediatrics and Geriatrics. *J. Drug Deliv.* **2015**, *2015*, 640529. [CrossRef] [PubMed]
7. Bizikova, P.; Papich, M.G.; Olivry, T. Hydroxyzine and Cetirizine Pharmacokinetics and Pharmacodynamics after Oral and Intravenous Administration of Hydroxyzine to Healthy Dogs. *Vet. Dermatol.* **2008**, *19*, 348–357. [CrossRef] [PubMed]
8. Durda, J.; Wedi, B.; Martin, V.; Breuer, K. Hyperresponsiveness to Antihistamines in Spontaneous Urticaria and Heat Urticaria. *Allergol Sel.* **2017**, *1*, 222–226. [CrossRef]
9. May, J.R.; Dolen, W.K. Management of Allergic Rhinitis: A Review for the Community Pharmacist. *Clin. Ther.* **2017**, *39*, 2410–2419. [CrossRef]
10. Avachat, A.M.; Gujar, K.N.; Wagh, K.V. Development and Evaluation of Tamarind Seed Xyloglucan-Based Mucoadhesive Buccal Films of Rizatriptan Benzoate. *Carbohydr. Polym.* **2013**, *91*, 537–542. [CrossRef]
11. Orlu, M.; Ranmal, S.R.; Sheng, Y.; Tuleu, C.; Seddon, P. Acceptability of Orodispersible Films for Delivery of Medicines to Infants and Preschool Children. *Drug Deliv.* **2017**, *24*, 1243–1248. [CrossRef]
12. Chachlioutaki, K.; Tzimtzimis, E.K.; Tzetzis, D.; Chang, M.-W.; Ahmad, Z.; Karavasili, C.; Fatouros, D.G. Electrospun Orodispersible Films of Isoniazid for Pediatric Tuberculosis Treatment. *Pharmaceutics* **2020**, *12*, 470. [CrossRef] [PubMed]
13. Macedo, A.S.; Castro, P.M.; Roque, L.; Thomé, N.G.; Reis, C.P.; Pintado, M.E.; Fonte, P. Novel and Revisited Approaches in Nanoparticle Systems for Buccal Drug Delivery. *J. Control. Release* **2020**, *320*, 125–141. [CrossRef] [PubMed]
14. Patel, V.F.; Liu, F.; Brown, M.B. Advances in Oral Transmucosal Drug Delivery. *J. Control. Release* **2011**, *153*, 106–116. [CrossRef] [PubMed]
15. Pamlényi, K.; Kristó, K.; Jójárt-Laczkovich, O.; Regdon, G. Formulation and Optimization of Sodium Alginate Polymer Film as a Buccal Mucoadhesive Drug Delivery System Containing Cetirizine Dihydrochloride. *Pharmaceutics* **2021**, *13*, 619. [CrossRef] [PubMed]
16. Nair, A.B.; Kumria, R.; Harsha, S.; Attimarad, M.; Al-Dhubiab, B.E.; Alhaider, I.A. In Vitro Techniques to Evaluate Buccal Films. *J. Control. Release* **2013**, *166*, 10–21. [CrossRef]
17. Hearnden, V.; Sankar, V.; Hull, K.; Juras, D.V.; Greenberg, M.; Kerr, A.R.; Lockhart, P.B.; Patton, L.L.; Porter, S.; Thornhill, M.H. New Developments and Opportunities in Oral Mucosal Drug Delivery for Local and Systemic Disease. *Adv. Drug Deliv. Rev.* **2012**, *64*, 16–28. [CrossRef]
18. Gibaja, V.; Javot, L.; Tournebize, J.; Gillet, P. Données récentes de pharmacosurveillance du fentanyl d'action rapide: Alerte sur le mésusage. *Therapies* **2021**, *76*, 165. [CrossRef]
19. Khan, S.; Boateng, J.S.; Mitchell, J.; Trivedi, V. Formulation, Characterisation and Stabilisation of Buccal Films for Paediatric Drug Delivery of Omeprazole. *AAPS PharmSciTech* **2015**, *16*, 800–810. [CrossRef]
20. Tejada, G.; Lamas, M.C.; Svetaz, L.; Salomón, C.J.; Alvarez, V.A.; Leonardi, D. Effect of Drug Incorporation Technique and Polymer Combination on the Performance of Biopolymeric Antifungal Buccal Films. *Int. J. Pharm.* **2018**, *548*, 431–442. [CrossRef]
21. Trastullo, R.; Abruzzo, A.; Saladini, B.; Gallucci, M.C.; Cerchiara, T.; Luppi, B.; Bigucci, F. Design and Evaluation of Buccal Films as Paediatric Dosage Form for Transmucosal Delivery of Ondansetron. *Eur. J. Pharm. Biopharm.* **2016**, *105*, 115–121. [CrossRef]
22. Kumria, R.; Nair, A.B.; Goomber, G.; Gupta, S. Buccal Films of Prednisolone with Enhanced Bioavailability. *Drug Deliv.* **2016**, *23*, 471–478. [CrossRef] [PubMed]
23. Kulkarni, U.D.; Mahalingam, R.; Li, X.; Pather, I.; Jasti, B. Effect of Experimental Temperature on the Permeation of Model Diffusants Across Porcine Buccal Mucosa. *AAPS PharmSciTech* **2011**, *12*, 579–586. [CrossRef]
24. Morales, J.O.; McConville, J.T. Manufacture and Characterization of Mucoadhesive Buccal Films. *Eur. J. Pharm. Biopharm.* **2011**, *77*, 187–199. [CrossRef] [PubMed]
25. Zaman, M.; Hanif, M.; Shaheryar, Z.A. Development of Tizanidine HCl-Meloxicam Loaded Mucoadhesive Buccal Films: In-Vitro and in-Vivo Evaluation. *PLoS ONE* **2018**, *13*, e0194410. [CrossRef] [PubMed]
26. Nair, A.B.; Al-Dhubiab, B.E.; Shah, J.; Vimal, P.; Attimarad, M.; Harsha, S. Development and Evaluation of Palonosetron Loaded Mucoadhesive Buccal Films. *J. Drug Deliv. Sci. Technol.* **2018**, *47*, 351–358. [CrossRef]
27. Okeke, O.C.; Boateng, J.S. Nicotine Stabilization in Composite Sodium Alginate Based Wafers and Films for Nicotine Replacement Therapy. *Carbohydr. Polym.* **2017**, *155*, 78–88. [CrossRef]
28. Tagami, T.; Ando, M.; Nagata, N.; Goto, E.; Yoshimura, N.; Takeuchi, T.; Noda, T.; Ozeki, T. Fabrication of Naftopidil-Loaded Tablets Using a Semisolid Extrusion-Type 3D Printer and the Characteristics of the Printed Hydrogel and Resulting Tablets. *J. Pharm. Sci.* **2019**, *108*, 907–913. [CrossRef]
29. Kumria, R.; Nair, A.B.; Al-Dhubiab, B.E. Loratidine Buccal Films for Allergic Rhinitis: Development and Evaluation. *Drug Dev. Ind. Pharm.* **2014**, *40*, 625–631. [CrossRef]
30. Deshmukh, K.; Basheer Ahamed, M.; Deshmukh, R.R.; Khadheer Pasha, S.K.; Bhagat, P.R.; Chidambaram, K. Biopolymer Composites With High Dielectric Performance: Interface Engineering. In *Biopolymer Composites in Electronics*; Elsevier: Amsterdam, The Netherlands, 2017; pp. 27–128. ISBN 978-0-12-809261-3.

31. Paolicelli, P.; Petralito, S.; Varani, G.; Nardoni, M.; Pacelli, S.; Di Muzio, L.; Tirillò, J.; Bartuli, C.; Cesa, S.; Casadei, M.A.; et al. Effect of Glycerol on the Physical and Mechanical Properties of Thin Gellan Gum Films for Oral Drug Delivery. *Int. J. Pharm.* **2018**, *547*, 226–234. [CrossRef]
32. Bonferoni, M.C.; Sandri, G.; Rossi, S.; Ferrari, F.; Gibin, S.; Caramella, C. Chitosan Citrate as Multifunctional Polymer for Vaginal Delivery. *Eur. J. Pharm. Sci.* **2008**, *33*, 166–176. [CrossRef]
33. Ibrahim, Y.H.-E.Y.; Regdon, G.; Kristó, K.; Kelemen, A.; Adam, M.E.; Hamedelniel, E.I.; Sovány, T. Design and Characterization of Chitosan/Citrate Films as Carrier for Oral Macromolecule Delivery. *Eur. J. Pharm. Sci.* **2020**, *146*, 105270. [CrossRef] [PubMed]
34. Kelemen, A.; Gottnek, M.; Regdon, G.; Pintye-Hódi, K. New Equipment for Measurement of the Force of Adhesion of Mucoadhesive Films. *J. Adhes. Sci. Technol.* **2015**, *29*, 1360–1367. [CrossRef]
35. Gottnek, M.; Süvegh, K.; Pintye-Hódi, K.; Regdon, G. Effects of Excipients on the Tensile Strength, Surface Properties and Free Volume of Klucel® Free Films of Pharmaceutical Importance. *Radiat. Phys. Chem.* **2013**, *89*, 57–63. [CrossRef]
36. Patel, V.F.; Liu, F.; Brown, M.B. Modeling the Oral Cavity: In Vitro and in Vivo Evaluations of Buccal Drug Delivery Systems. *J. Control. Release* **2012**, *161*, 746–756. [CrossRef] [PubMed]
37. Sander, C.; Nielsen, H.M.; Jacobsen, J. Buccal Delivery of Metformin: TR146 Cell Culture Model Evaluating the Use of Bioadhesive Chitosan Discs for Drug Permeability Enhancement. *Int. J. Pharm.* **2013**, *458*, 254–261. [CrossRef]
38. Tetyczka, C.; Griesbacher, M.; Absenger-Novak, M.; Fröhlich, E.; Roblegg, E. Development of Nanostructured Lipid Carriers for Intraoral Delivery of Domperidone. *Int. J. Pharm.* **2017**, *526*, 188–198. [CrossRef]
39. Nielsen, H.M.; Verhoef, J.C.; Ponec, M.; Rassing, M.R. TR146 Cells Grown on Filters as a Model of Human Buccal Epithelium: Permeability of Fluorescein Isothiocyanate-Labelled Dextrans in the Presence of Sodium Glycocholate. *J. Control. Release* **1999**, *60*, 223–233. [CrossRef]
40. Azarmi, S.; Roa, W.; Löbenberg, R. Current Perspectives in Dissolution Testing of Conventional and Novel Dosage Forms. *Int. J. Pharm.* **2007**, *328*, 12–21. [CrossRef]
41. Jacobsen, J.; van Deurs, B.; Pedersen, M.; Rassing, M.R. TR146 Cells Grown on Filters as a Model for Human Buccal Epithelium: I. Morphology, Growth, Barrier Properties, and Permeability. *Int. J. Pharm.* **1995**, *125*, 165–184. [CrossRef]
42. Pham Le Khanh, H.; Nemes, D.; Rusznyák, Á.; Ujhelyi, Z.; Fehér, P.; Fenyvesi, F.; Váradi, J.; Vecsernyés, M.; Bácskay, I. Comparative Investigation of Cellular Effects of Polyethylene Glycol (PEG) Derivatives. *Polymers* **2022**, *14*, 279. [CrossRef]
43. Reddy, N.; Yang, Y. Citric Acid Cross-Linking of Starch Films. *Food Chem.* **2010**, *118*, 702–711. [CrossRef]
44. Uranga, J.; Puertas, A.I.; Etxabide, A.; Dueñas, M.T.; Guerrero, P.; de la Caba, K. Citric Acid-Incorporated Fish Gelatin/Chitosan Composite Films. *Food Hydrocoll.* **2019**, *86*, 95–103. [CrossRef]
45. Rangel-Marrón, M.; Mani-López, E.; Palou, E.; López-Malo, A. Effects of Alginate-Glycerol-Citric Acid Concentrations on Selected Physical, Mechanical, and Barrier Properties of Papaya Puree-Based Edible Films and Coatings, as Evaluated by Response Surface Methodology. *LWT* **2019**, *101*, 83–91. [CrossRef]
46. Szekalska, M.; Wróblewska, M.; Trofimiuk, M.; Basa, A.; Winnicka, K. Alginate Oligosaccharides Affect Mechanical Properties and Antifungal Activity of Alginate Buccal Films with Posaconazole. *Mar. Drugs* **2019**, *17*, 692. [CrossRef]
47. Juliano, C.; Gavini, E.; Cossu, M.; Bonferoni, M.C.; Giunchedi, P. Mucoadhesive Alginate Matrices Containing Sodium Carboxymethyl Starch for Buccal Delivery: In Vitro and in Vivo Studies. *J. Drug Deliv. Sci. Technol.* **2004**, *14*, 159–163. [CrossRef]
48. Majumder, J.; Deb, J.; Husain, A.; Jana, S.S.; Dastidar, P. Cetirizine Derived Supramolecular Topical Gel in Action: Rational Design, Characterization and in Vivo Self-Delivery Application in Treating Skin Allergy in Mice. *J. Mater. Chem. B* **2015**, *3*, 6634–6644. [CrossRef]
49. Salimi, A.; Razian, M.; Pourahmad, J. Analysis of Toxicity Effects of Buspirone, Cetirizine and Olanzapine on Human Blood Lymphocytes: In Vitro Model. *Curr. Clin. Pharmacol.* **2018**, *13*, 120–127. [CrossRef]

III.

Heliyon 8 (2022) e10364

Contents lists available at ScienceDirect

Heliyon

journal homepage: www.cell.com/heliyon

Research article

Development and evaluation of bioadhesive buccal films based on sodium alginate for allergy therapy

Krisztián Pamlényi, Katalin Kristó, Tamás Sovány, Géza Regdon jr. *

University of Szeged, Institute of Pharmaceutical Technology and Regulatory Affairs, Eötvös u. 6., H-6720, Szeged, Hungary

ARTICLE INFO

Keywords:
Innovative drug delivery system
Buccal polymer film
Sodium alginate
Antihistamine
Allergy

ABSTRACT

Buccal drug administration is a less explored area, therefore researchers and companies focus on its research because of its innovative potential and opportunities. Buccal polymer films (patches) are considered to be an innovative form and have a great number of advantageous properties. Firstly, patients who suffer from swallowing problems and children can also apply them. The active pharmaceutical ingredient enters the systemic circulation directly without degradation and transformation. The aim of this study was to formulate buccal films with sodium alginate (SA) because it is a rarely used, innovative polymer for the formulation of buccal films. The mechanical, chemical properties and dosage forms of the prepared films were investigated with different methods. To formulate the films, cetirizine dihydrochloride (CTZ) was used as model drug, and glycerol (GLY) was added to make the films more elastic. The samples were prepared and stored at room temperature. As a result, it can be seen that the mechanical properties of all film compositions show good results, especially breaking hardness. The films with high SA concentration containing CTZ had appropriate mucoadhesion forces, so these samples are suitable for application on the buccal mucosa. The results of dissolution confirmed this finding. Finally, it can be said we formulated fast dissolving films and it can be concluded that the films prepared with 3% SA concentration containing 1% and 3% GLY can be recommended for buccal application.

1. Introduction

Bioadhesive drug delivery systems are becoming increasingly frequent on the market. One such system is buccal tablets, films and gels. This administration route is easy to use, so patient compliance is better than in the case of the intravenous or per os route, etc. [1]. Children, elderly people and people who suffer from swallowing problems can also use it [2]. A further advantage of this alternative route is that the active pharmaceutical ingredient can enter the systemic circulation without transformation because it avoids the first-pass effect of the liver [3]. Furthermore, local and fast systemic effects can be achieved with these systems, therefore they can be used in emergencies such as hypertensive crisis or anaphylactic shock, and also in chronic illnesses like asthma, allergy, hypertension or other chronic diseases [4, 5, 6, 7].

Mucoadhesion is the process when the materials and the mucin of the mucous membrane are held together for a long time by attractive bonding. It is defined as bioadhesion when both connecting materials are biological. Mucin is a hydrophilic macromolecule and possesses a great number of hydrogen atoms and hydroxyl groups and can therefore create primary (covalent, ionic glycosides, ester bonding) and secondary (hydrogen bonding, van der Waals forces) bonding with biological structures [8, 9]. Mucoadhesion includes several types of bonding, the major categories are adsorption theory, diffusion theory, wetting theory, fracture theory, and electrostatic theory [10]. Mucoadhesion force and the time of mucoadhesion are also important for the application because if one of these two parameters is not sufficient, the absorption of the active pharmaceutical ingredient (API) cannot occur.

The first step in the development is the selection of the polymer material with mucoadhesive properties. Many polymers are available with different parameters [11]. Polymers can be from natural sources, semi-synthetic, and synthetic. The most commonly used polymers are cellulose derivatives such as hydroxypropyl cellulose (HPC), hydroxypropyl-methylcellulose (HPMC), but chitosan, sodium alginate (SA), polyacrylic acid (PAA) and polyethylene glycol (PEG) are also common [12, 13, 14, 15, 16]. Plasticizers are also important additives in the formulation. They can increase the elasticity of the films and make the application easier, such are, for example, glycerol and mannitol [17]. In addition, many additives can be applied in polymer films, such as solvents, taste-masking agents, permeation enhancers, saliva-stimulating agents, etc. [18, 19, 20].

* Corresponding author. ,
E-mail addresses: geza.regdon@pharm.u-szeged.hu, geza.regdon@gmail.com (G. Regdon jr.).

https://doi.org/10.1016/j.heliyon.2022.e10364
Received 29 March 2022; Received in revised form 16 July 2022; Accepted 15 August 2022

In the literature, there are some studies that investigated the effect of the polymer material and the plasticizer or any other ingredient in films, but in these studies the authors did not apply an API despite the fact that the API can remarkably change the properties of films and in terms of use, it would be important to investigate them together [14, 21, 22, 23]. The selected API has to meet some criteria. The applied amount of the API should not exceed 40–50 mg per one dose, it should be soluble in water or in other solvent, and without these criteria formulation is not possible [23, 24].

SA is a rarely used polymer in the formulation of mucoadhesive systems, but it has many advantageous properties [25]. SA is an anionic, natural, non-toxic, biodegradable, biocompatible polymer with appropriate mucoadhesive properties [26, 27]. It can be extracted from brownseeds. SA has many hydroxyl and carboxyl groups, which allow it to create bonding with the mucin of the buccal mucosa [28].

In our previous work, we formulated buccal films with HPMC and SA [27]. HPMC is a conventional and much studied excipient in pharmaceutical technology, therefore we mixed it with SA in that work [27]. In our current project, we used only SA as a polymer film-forming agent without HPMC because the film-forming properties of SA seem to be promising based on our previous work. The aim of the current project was to investigate the film-forming ability of SA and to formulate polymer films from SA which can be applied on the buccal mucosa. This would be a novel additive from the aspect of administration. Our further aim was to incorporate other components in the films, such as glycerol (GLY) and cetirizine dihydrochloride (CTZ). GLY was used as a plasticizer, while CTZ was the model drug. It is a second-generation (non-sedative) antihistamine and a common drug in the oral treatment of allergy [29]. Another purpose of our work was to investigate the mechanical, *in vitro* mucoadhesive and physical-chemical properties of prepared films. In addition, we studied the effect of the plasticizer and the API on the mechanical properties of these films.

2. Materials and methods

2.1. Materials

SA (Biochemica GmbH, Germany) (10,000–600,000 g/mol) was used as a film-forming agent in the preparation of buccal films. GLY 85% (w/w %) was added to the film as a plasticizer (Ph. Eur. 8.). CTZ (Ph. Eur. 8.) was applied as an active ingredient in the polymer films. It was a gift from Extractum Pharma Pharmaceutical Manufacturing, Marketing and Consulting Inc. Distilled water was used as a solvent.

2.2. Preparation of the films

Buccal films were prepared at room temperature with the solvent casting method. At the beginning of preparation, SA (2, 3 w/w%) was dissolved in distilled water and mixed (900 rpm) at room temperature. After solvation, CTZ was added to the polymer solution (0.5523 g/100 g solution) for 8 h. In the third step, GLY (1, 3, 5 w/w%) was incorporated into the solution the following day. Mixing was decreased to 100 rpm for 3 h to make the air bubbles disappear from the solution. The solution was cast on Teflon surface in rubber rings with a diameter of 6.7 cm, with 10 g of solution/ring, then the solvent was evaporated at room temperature (25 ± 0.5 °C) for 72 h. The Teflon surface was selected because the films can be removed easily from the surface and the films do not stick to it. At the same time, Teflon is an inert material, no chemical interactions can take place between the film components and the surface. The dried polymer films were removed from the Teflon surface, were put in closed containers and were stored at room temperature during the investigations. The preparation method was the same for all films to ensure the same conditions.

As can be seen, Table 1 contains Samples 1–18. Four compositions contained 4% SA (Sample 3, Samples 16–18). The preparation of these samples was difficult because of their high viscosity due to the high concentration of the polymer. Also, these samples had several disadvantages in terms of application, such as large thickness and breaking hardness, low flexibility. Therefore no further investigations were done with Sample 3, Samples 16–18.

Table 1. Composition of prepared films.

Samples	SA (w/w%)	GLY (w/w%)	CTZ (10 mg)
1	2	-	-
2	3	-	-
3	4	-	-
4	2	1	-
5	2	3	-
6	2	5	-
7	3	1	-
8	3	3	-
9	3	5	-
10	2	1	+
11	2	3	+
12	2	5	+
13	3	1	+
14	3	3	+
15	3	5	+
16	4	1	-
17	4	3	-
18	4	5	-

Table 1 shows the prepared polymer films of different compositions. Samples 10 to 15 are marked in grey because these films contain CTZ.

2.3. Thickness of the films

The thickness of the polymer films was measured with a screw micrometre (Mitutoyo Co. Ltd, Japan), sensitivity was 0.001 mm. Six points were selected randomly from all films (n = 6). The means and standard deviations (SD) were evaluated from these data.

2.4. Breaking hardness of the films

Breaking hardness was tested with a self-developed device and software. The device, seen in Figure 1, and the software were developed at our institute [21, 30]. The device has two different types of sample holder as probes (needle-like probe, rod-like probe). The equipment has a fix disc and a vertically moving jowl. Force, force-displacement and time can be registered. A different sample holder can be applied depending on the test. The breaking hardness of the films can be examined with the needle-like probe (its area was 201 mm^2). At the beginning of the test, the sample was fixed on the bottom part of the equipment and the probe was lowered at constant speed (20 mm/min). The probe moved towards the film and finally it broke the film. The equipment detected the time, force and deformation during the test. The test was finished when the film was broken. The measuring range was 0–200 N, the sampling rate was 50 Hz, the output was 0–5 V, and the sensitivity was ±0.1 N [14]. The test was repeated six times (n = 6) for each film. Tablets, pellets, films can also be investigated with this equipment. The means and standard deviations were calculated.

2.5. In vitro mucoadhesivity study

Mucoadhesion was tested with the same self-developed analyser with different parameters and modifications. During the investigation, the rod-like probe was used as sample holder with a diameter of 5 mm. A double-sided adhesive tape was put on the surface of the sample holder, and the polymer samples were fixed on the other side of the adhesive tape. A 35-mm-diameter disc was fixed on the bottom part of the

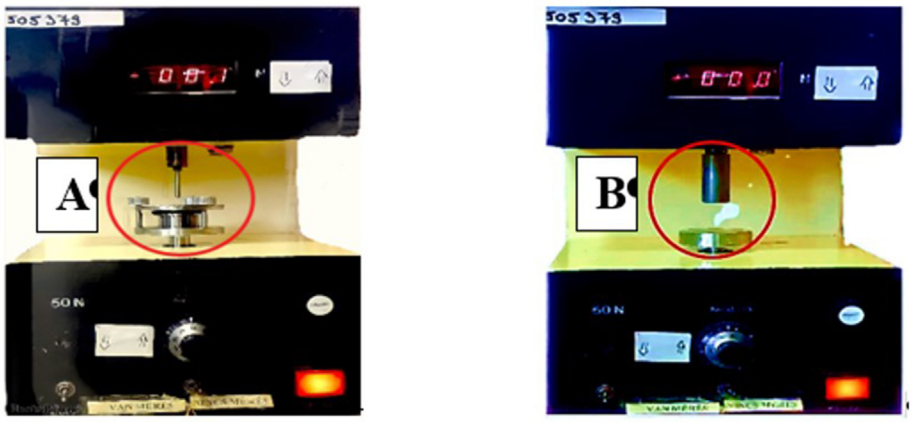

Figure 1. Schematic picture of the self-developed texture analyser. A measures the breaking hardness of films, while B measures the mucoadhesion force of films [31].

equipment. To this area, 40 μl of freshly prepared mucin dispersion was injected from measurement to measurement. The mucin dispersion was prepared in situ before the investigation, 1 g of mucin was mixed in 10 g of distilled water (10 w/w%). The rod-like sample holder was moved downward and squeezed to the bottom disc, which contained the mucin, with 30 ± 0.1N for 30 s. This constant state part, which can be seen in the force-time curve, is the first phase of the study. During the second phase, the sample holder went upwards, and the force was decreased until the sample started to separate from mucin, which can be detected as a well-defined peak in the force -time curve. The peak maximum indicates mucoadhesion force. The test was repeated five times (n = 5) and the means and standard deviations were calculated.

2.6. HATR FT-IR spectroscopy measurement

The FTIR spectra of the raw materials and the polymer films were investigated with an Avatar 330 FT-IR apparatus (Thermo-Scientific, USA). The equipment was coupled with a Zn/Se HATR (horizontal attenuated total reflectance) plate. The films were put directly on a clean crystal of the apparatus. The applied spectral range was 600–4000 cm^{-1} during the investigation. The spectra were collected from 128 scans to obtain smooth spectra, at the spectral resolution of 4 cm^{-1} with CO_2 and H_2O correction. The aim of the FTIR measurement was to investigate and determine the chemical interactions between the components of the films. FTIR spectroscopy demonstrated the different interactions that take place in the polymer film system, as can be seen in the results. The explanation of physical phenomena usually derives from chemical processes, therefore it is required to know the chemical background. We tried to find a connection between the chemical interactions and the other properties of the films.

2.7. Thermoanalytical measurement (thermogravimetric analysis (TGA), differential scanning calorimetry (DSC))

The thermoanalytical measurement of the prepared films was carried out with a Mettler-Toledo TGA/DSC1 instrument (Mettler Toledo, Switzerland). Small pieces of films (approximately 10 mg) were placed in aluminum pans (100 μL), and were inserted into the instrument. During the measurement, the start temperature was 25 °C and the end temperature was 500 °C. The heating rate was 10 °C/min. The samples were investigated in flowing nitrogen atmosphere, the flow rate was 50 ml/min. The curves were evaluated from the average of two parallel measurements with STARe software [32, 33].

2.8. Dissolution test

Pieces of film of the size of 2 × 2 cm (containing 10 mg of cetirizine dihydrochloride) were used in the dissolution test. Erweka DT700 dissolution equipment with basket tester was used in the investigation. The mixing speed was 100 rpm and the temperature was 37 °C. The dissolution medium was 900 ml of phosphate buffer (pH = 6.8). Aliquots were 5 ml and were analysed in 5, 10, 15, 20, 30, 40, 50, 60, 90, 120 min with Genesys 10S UV-VIS (Thermo Fisher Scientific, USA) UV-spectrophotometry at λ = 207 nm, which was a sharp and characteristic peak of the raw material CTZ. This peak was determined to create a calibration solution from CTZ with distilled water. The UV spectra of the raw materials were collected and the peak of the raw materials did not interfere with the peak of CTZ at 207 nm.

2.9. Statistical analyses

The significance test of breaking hardness and *in vitro* mucoadhesivity was evaluated with Microsoft Excel (version 15, Redmond, Washington USA) as software. A Two-Sample T-Test was applied. The test was run six times for each sample. In all cases, the samples were compared to the composition without CTZ. In each case, we used a significance level $p < 0.05$. Significance is labelled as ns = $p < 0.05$; *

3. Results

3.1. Thickness of the films

Table 2 shows the thickness of the films prepared in different compositions. As we can see, the thinnest film is Sample 1 (67.45 μm), which was formulated without GLY and CTZ, and it contained the least amount of SA. The concentration of SA can increase thickness, and a similar effect can be observed in the case of raising the GLY concentration. Sample 3 is thicker (212.43 μm) than Sample 2 (99.34 μm), and Sample 9 (177.38 μm) is also thicker than Sample 7 (106.63 μm). CTZ can also increase thickness, the films containing CTZ have greater thickness than their CTZ-free counterparts (Sample 10–105.23 μm, Sample 4–98.29 μm). However, it can be stated that GLY increased thickness to a greater extent than CTZ due to the fact that GLY has a water retention effect [34]. At the same time, SA can also increase the thickness of the films because SA and CTZ can enhance the dry matter content of the films.

3.2. Breaking hardness of the films

The breaking hardness of films is an important investigation with respect to application. The patient has to place the film on the buccal mucosa. During application, the patient exerts force on the film, therefore the film must have sufficient breaking hardness to resist the force and have adequate flexibility. During the preformulation study, we tried to simulate the application force to the mucosa with our fingers. The moving part of our equipment was removed and the film was pressed with fingers, with a force similar to that applied by the patients when

Table 2. Thickness of the polymer films.

Samples	Thickness (μm)	Standard deviation of thickness (μm)
1	67.45	±8.53
2	99.34	±10.38
3	212.43	±4.92
4	98.29	±6.38
5	135.66	±9.86
6	199.33	±7.53
7	106.63	±8.42
8	123.12	±3.36
9	177.38	±6.92
10	105.23	±5.18
11	148.03	±13.88
12	212.32	±3.43
13	158.05	±4.34
14	194.14	±2.97
15	253.17	±11.30

pressing it to the mucosa. We concluded that a force of 120 N is sufficient to create mucoadhesion to the buccal mucosa. So films must have breaking hardness greater than 120 N to be appropriate for application. Figure 2 shows the breaking hardness of films of different compositions. The significance results are marked with * (*; $p < 0.05$). The breaking hardness of SA-based films is high because the chains of SA can create a strong cohesive structure [27]. This hardness was decreased by GLY, probably GLY increases the bonding distance between the molecules, therefore the film has a lower breaking point despite the higher amount of plasticizer. Before the breaking point, these films were more elastic due to the plasticizer. CTZ can also influence this parameter of films, it can enhance the strength of films due to creating bindings with SA and GLY. The investigation of Samples 16–18 reveals that in the films containing 4% polymer concentration the effect of GLY cannot prevail, presumably the large number of polymer chains can create a very strong structure and GLY cannot degrade the structure. During preparation, this great hardness was also experienced because of high viscosity. Overall, it can be said that most of the compositions have appropriate breaking hardness because all the films containing CTZ have greater breaking hardness than 120 N, except for Sample 12.

3.3. *In vitro* mucoadhesivity study

In vitro mucoadhesivity study is another important investigation in terms of application because the films must adhere to the mucosa for the absorption of the API. Figure 3 shows the results of this study. The significance results are marked with * (*; $p < 0.05$).

As SA is a mucoadhesive polymer, it can noticeably increase the mucoadhesion force of films due to the high number of free chains which can bind to the mucin of the buccal mucosa. Sample 3 has the largest mucoadhesion force from among the films of different compositions. The 2 and 3% films, which contain GLY but no CTZ, have similar mucoadhesive properties. The addition of a low amount of GLY to the film can cause higher mucoadhesion force. This observation can be explained by the plasticizer effect of GLY. As a result, the films become more elastic and fit better with the probe and with the bucca than without plasticizer. The higher GLY concentration causes less mucoadhesion force, so GLY reduces the mucoadhesivity of the prepared films. The reason for this conclusion may be that an interaction may occur between the carboxyl group of GLY and CTZ and SA, leaving fewer free carboxyl groups which can bind to the oligosaccharide units of mucin. This observation can be confirmed by the results of FT-IR measurements.

From the mucoadhesivity data, we found that the films with 2% SA concentration have 7.44 ± 0.23 N. The films with 3% SA concentration have a value close to 18 N with our equipment. It is known from the literature that the SA has smaller mucoadhesivity (with our equipment more than 7 N) than cellulose derivatives, but its mucoadhesivity is also sufficient to bind to the buccal mucosa [35]. We drew the limit at 7 N. So if the mucoadhesivity of the different compositions is larger than 7 N, it means they have sufficient force for buccal mucoadhesion.

Films containing CTZ have less mucoadhesion force compared to their counterparts without CTZ, as can be seen in Figure 3. It can be concluded that CTZ decreases the mucoadhesion force of films. The 2% polymer films containing CTZ have very low mucoadhesivity, their force is less than 5 N. Because of the low forces, these compositions are not suitable for application on the buccal mucosa. The 3% polymer films containing CTZ have better mucoadhesivity properties, their force is almost 10 N, except for Sample 15 containing 5% GLY.

3.4. *FT-IR spectroscopy measurement*

FT-IR spectroscopy as an interaction study was carried out to obtain information about the interactions between the API and other excipients

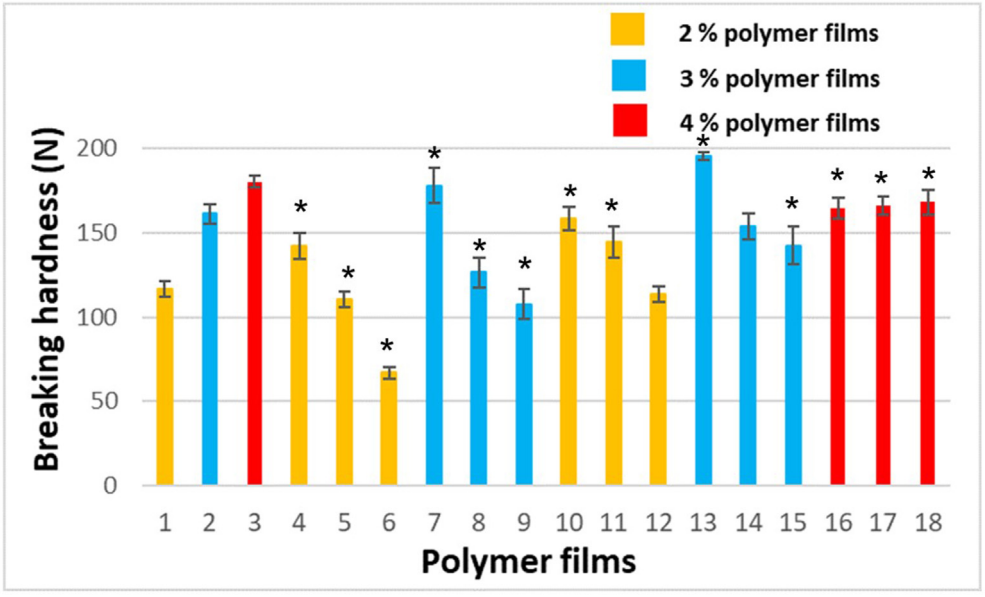

Figure 2. Breaking hardness of the prepared films.

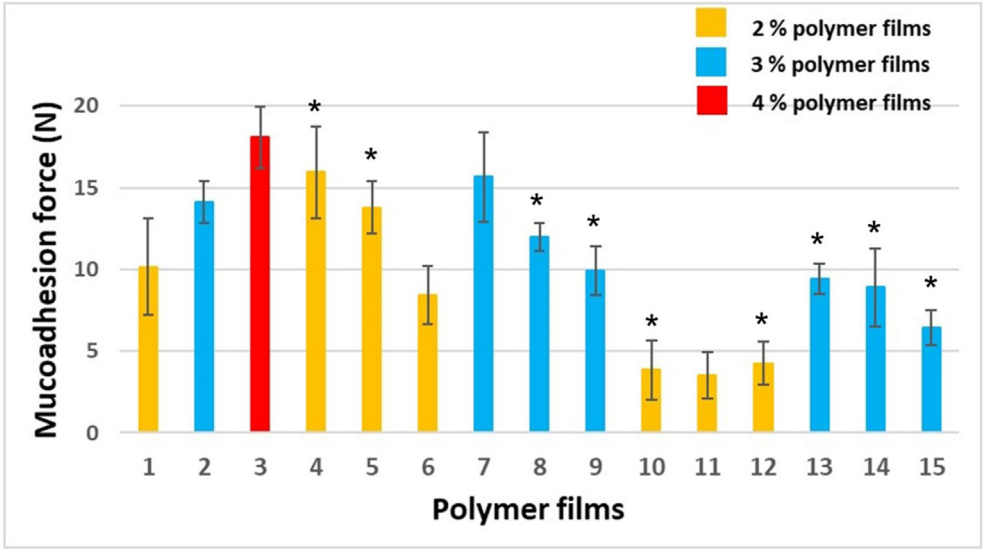

Figure 3. Mucoadhesion force of the prepared films.

in the film. The results of the FT-IR investigation can be seen in Figure 4 and Figure 5. In both spectra, there is a peak at 3340 cm^{-1}, which corresponds to the O–H stretching vibration of GLY [36]. This peak shifts to the lower frequency zone and its intensity increases with higher GLY concentration. This observation can be attributed to weak interactions, intermolecular hydrogen bonds between SA, GLY and CTZ.

The peak at 1739 cm^{-1} may appear, which determines the carboxyl group of the API [37]. This peak disappears as the amount of the polymer and the plasticizer increases. Figure 4 shows a peak shifted to the lower wavenumber in the case of the 2% polymer films, and the shifted peak is larger when increasing the GLY concentration. With 3% SA and high concentrations of GLY, this peak totally disappears and becomes unidentifiable (Figure 5). This phenomenon shows a strong interaction (hydrogen bonding) between the carboxylic group of CTZ and the OH^- group of the polymer and the plasticizer.

In the spectra, there are two characteristic peaks at 1586 cm^{-1} and 1412 cm^{-1}. These peaks represent the asymmetrical and symmetrical stretching vibration of COO^- groups. As a function of GLY concentration, the intensity of the peak may increase in the case of films with 3% polymer concentration, as shown in Figure 4 and Figure 5. This

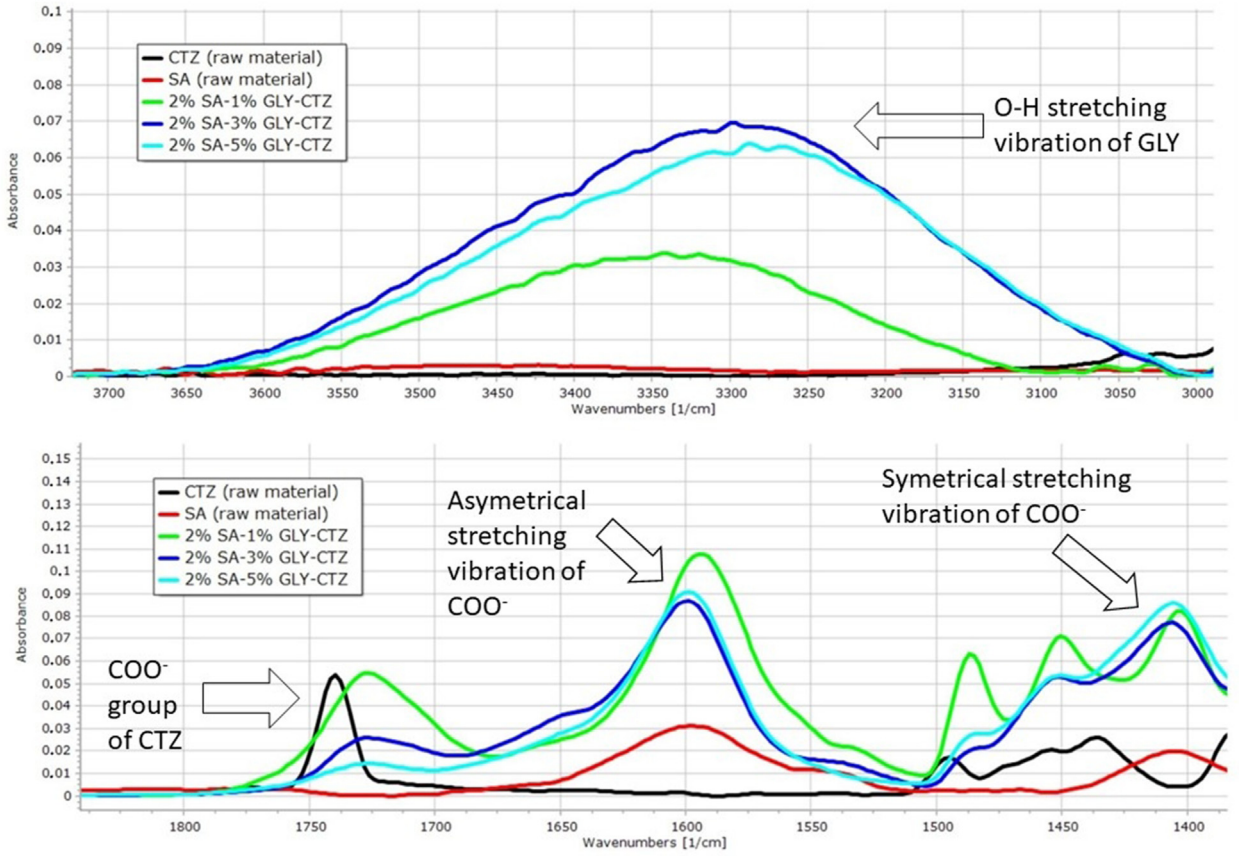

Figure 4. Spectra of raw materials and 2% polymer films.

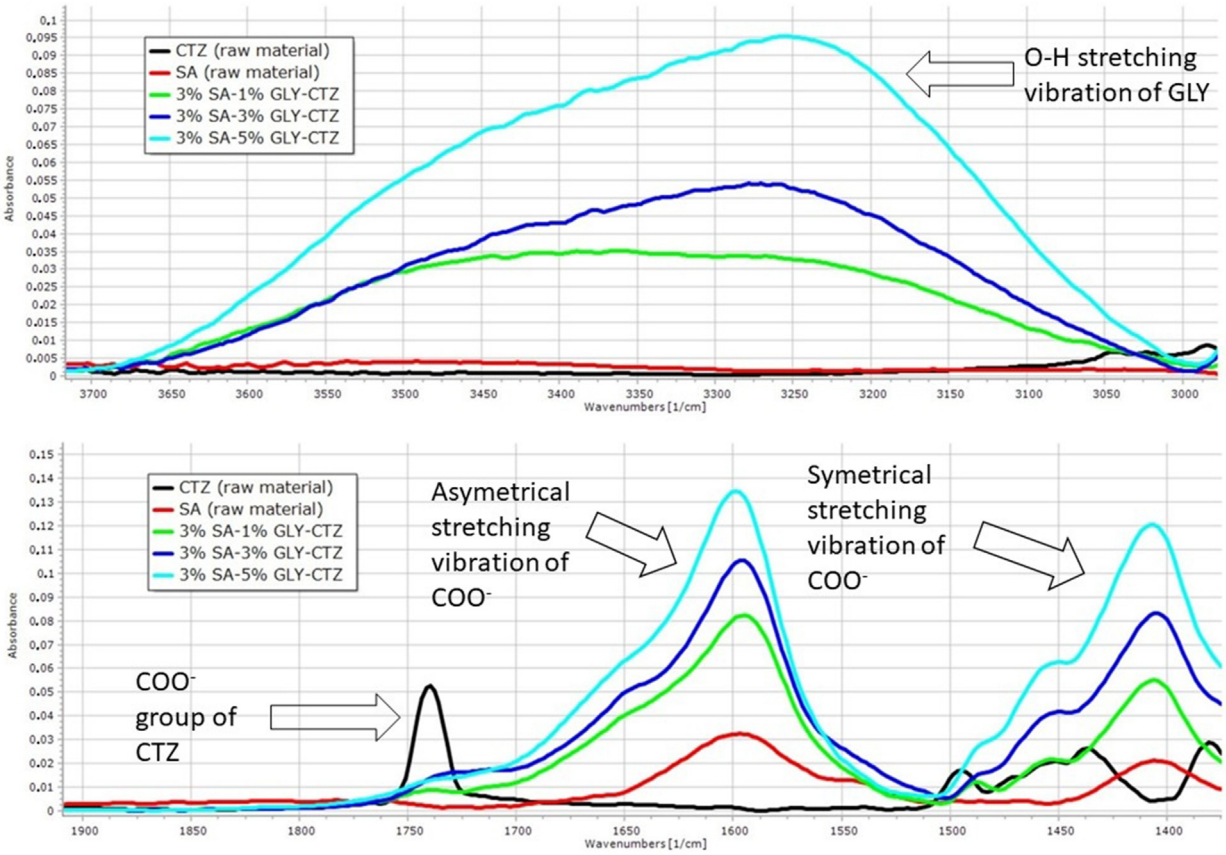

Figure 5. Spectra of raw materials and 3% polymer films.

phenomenon is due to the interaction between CTZ, SA and GLY, as can be seen at 1739 cm^{-1} also. The reason for this observation is that the 3% polymer films contain more free COO^{-} groups than the 2 % polymer films, therefore a higher peak can be detected in this area in Figure 5.

The results of the FT-IR measurement can be related to the mechanical properties of the films and the dissolution test. As can be seen from the FT-IR measurements, at 1739 cm^{-1} a strong interaction can occur in the 3% polymer films, which means these films have a cohesive, stable structure with higher breaking hardness and higher mucoadhesivity than the 2% polymer films. At the same time, these strong interactions can slow drug release because the hydrogen bond can cause a stable structure and it is more resistant to the degradation effect during the dissolution

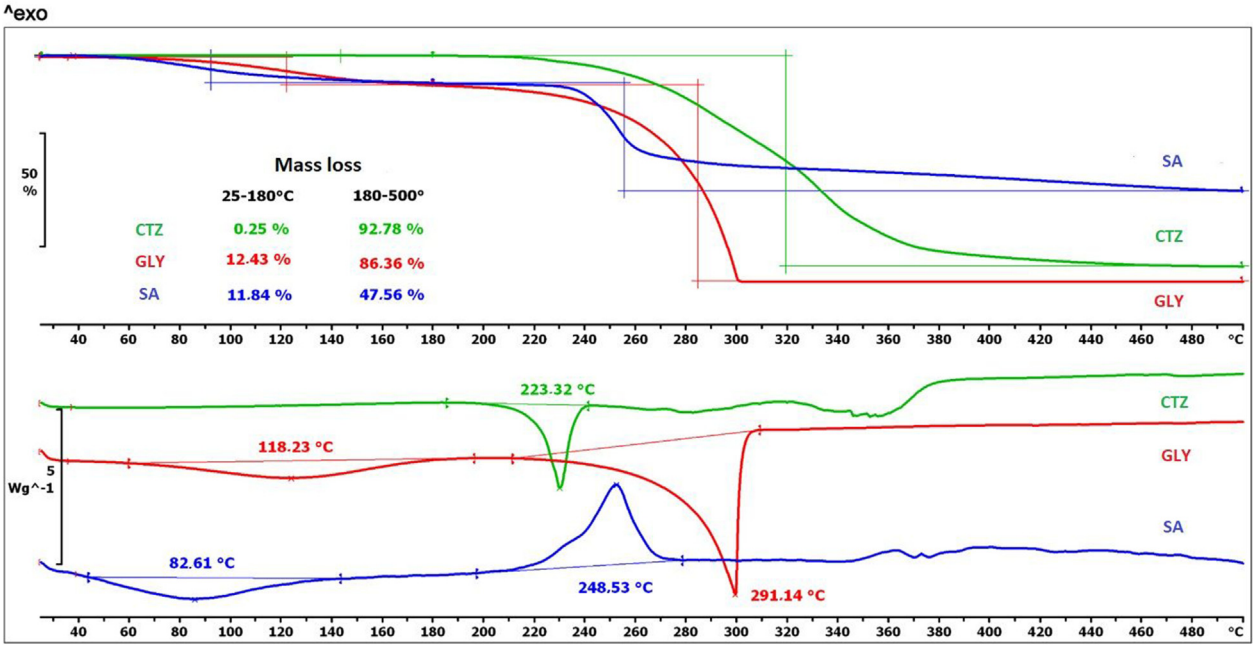

Figure 6. Thermal properties of raw materials as shown by TGA and DSC curves.

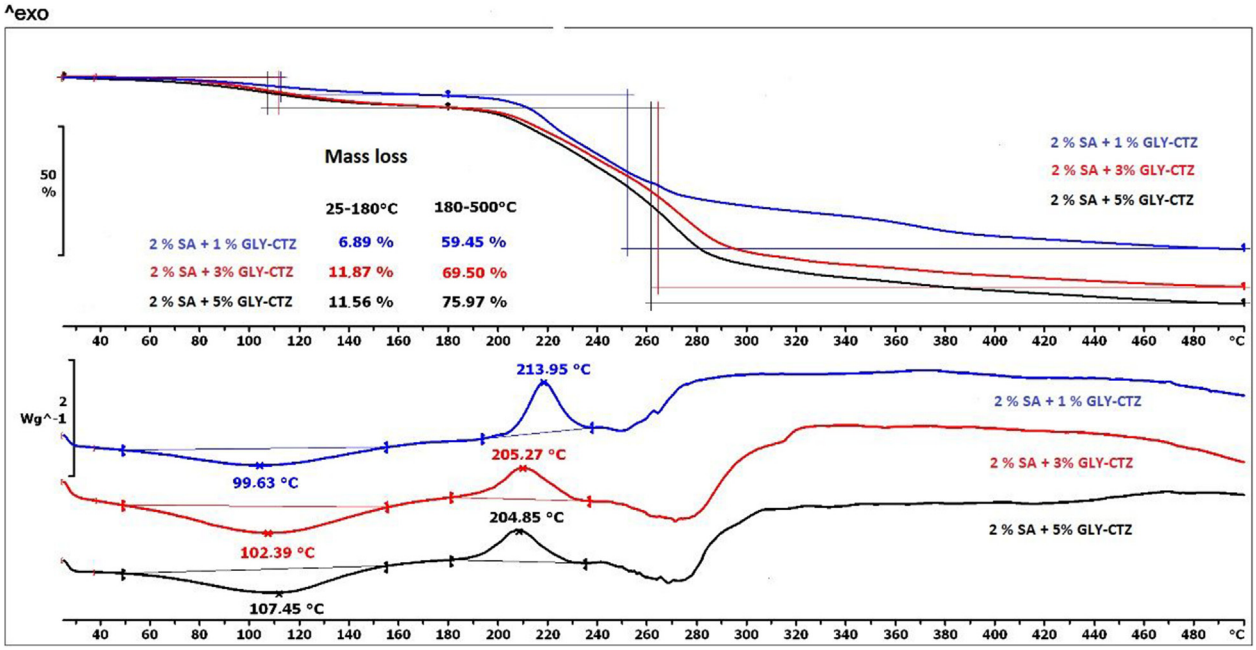

Figure 7. Thermal properties of the 2% polymer films as shown by TG and DSC curves.

test. The effect of GLY concentration on drug release is connected to the interaction at 3300 cm^{-1}, so the films with the highest GLY concentration can form the strongest interactions, therefore the dissolution is the slowest in the case of this film composition.

As a conclusion, we focused on identifying the chemical interactions between the components of films with FT-IR spectroscopy. It is important to know because chemical interactions can influence the physical parameters of the film. From our results, it can be concluded that strong interactions can occur between SA, GLY and CTZ. Typically, hydrogen bonds can be formed in the films, and the strength of the bond depends on the polymer concentration. These interactions affect mostly the dissolution of the API. The purpose of the FT-IR measurement was achieved.

3.5. Thermoanalytical measurement (TGA, DSC)

In Figure 6 the TGA and DSC curves of the raw materials can be seen. The TGA curves in Figure 6 show that the mass loss of the film-forming agent is 11.84% until 180 °C, and 47.56% until 500 °C. The decomposition process starts from 75 °C. For GLY, the mass loss is almost similar until 180 °C, but it is more than 86% until 500 °C. The mass loss curve of CTZ reveals that the decomposition starts above 200 °C, so CTZ can be said to be a thermostable API.

The DSC curve of SA shows an endothermic peak from 40 °C to 150 °C and an exothermic peak is visible from 200 °C to 280 °C. For GLY, 2 peaks can also be detected. The first peak appears at 118.23 °C, it is an endothermic peak. The second peak starts from 215 °C and ends at 320 °C.

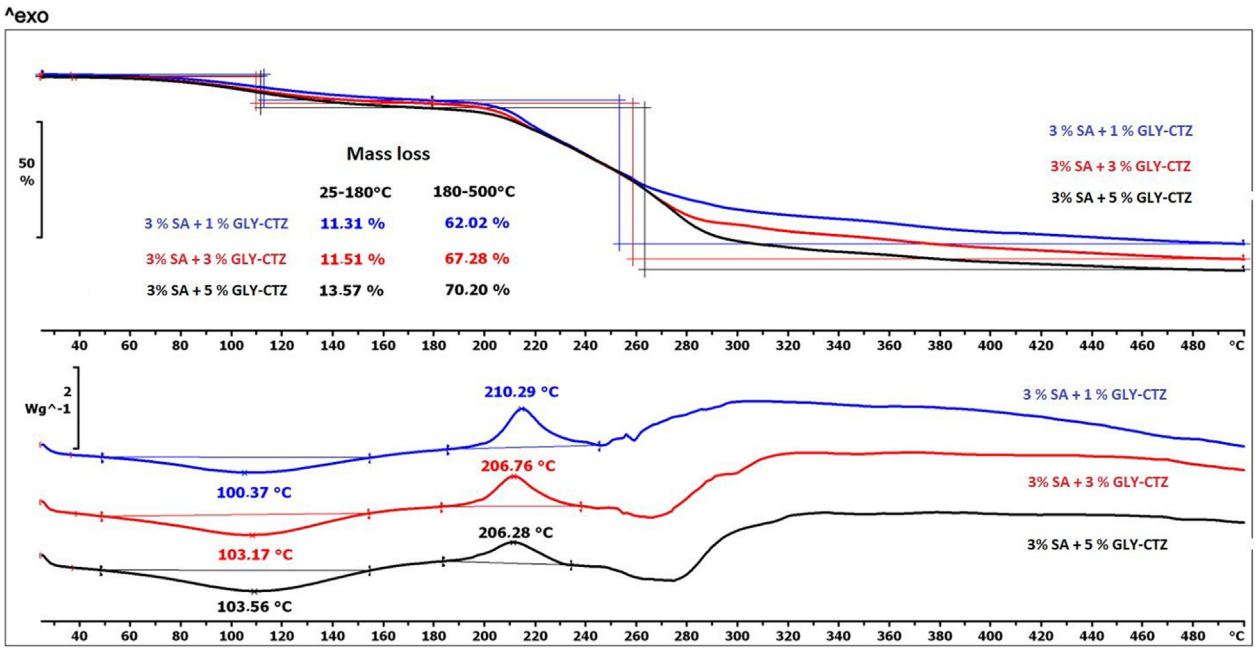

Figure 8. Thermal properties of the 3% polymer films as shown by TG and DSC curves.

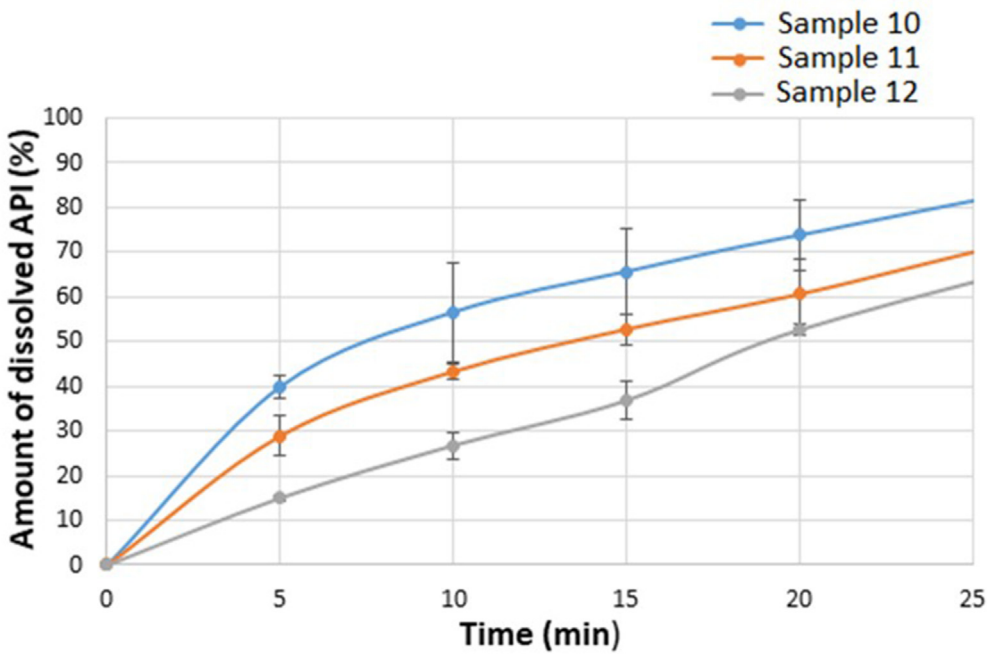

Figure 9. Dissolution curves of the 2% polymer concentration films under 20 min.

This peak indicates the decomposition of GLY. The decomposition of CTZ starts after the melting point, which can be seen at 223.32 °C, followed by the general decomposition of CTZ.

After the examination of the excipients, we wished to investigate the behaviour of the prepared films and explore the interaction between the excipients. The results of the thermal behaviour of films can be found in Figure 7 and Figure 8. Figure 7 shows the thermal behaviour of 2% polymer films, and in Figure 8 the thermoanalytical curves of 3% polymer films can be seen. The decomposition of buccal films can take place in two steps. In the first step (until 180 °C), it is visible that films with the lowest GLY concentration (Sample 10) have the lowest mass loss, which can be explained by the lower water content of films with low GLY concentration. In the case of larger GLY and SA concentrations, which result in a higher water content, there is no significant difference in the mass loss of Samples 11–15.

In the second step of Figure 7 and Figure 8, the same observations can be made, but the values of the mass loss of the films with different compositions are higher and can be detected from 60% to 75% due to the remarkable decomposition of CTZ and GLY and a little bit of SA.

Two characteristic peaks of SA can be found in the DSC curves of the films with different compositions (Figure 7 and Figure 8). The first peak shifts towards higher temperature with increasing GLY concentration. This observation may reveal a moderate interaction between the excipients of the films, which may indicate the presence of hydrogen bonds. This fact confirms the results of FT-IR spectroscopy. The second (exothermic) peak of the DSC curves also shows a shift with increasing

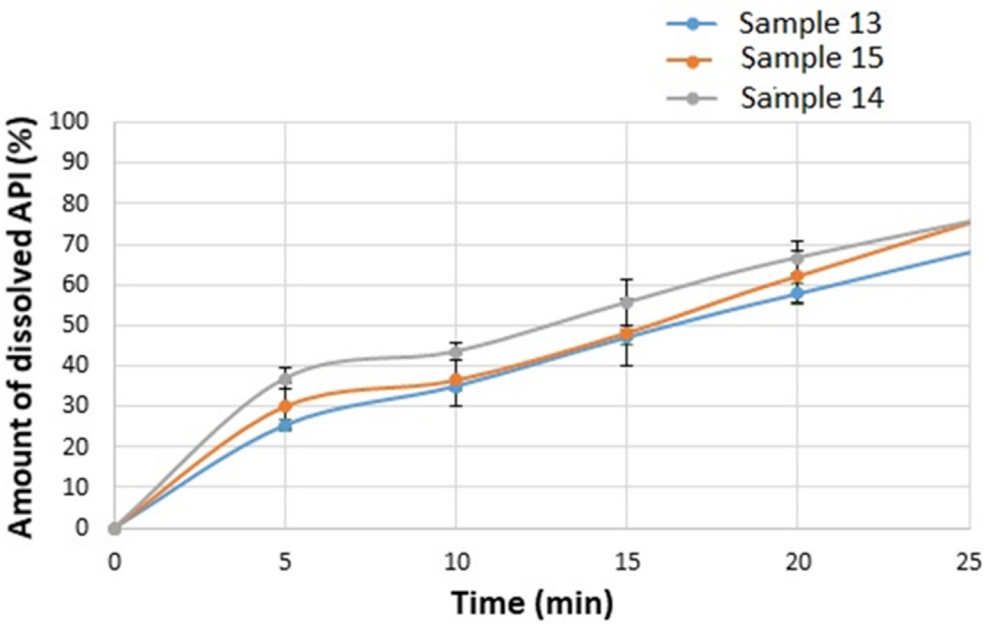

Figure 10. Dissolution curves of the 3% polymer concentration films under 20 min.

GLY concentration, the exothermic peak moves towards the lower temperature. This correlation appears to be notable for the films with 1% and 3% GLY concentrations, but it is not noticeable for films with medium and high GLY concentrations. The correlation can be applied to films with 2% and 3% SA concentrations.

In summary, the decomposition processes generally start from 70 °C, so the polymer films can be considered thermally stable up to this temperature.

3.6. Dissolution test

The dissolution study is one of the most important dosage form tests. The results of the dissolution study of the films with 2 % polymer concentration are shown in Figure 9. During the whole test (120 min), the total amount of CTZ dissolved from the different compositions of the films. In the first 20 min, the largest amount dissolved from the composition containing less GLY, around 73% more than from films with a higher GLY content. Less API could dissolve from the film with 5% GLY concentration, in this case less than 55%. GLY can remarkably reduce the speed of dissolution. This fact is the most likely related to the stronger bonding between the components.

Figure 10 shows the dissolution of the 3% polymer films. From these films, the total amount of CTZ could also dissolve during the whole test. There is no significant difference between the amount of the dissolved API and the different plasticizer concentrations of the 3% polymer films. A difference can be detected in the shape of the curves. In the case of 2% polymer films, the curves are comparable to a saturation curve without steady state stage. The curves of the films with 3% polymer concentration have a step between 7 and 10 min, in this period steady state can be detected, which can also be explained by the structural relationships between SA, GLY and CTZ, which is supported by FT-IR spectroscopy measurement. A more stable structure can be created, therefore it takes time for the cohesive and adhesive structure to degrade and for the drug to be released.

4. Conclusion

In our present research, we focused on the film-forming ability of SA and on formulating buccal films with SA. In the films, CTZ was applied as a drug. The mechanical properties of the films showed that SA can create a strong, cohesive structure, and due these properties all compositions had a very large breaking hardness. It can be concluded from the result that the amount of SA and CTZ can increase this film parameter, but GLY reduces it.

From the mucoadhesion study, we can observe the good mucoadhesive properties of SA, while GLY and CTZ reduce the mucoadhesion force of films. The films with 2% polymer concentration containing API had no satisfactory mucoadhesivity, so Samples 10–12 cannot be used on the buccal mucosa, whereas the films with 3% polymer concentration containing CTZ had fine mucoadhesivity property.

By the FT-IR measurement, weak and strong interactions between the different excipients can also be detected. These interactions can typically be identified as hydrogen bondings, which confirmed the results of the mechanical properties of the films, especially breaking hardness.

Thermal analysis can also detect interactions between the different materials in the films. This interaction determines that hydrogen bondings can be created in the films. The observation of interaction between the excipients was proved with two different measurements. Due to this phenomenon, the thermal stability of films can increase in the first place, but it can also increase mechanical stability. The films are thermally stable up to 70 °C, so it is possible to increase the temperature of preparation to speed up the production.

Overall, it can be stated that we formulated a fast dissolving buccal film from SA and found promising compositions, especially Sample 13 (3 % SA+1% GLY-CTZ) and Sample 14 (3 % SA+1% GLY-CTZ), which are suitable and possible to apply as a buccal drug delivery system.

Declarations

Author contribution statement

Krisztián Pamlényi: Conceived and designed the experiments; Performed the experiments; Analyzed and interpreted the data; Wrote the paper.

Katalin Kristó: Conceived and designed the experiments; Analyzed and interpreted the data; Wrote the paper.

Tamás Sovány: Analyzed and interpreted the data; Wrote the paper.

Géza Regdon jr: Conceived and designed the experiments; Analyzed and interpreted the data; Contributed reagents, materials, analysis tools or data; Wrote the paper.

Funding statement

This work was supported by The University of Szeged Open Access Fund (FundRef, Grant No. 5651), was also supported by Richter Gedeon Talentum Foundation (Grant No. 010819) and the ÚNKP-21-3 New National Excellence Program of the Ministry for Innovation and Technology from the Source of the National Research, Development and Innovation Fund (Grant No. ÚNKP-21-3).

Krisztián Pamlényi was supported by Richter Gedeon Talentum Foundation (Grant No. 100108190822).

Data availability statement

Data will be made available on request.

Declaration of interest's statement

The authors declare no conflict of interest.

Additional information

No additional information is available for this paper.

Acknowledgements

The authors thank Extractum Pharma Pharmaceutical Manufacturing, Marketing and Consulting Inc. for supplying cetirizine dihydrochloride.

References

[1] A.S. Macedo, P.M. Castro, L. Roque, N.G. Thomé, C.P. Reis, M.E. Pintado, P. Fonte, Novel and revisited approaches in nanoparticle systems for buccal drug delivery, J. Contr. Release 320 (2020) 125–141.

[2] B. Fonseca-Santos, M. Chorilli, An overview of polymeric dosage forms in buccal drug delivery: state of art, design of formulations and their in vivo performance evaluation, Mater. Sci. Eng. C 86 (2018) 129–143.

[3] J. Xu, S. Strandman, J.X.X. Zhu, J. Barralet, M. Cerruti, Genipin-crosslinked catechol-chitosan mucoadhesive hydrogels for buccal drug delivery, Biomaterials 37 (2015) 395–404.

[4] A.I. Raafat, G.A. Mahmoud, A.E.-H. Ali, N.A. Badawy, M.F. Elshahawy, *In vitro* evaluation of mucoadhesive and self-disinfection efficiency of (acrylic acid/polyethylene glycol)-silver nanocomposites for buccal drug delivery, J. Bioact. Compat Polym. 33 (2018) 95–115.

[5] M.A. Rogawski, A.H. Heller, Diazepam buccal film for the treatment of acute seizures, Epilepsy Behav. 101 (2019), 106537.

[6] R. Kumria, A.B. Nair, G. Goomber, S. Gupta, Buccal films of prednisolone with enhanced bioavailability, Drug Deliv. 23 (2016) 471–478.

[7] A. Flo, A.C. Calpena, L. Halbaut, E.I. Araya, F. Fernández, B. Clares, Melatonin delivery: transdermal and transbuccal evaluation in different vehicles, Pharm. Res. (N. Y.) 33 (2016) 1615–1627.

[8] G. Sandri, M. Ruggeri, S. Rossi, M.C. Bonferoni, B. Vigani, F. Ferrari, (Trans)buccal drug delivery, in: Nanotechnology for Oral Drug Delivery, Elsevier, 2020, pp. 225–250.

[9] P. Laurén, H. Paukkonen, T. Lipiäinen, Y. Dong, T. Oksanen, H. Räikkönen, H. Ehlers, P. Laaksonen, M. Yliperttula, T. Laaksonen, Pectin and mucin enhance the bioadhesion of drug loaded nanofibrillated cellulose films, Pharm. Res. (N. Y.) 35 (2018) 145.

[10] M.L. Bruschi, S.B. de Souza Ferreira, J. Bassi da Silva, Mucoadhesive and mucus-penetrating polymers for drug delivery, in: Nanotechnology for Oral Drug Delivery, Elsevier, 2020, pp. 77–141.
[11] F. Laffleur, Mucoadhesive polymers for buccal drug delivery, Drug Dev. Ind. Pharm. 40 (2014) 591–598.
[12] O.C. Okeke, J.S. Boateng, Composite HPMC and sodium alginate based buccal formulations for nicotine replacement therapy, Int. J. Biol. Macromol. 91 (2016) 31–44.
[13] R. Trastullo, A. Abruzzo, B. Saladini, M.C. Gallucci, T. Cerchiara, B. Luppi, F. Bigucci, Design and evaluation of buccal films as paediatric dosage form for transmucosal delivery of ondansetron, Eur. J. Pharm. Biopharm. 105 (2016) 115–121.
[14] A. Kelemen, B. Katona, S. Módra, Z. Aigner, I. Sebe, K. Pintye-Hódi, R. Zelkó, G. Regdon, K. Kristó, Effects of sucrose palmitate on the physico-chemical and mucoadhesive properties of buccal films, Molecules 25 (2020) 5248.
[15] A. Kazsoki, A. Domján, K. Süvegh, R. Zelkó, Microstructural characterization of papaverine-loaded HPC/PVA gels, films and nanofibers, Eur. J. Pharmaceut. Sci. 122 (2018) 9–12.
[16] K.-G.H. Desai, S.R. Mallery, A.S. Holpuch, S.P. Schwendeman, Development and in vitro-in vivo evaluation of fenretinide-loaded oral mucoadhesive patches for site-specific chemoprevention of oral cancer, Pharm. Res. (N. Y.) 28 (2011) 2599–2609.
[17] M. Montenegro-Nicolini, J.O. Morales, Overview and future potential of buccal mucoadhesive films as drug delivery systems for biologics, AAPS PharmSciTech 18 (2017) 3–14.
[18] J.O. Morales, J.T. McConville, Manufacture and characterization of mucoadhesive buccal films, Eur. J. Pharm. Biopharm. 77 (2011) 187–199.
[19] S. Farias, J.S. Boateng, *In vitro*, ex vivo and in vivo evaluation of taste masked low dose acetylsalicylic acid loaded composite wafers as platforms for buccal administration in geriatric patients with dysphagia, Int. J. Pharm. 589 (2020), 119807.
[20] Y.H.-E.Y. Ibrahim, G. Regdon, K. Kristó, A. Kelemen, M.E. Adam, E.I. Hamedelniel, T. Sovány, Design and characterization of chitosan/citrate films as carrier for oral macromolecule delivery, Eur. J. Pharmaceut. Sci. 146 (2020), 105270.
[21] M. Gottnek, K. Süvegh, K. Pintye-Hódi, G. Regdon, Effects of excipients on the tensile strength, surface properties and free volume of Klucel® free films of pharmaceutical importance, Radiat. Phys. Chem. 89 (2013) 57–63.
[22] A.M. Ili Balqis, M.A.R. Nor Khaizura, A.R. Russly, Z.A. Nur Hanani, Effects of plasticizers on the physicochemical properties of kappa-carrageenan films extracted from Eucheuma cottonii, Int. J. Biol. Macromol. 103 (2017) 721–732.
[23] A. Miro, I. d'Angelo, A. Nappi, P. La Manna, M. Biondi, L. Mayol, P. Musto, R. Russo, M.I.L. Rotonda, F. Ungaro, F. Quaglia, Engineering poly(ethylene oxide) buccal films with cyclodextrin: a novel role for an old excipient? Int. J. Pharm. 452 (2013) 283–291.
[24] A.B. Nair, R. Kumria, S. Harsha, M. Attimarad, B.E. Al-Dhubiab, I.A. Alhaider, *In vitro* techniques to evaluate buccal films, J. Contr. Release 166 (2013) 10–21.
[25] M. Szekalska, M. Wróblewska, M. Trofimiuk, A. Basa, K. Winnicka, Alginate oligosaccharides affect mechanical properties and antifungal activity of alginate buccal films with posaconazole, Mar. Drugs 17 (2019) 692.
[26] L. Wang, Y. Wu, J. Li, H. Qiao, L. Di, Rheological and mucoadhesive properties of polysaccharide from Bletilla striata with potential use in pharmaceutics as bio-adhesive excipient, Int. J. Biol. Macromol. 120 (2018) 529–536.
[27] K. Pamlényi, K. Kristó, O. Jójárt-Laczkovich, G. Regdon, Formulation and optimization of sodium alginate polymer film as a buccal mucoadhesive drug delivery system containing cetirizine dihydrochloride, Pharmaceutics 13 (2021) 619.
[28] K. Haugstad, A. Håti, C. Nordgård, P. Adl, G. Maurstad, M. Sletmoen, K. Draget, R. Dias, B. Stokke, Direct determination of chitosan–mucin interactions using a single-molecule strategy: comparison to alginate–mucin interactions, Polymers 7 (2015) 161–185.
[29] F. Horak, P. Zieglmayer, R. Zieglmayer, P. Lemell, The effects of bilastine compared with cetirizine, fexofenadine, and placebo on allergen-induced nasal and ocular symptoms in patients exposed to aeroallergen in the Vienna Challenge Chamber, Inflamm. Res. 59 (2010) 391–398.
[30] A. Kelemen, M. Gottnek, G. Regdon, K. Pintye-Hódi, New equipment for measurement of the force of adhesion of mucoadhesive films, J. Adhes. Sci. Technol. 29 (2015) 1360–1367.
[31] K. Kristó, O. Kovács, A. Kelemen, F. Lajkó, G. Klivényi, B. Jancsik, K. Pintye-Hódi, G. Regdon, Process analytical technology (PAT) approach to the formulation of thermosensitive protein-loaded pellets: multi-point monitoring of temperature in a high-shear pelletization, Eur. J. Pharmaceut. Sci. 95 (2016) 62–71.
[32] M. Gottnek, K. Pintye-Hódi, G. Regdon, Tracking of the behaviour of lidocaine base containing hydroxypropylcellulose free films with thermoanalytical method, J. Therm. Anal. Calorim. 120 (2015) 201–208.
[33] G. Regdon, A. Kósa, I. Erős, K. Pintye-Hódi, Thermoanalytical behaviour of some coating free films, J. Therm. Anal. Calorim. 89 (2007) 793–797.
[34] M. Jouki, N. Khazaei, M. Ghasemlou, M. HadiNezhad, Effect of glycerol concentration on edible film production from cress seed carbohydrate gum, Carbohydr. Polym. 96 (2013) 39–46.
[35] K. Kesavan, Sodium alginate based mucoadhesive system for gatifloxacin and its *in vitro* antibacterial activity, Sci. Pharm. 78 (2010) 941–957.
[36] M. Ionita, M.A. Pandele, H. Iovu, Sodium alginate/graphene oxide composite films with enhanced thermal and mechanical properties, Carbohydr. Polym. 94 (2013) 339–344.
[37] M. Paczkowska, M. Mizera, K. Lewandowska, M. Kozak, A. Miklaszewski, J. Cielecka-Piontek, Effects of inclusion of cetirizine hydrochloride in β-cyclodextrin, J. Inc. Phenom. Macrocycl. Chem. 91 (2018) 149–159.